



University of Nairobi

Aerosol Remote Sensing and Modelling: Estimation of Vehicular Emission Impact on Air Pollution in Nairobi, Kenya

by

Nyaga Ezekiel Waiguru

S56/9306/2017

BSc. Physics


Masinde Muliro University of Science and Technology

A thesis submitted in partial fulfilment for the degree of Master of Science in Nuclear Science and Technology in the Institute of Nuclear Science and Technology in the University of Nairobi.

@ 2021

Declaration

This thesis is my original work and has not been presented for a degree in any other University.

Sign: 

Date 25th May 2021

Mr. Nyaga, Ezekiel Waiguru

(S56/9306/2017)

Supervisors' Approval

This thesis has been submitted for examination with our knowledge as university supervisors.

Prof Michael Gatari
Institute of Nuclear Science and Technology
University of Nairobi

Sign: 

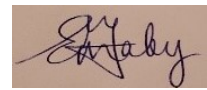
Date: **25 May 2021**

Dr. Andrea Mazzeo
School of Geography, Earth and Environmental Science
University of Birmingham, UK.

Sign: 

Date: **25th of May 2021**

Prof Elijah Mwangi
School of Engineering
University of Nairobi.

Sign: 

Date: **25 May 2021**

Dedication

This thesis is dedicated to my parents, brothers and sisters due to their unwavering encouragement and support throughout my education journey.

Acknowledgement

I am thankful to Gandhi Smarak Nidhi Fund for sponsoring my MSc studies in Nuclear Science and Technology. I wish to express my gratitude to my supervisors Prof. Michael Gatari, Dr Andrea Mazzeo and Prof Elijah Mwangi. Their expertise, guidance and support made me pursue the project to conclusion. I am thankful to Dr Andrea Mazzeo for helping customize the HDM-4 model software for the local conditions in Nairobi besides offering useful insights during this work.

I appreciate the training on air quality modelling which I received from Prof E. Marais and Dr Joshua Vande Hey at the University of Leicester in the UK.

I sincerely appreciate the support of the ASAP (A Systems Approach to Air Pollution) East Africa project for provided the HDM-4 model software which made the modelling work possible. I wish to acknowledge the Kenya Urban Roads Authority (KURA) for providing database for the road networks and the vehicle fleet in Nairobi.

I acknowledge the use of Copernicus for mapping the spatial distribution of NO₂ in Nairobi area. The Research and User Support (RUS) Copernicus training enabled me to learn how to extract and process the data.

I am very grateful to students and members of staff at the Institute of Nuclear Science and Technology for supporting me in one way or another. I sincerely appreciate the support of David and Cynthia (Institute for Climate Change) for having taken part in data collection.

Table of Contents	
Declaration	ii
Dedication	iii
Acknowledgement	iv
List of Tables	vii
List of Figures	viii
List of Appendices	x
List of Abbreviations	xi
Abstract	xiii
CHAPTER ONE	14
INTRODUCTION	14
1.1 Background	14
1.2 Problem Statement	16
1.3 Objectives of the Study	17
1.3.1 Main Objective.....	17
1.3.2 Specific Objectives	17
1.4 Justification	17
1.5 Scope and Limitations of the Study	18
CHAPTER TWO	19
LITERATURE REVIEW	19
2.0 Background	19
2.1 Ground Level Air Quality	20
2.2 Air Pollution Studies in Nairobi.....	21
2.3 Health Effects of Air Pollutants	22
2.4 WHO Air Quality Guidelines	23
2.5 Vehicle Exhaust Emissions	24
2.6 Satellite Remote Sensing of Air Quality	25
2.6.1 TROPOMI Air Quality Detector.....	26
2.6.2 TROPOMI Working Principle	27
2.7 The Highway Development and Management Model (HDM-4).....	27
2.7.1 HDM-4 Data Requirement.....	28
2.8 Modelling Vehicle Emissions in HDM-4	29
2.8.1 Road Characteristics	29

2.8.2 Traffic Characteristics	31
2.8.3 Modelling Vehicle Speed	31
2.8.4 Fuel Consumption	34
2.9 Calibration of Vehicle Emission Models	36
2.10 Format of Vehicle Emission Models in HDM-4	36
2.11 Summary	39
CHAPTER THREE.....	40
METHODOLOGY.....	40
3.0 Customization and Calibration of HDM-4 Model v2.0	40
3.1 Sensitivity Test.....	41
3.2 Modelling Annual Exhaust Emissions	41
3.3 Effects Traffic Growth on Vehicle Exhaust Emissions	42
3.4 Mapping NO ₂ Concentration Over Nairobi	42
CHAPTER FOUR.....	44
RESULTS AND DISCUSSION	44
4.0 Sensitivity Test Results	44
4.1 Modelled Exhaust Emissions	45
4.2.1 Jogoo Road Results	47
4.2.2 Mombasa Road Results.....	49
4.2.3 Ngong Road Results.....	51
4.2.4 Outer-Ring Road Results	54
4.2.5 Waiyaki Way Results.....	56
4.2.6 Thika Road Results	58
4.2.7 Langata Road Results.....	60
4.3 Predicted Cumulative Exhaust Emissions for Nairobi Road Networks.....	62
4.4 Spatial Distribution of NO ₂ Emissions over Nairobi	64
CHAPTER FIVE.....	66
CONCLUSION	66
RECOMMENDATIONS	67
References	68

List of Tables

Table 2. 1 NEMA Air Quality Guidelines	24
Table 2. 2 Road Surface Classification (Morosiuk et al., 2004)	29
Table 2. 3 Vehicle Categories Included in HDM-4 (H. G. Kerali et al., 2000)	31

List of Figures

Figure 2. 1 Sentinel 5P satellite carrying TROPOMI detector on board (RBISA, 2020).....	26
Figure 2. 2 Spectral bands for TROPOMI and its predecessors OMI, SCIAMACHY and GOME (Vries et al., 2009).	27
Figure 2. 3 International roughness index for various roads (Sayers, 1986)	30
Figure 2. 4 Speed flow model in HDM-4 (Hoban et al., 1994).	33
Figure 3. 1. Illustrates the horizontal grid over which NO ₂ tropospheric column data was retrieved (source:(Wikipedia, 2018).	43
Figure 4. 1 Tornado plots showing sensitivity of the model input variables to (a) CO, (b) HC, (c) NO _x , and (d) PM _{2.5} emissions.....	45
Figure 4. 2 Comparison of un-calibrated HDM-4 exhaust emissions Edgar-DICE emissions.....	46
Figure 4. 3 Illustrates comparison between HDM-4 and Edgar-DICE emissions	47
Figure 4. 4 (a). Shows variation in IRI and (b) is the vehicle operating speed.....	47
Figure 4. 5 The modelled annual average fuel consumption for Jogoo road.....	48
Figure 4. 6 Illustrates the modelled exhaust emissions for Jogoo road	49
Figure 4. 7 (a) Variation in pavement IRI and (b) are the changes in annual average operating speed.	50
Figure 4. 8 Shows the modelled annual average fuel consumption for Mombasa road	50
Figure 4. 9 Predicted exhaust emissions for Mombasa road.....	51
Figure 4. 10 (a) Illustrates predicted pavement surface condition (IRI) and (b) is the annual average vehicle operating speed.	52
Figure 4. 11 illustrates the modelled annual average fuel consumption for Ngong road	53
Figure 4. 12 Illustrate predicted vehicle exhaust emissions for Ngong road.	54
Figure 4. 13 Illustrates change in modelled pavement surface condition (a), and variations in modelled vehicle average operating speeds (b)	54
Figure 4. 14 The modelled annual average fuel consumption for Outer-Ring road.	55
Figure 4. 15 Predicted exhaust emissions for Outer-ring road	56
Figure 4. 16 Predicted annual pavement surface roughness (IRI) (a), and the modelled vehicle operating speed.	57

Figure 4. 17 Illustrate changes in modelled vehicle exhaust emissions.....	58
Figure 4. 18 illustrates predicted IRI and the average vehicle speed.....	59
Figure 4. 19 Illustrates modelled exhaust emissions for Thika road	60
Figure 4. 20 (a) illustrates variation in pavement roughness and (b) is the annual average traffic operating speed.	60
Figure 4. 21 The annual average vehicle fuel consumption along Langata road.....	61
Figure 4. 22 Reports changes in vehicle emissions for Langata road.....	62
Figure 4. 23 Cumulative vehicle emissions for Nairobi road networks and their annual variations for the three test scenarios.....	63
Figure 4. 24 Relative change in emissions for the high and low traffic growth in comparison to the base scenario	64
Figure 4. 25 Total NO ₂ tropospheric column over Nairobi observed in different days of the year.	65

List of Appendices

- Appendix A: Vehicle Growth Rates for Different Road Categories (source: KENHA)
- Appendix B: Vehicle Parameters Required for Modelling; source (Notter et al., 2019)
- Appendix C: The Study Road Networks (Google.(n.d))
- Appendix D: Model Input parameters for the Road Networks

List of Abbreviations

BC	Black Carbon
CPF	Catalytic Pass Fraction
EOS	Earth Observation System
ESA	European Space Agency
GOME	Global Ozone Monitoring Experiment
GOMOS	Global Ozone Monitoring by Occultation of Stars
IRI	International Roughness Index
ISOHDM	International Study of Highways Development and Management
KeNHA	Kenya National Highways Authority
KeRRA	Kenya Rural Roads Authority
KRB	Kenya Roads Board
KURA	Kenya Urban Roads Authority
LHS	Latin Hypercube Samples
MODIS	Moderate Resolution Imaging Spectroradiometer
NEMA	National Environmental Management Authority
NRT	Near Real Time
NRTI	Near Real Time
NTSA	National Transport and Safety Authority
OMI	Ozone Monitoring Instrument
PCSE	Passenger Car Space Equivalent
RDWE	Road Deterioration and Work Effects
RUE	Road User Effects

RUS	Research and User Support
TOA	Top-of-atmosphere
TOMS	Total Ozone Mapping Spectrometer
TROPOMI	Tropospheric Ozone Monitoring Instrument
TSP	Total suspended particulate
VOC	Volatile organic compounds
WHO	World Health Organisation
DICE Africa	Emission Inventory for the Africa Region
NCIDP	Nairobi county integrated development plan

Abstract

In cities experiencing rapid urbanisation and motorisation like Nairobi, deterioration of air quality is bound to occur due to vehicular emissions. Exposure to ambient aerosols is a leading risk factor which is attributed to respiratory diseases, cardiovascular diseases, lung cancer and stroke. Regular monitoring of air quality is therefore important for constant assessment of the abundance of air pollutants in the air we breathe. The model for Highway Development and Management (HDM-4) was calibrated against Edgar-DICE emissions. Calibration of vehicle Engine Output Models (EOM) involved adjustment of default emission coefficients till the model output emissions was in agreement with the Edgar-DICE emissions. Calibrated model was used to predict annual exhaust emissions within Nairobi. The effect of traffic growth on exhaust emissions was investigated for a twenty-year period. Sentinel 5P satellite measurements of total NO₂ tropospheric column was used to map spatial distribution of NO₂ in the study area. Spearman's rank correlation coefficient was used to rank the degree of sensitivity of the model input variables and then visualized as Tornado plots. According to this test, vehicle life, vehicle operating weight, and road geometry had the highest influence on the exhaust emissions. The HDM-4 annual modelled quantities of CO, NO_x, and PM_{2.5} were 60324, 4582, and 4273 tonnes respectively. For the same pollutants, the Edgar-DICE emissions predicted 42420 tonnes, 1458 tonnes, and 3188 tonnes respectively. The improvement in HDM-4 predictions was attributed to its bottom-up approach unlike the Edgar-DICE emissions which were generated through a top-down approach. Exhaust emissions forecasting showed possible increment of PM_{2.5} and CO by 11.5% and 2.20% respectively for the high traffic growth scenario while NO_x reduced by 0.22%. In low traffic growth scenario, PM_{2.5} and CO recorded a reduction of 1.33% and 0.1% respectively, contrary to NO_x which increased by 0.5%. This behaviour was attributed to the fact that traffic congestion has negative influence on NO_x emissions. Observation from Tropospheric Ozone Monitoring Instrument (TROPOMI) satellite showed patterns of high NO₂ concentration along busy highways connecting the city. The study has demonstrated alternative tools which can not only provide information on air quality in areas with limited coverage of ground monitoring but also form new frontier in air quality research through modelling and satellite remote sensing. Adequate understanding of the of source contribution to overall emissions is key to formulation of target control measures.

CHAPTER ONE

INTRODUCTION

1.1 Background

Because of the widespread evidence of the health effects arising from exposure to poor air quality (Manisalidis et al., 2020), there is need for regular assessment of air quality to prevent associated risks. The causes of air pollution range from vehicle emissions, industrial emissions, uncontrolled burning of municipal waste, mineral dust, biomass burning among others. These emissions include historically defined criteria pollutants namely PM_{2.5}, SO₂, NO_x, CO, and a variety of toxic species of hydrocarbons (HCs), which pose risk to human health (Saxena and Sonwani, 2019). For this reason, robust monitoring of air quality is necessary to constantly assess the level of ambient aerosols.

Air quality studies in Kenya have been based on sparse datasets collected from random monitoring campaigns, mostly conducted in learning institutions (Gichuru et al., 2005). The studies have given insights on the poor state of air quality in the city (Kinney et al., 2011). Measurements taken in the central business district and areas in close proximity to busy traffic road links have recorded levels of air pollution which exceeded the World Health Organisation (WHO) guidelines (Gaita et al., 2014). Air pollution hotspots have been identified in the neighbourhood of motorways and around the bus parks (Kinney et al., 2011). The situation is only expected to get worse owing to the quality and quantity of fuel consumed (Ndegwa, 2017), traffic congestion (Gachanja, 2015), lack of public awareness about air quality (Egondi et al., 2013), and deficiencies in relevant legislation due to incomplete data which is necessary for policy formulation (Gichuru et al., 2005).

As of 2019, the main mode of transport for approximately 4.4 million residents of Nairobi was road and walking (KNBS, 2019). Railway transport is available during rush hours and covers limited routes within the city. The number of registered vehicles in 2019 was 3.6 million, rising from 2.5 in 2015, which represented approximately 11.7% annual increment during that period (KNBS, 2016, 2020). About 30% of registered vehicles nationally operate in Nairobi (Omwenga, 2011). Majority of the vehicle fleet are second-hand imported vehicles. Fuel consumption is also bound to increase due to the old vehicle technology, poor maintenance practices, frequent traffic congestion and deteriorated road conditions, all of which are likely to contribute to high exhaust emissions.

Exposure to PM_{2.5} is associated with respiratory disease, cardiovascular disease, lung cancer and stroke (Landrigan et al., 2018). The risk is especially high to the elderly, children and people with underlying conditions. In 2019, respiratory system disease was leading cause of ill health in Nairobi with about 820 thousand reported cases (KNBS, 2020). The three-leading cause of mortality for children aged below five were pneumonia, prematurity and diseases of respiratory system (NCIDP, 2018). Studies have shown high pollutant concentrations along busy traffic networks within the city owing to high traffic volumes. City drivers, traffic police, street vendors, and motorbike operators are therefore at great risk of occupational exposure (Mukaria, 2017; Ngo et al., 2015). Additionally, passengers and pedestrians get exposed as they undertake their daily activities. It has also been shown that since 1974 to 2018, visibility in Nairobi reduced by approximately 60% owing to increase in anthropogenic emissions over time (Singh et al., 2020). Since 2015, Nairobi has recorded the highest number of road accidents followed by Nakuru and Kiambu counties (Muguro et al., 2020), which could be attributed to degradation of eyesight.

Traditionally, air quality measurements taken from ground stations (reference stations) has been considered as ground truth (Sadd et al., 2014). PM_{2.5} is the widely monitored pollutant owing to the widespread evidence of its health effects even in low concentrations. The sampling techniques and quantification of PM_{2.5} mass concentration has been documented widely (Cheng et al., 2015; Koistinen et al., 1999). Pre-weighed filter is deployed in a sampler and allowed to run, mostly for twenty-four hours and the mass of PM_{2.5} is then determined by the mass difference. The use of optical particle counters has also increased recently owing to their relatively low cost and the ease of deployment (Kumar et al., 2015; Munir et al., 2019). They have therefore become suitable alternatives in places without existing monitoring networks. However, good understanding of their limitations and proper calibration is paramount in order to achieve reasonably accurate results (Pope et al., 2018).

In the recent years, satellite remote sensing has received wide application in air quality studies. A good example is the Moderate Resolution Imaging Spectroradiometer (MODIS) which provide vertically resolved aerosol measurements emanating from industries, transport, biomass burning, forest fires, dust storms, and volcanic eruptions (Xiong et al., 2009). The TROPOspheric Monitoring Instrument (TROPOMI) is a low orbit atmospheric detector onboard Sentinel 5P satellite. TROPOMI provides information about tropospheric composition of aerosols and clouds.

Air quality models predict air quality at different spatial and temporal scales. They are effective tools which not only supplement air quality monitoring but also perform tasks such as scenario analysis and forecasting, which cannot be achieved through monitoring (Castell et al., 2017). The Highway Development and Management-4 (HDM-4) model has been developed by World Bank for the purposes of pavement management. Vehicle exhaust emission models are also incorporated in the HDM-4 for the purpose of environmental impact assessment.

The Engine Out Emissions models in HDM-4 were calibrated and used to model vehicle exhaust emissions in Nairobi. The model simulates emissions by taking into account complex interactions between pavement characteristics, vehicle engine and physical characteristics, and the environment (Prasad et al., 2013a). Other sub-models in HDM-4 include pavement performance prediction, vehicular performance prediction and economic analysis tools (Prasad et al., 2013a). The components of exhaust emissions simulated by the models include HC, CO, CO₂, SO₂, NO_x, and particulate matter (Sassykova et al., 2019).

While huge sets of air pollution data exist from different satellite missions, it has been scarcely applied to study air quality, especially in a city like Nairobi where only limited ground measurements exist. The mapping of NO₂ emissions within Nairobi was done using tropospheric column data from Sentinel 5P satellite. Data analysis was done using python packages developed by Copernicus Research and User Support Service (RUS, 2018). The synergy provided by vehicle emission models and the satellite data provided good understanding of the relative contribution of vehicle emissions to the overall air quality as well as identification of air pollution hotspots within the city.

1.2 Problem Statement

While short term air quality monitoring campaigns have revealed the deteriorating state of air quality in Nairobi, traffic emission is the major source of atmospheric pollution. This is occasioned by huge traffic volume which is estimated to grow by approximately 13% annually. Frequent incidences of traffic congestion experienced in the city contribute to increased fuel consumption which has potential to cause increased exhaust emissions.

Road transport is responsible for most of PM_{2.5}, HC, CO, CO₂, NO_x, and SO₂ emissions in urban centres. The PM_{2.5} particles pose great dangers to human health, they are capable of penetrating through the alveoli of the lungs into the blood streams owing to their small size. Exposure to PM_{2.5} is attributed to acute lower respiratory infections, cardiovascular, chronic

obstructive pulmonary diseases and lung cancer (WHO, 2006). HC emissions contribute to formation of smog in urban areas which reduces visibility and can result to accidents. In presence of sunlight, NO_x, CO and HC reacts to form ground level O₃ which has potential to trigger asthma, reduce lung function as well as causing of lung diseases (WHO, 2006). The SO₂ exposure is linked to inflammatory condition to respiratory tract which cause coughing, mucus secretion and aggravation of chronic bronchitis and asthma.

The National Economic survey of 2019 recorded respiratory diseases as leading cause of illness among children in Nairobi. Cumulatively, 154,636 and 489 cases of respiratory and cardiovascular conditions constituted 12% and 11% of the nationally statistics respectively (KNBS, 2020). These estimates could be higher given that many cases go unreported and therefore unaccounted for.

1.3 Objectives of the Study

1.3.1 Main Objective

The study aimed to estimate the impact of motorised traffic to atmospheric emissions using research tools which can effectively supplement ground measurements and ensure improvement of air quality prediction in cities with limited coverage of ground monitoring networks like Nairobi.

1.3.2 Specific Objectives

- i. To prepare and carryout Level 1 calibration of HDM-4 vehicle emission models for Nairobi.
- ii. To model annual vehicle emissions of CO, HC, NO_x, SO₂, and PM_{2.5}.
- iii. To evaluate the relative changes in these emissions for a period of twenty years due to traffic growth.
- iv. To map out the spatial distribution of NO₂ over Nairobi using total NO₂ tropospheric column data derived from Sentinel 5P satellite.

1.4 Justification

The city of Nairobi with an estimated population of about 4 million people has experienced rapid urbanization and motorization which in many ways is typical of most cities in developing countries thus facing similar air pollution problems (NCAQAP, 2018). The sparse air quality datasets drawn from randomly conducted studies (NCAQAP, 2018) has hindered the spatial-temporal analysis of air pollution. Thus causing inconclusive findings on health effects of exposure to airborne aerosols in Nairobi (Gaita et al., 2014; Kinney et al., 2011;

Pope et al., 2018). These incomprehensive datasets have derailed both regulation of air quality in as well as formulation of appropriate policies to mitigate air pollution. In the absence of the ground monitoring network, it is necessary to innovate and embrace opportunities offered by emission models and satellite remote sensing to study air quality.

Vehicle emission models have been widely developed and used to predict vehicle contribution to atmospheric emissions. These tools are not only effective to supplement air quality monitoring, but also important in performing tasks such as scenario analysis and forecasting, which cannot be achieved through monitoring (Castell et al., 2017). The Highway Development and Management-4 (HDM-4) emission models are capable to perform these tasks. The models compute vehicle emissions from a section of road to the complete road network (Prasad et al., 2013).

1.5 Scope and Limitations of the Study

The study involved estimation of vehicle emissions in Nairobi county using HDM-4 emission models and Sentinel 5P datasets. Only **Level 1** calibration of HDM-4 models was carried out at this stage. **Level 2** and **Level 3** require huge time and resource investment therefore not in this project. The vehicle emission models were calibrated against Edgar-DICE emissions due to lack of vehicle emissions monitoring data (Mazzeo et al., 2019). The period of vehicle exhaust emissions forecasting was taken to be twenty years which is considered as the pavement lifecycle in the HDM-4 model. Sentinel 5P tropospheric column measurement was then used to demonstrate the spatial distribution of NO₂ in Nairobi. Thirteen major roads links were assumed to represent Nairobi road networks. The road transport was also assumed to be main source of atmospheric NO₂ within Nairobi.

CHAPTER TWO

LITERATURE REVIEW

2.0 Background

Transport has played a fundamental role in human development. It creates a competitive business environment and is the means through which social-economic and environmental objectives can be achieved (Chama, 2013). However, rapid convergence of people in cities of emerging and developing economies has not only increased motorization but also intensified strain on the limited and poorly developed transport infrastructure (Rajé et al., 2018). High volume in developing cities has the effect of causing congestion, accidents and air pollution (Díaz et al., 2020). Fuel combustion in vehicle engines generates air pollutants in form of nitrogen oxides (NO_x), hydrocarbons (HC) which is also known as volatile organic compounds (VOCs), carbon monoxide (CO), particulate matter (PM_{2.5}, PM₁₀) and black carbon (BC) (Winkler et al., 2018). The light-duty gasoline powered vehicle is generally known for high VOCs, CO and NO_x emissions, whereas heavy-duty diesel vehicles are major emitters of NO_x and PM_{2.5} (Sawyer, 2010). Besides increased traffic volume, majority of vehicles in developing countries are composed of second-hand imported vehicles which are likely to cause more emissions due to old emissions control technologies in these vehicles (Ebinger and Vergara, 2011). In 2017, approximately 70% of the global used light duty vehicles was imported by developing countries (Baskin et al., 2020). This figure is set to at least double by 2050 due to factors such as population growth, limited regulations governing the quality of imported vehicles and inadequate implementation of existing regulations (Baskin et al., 2020).

The city of Nairobi has experienced rapid growth in vehicle fleet to meet high transport demand for approximately 4.2 million inhabitants (KNBS, 2020). The number of in-service vehicles in Kenya is estimated at 1.6 million (Ogot et al., 2018), about 30% of the fleet is estimated to operate in Nairobi (Omwenga, 2011). The fleet is composed of motorcycles, cars, buses, matatus (14-seater public transport vans) and trucks. The fleet is characterised by old and poorly maintained vehicles which get frequently overloaded during use, all these factors increase tailpipe emissions resulting to enhanced air pollution (Mbandi et al., 2019).

Road transport system in Nairobi is characterized with paved roads which emanate radially from the centre of the city (Nakagawa et al., 2018). The roads are however linked to limited networks of radial arterials outside of the city to surrounding neighbourhoods and to the communities beyond (Gonzales et al., 2009). The major road intersections are managed with roundabouts and the flow is mostly

controlled manually by traffic police, traffic signals are only available in a few junctions in the CBD (Gonzales et al., 2009). Inefficient traffic flow has the effect of causing incidences of traffic congestion which not only raise vehicle fuel consumption but also the quantity of vehicle emissions.

The Highway Development and Management (HDM-4) model has received wide application globally for pavement management (Prasad et al., 2013). HDM-4 provide opportunity for analysis of pavement investment from feasibility study, design stage, construction, future improvements, maintenance and the cost. The HDM-4 model structure can be classified into two broad sub-model namely Road Deterioration and Work Effects (RDWE) models and the Road User Effects models. The vehicle emission is modelled in RUE sub-models. Vehicle emission modelling is important for assessment of effects in terms of pollutant quantities, changes in road characteristics, traffic congestion and vehicle technology. HDM-4 predicts the different components of vehicle exhaust and tailpipe emissions as a function of fuel consumption and speed. The predicted quantities of NO_x, HC, CO, CO₂, SO₂ and PM_{2.5} emissions are computed based on equations given in HDM-4 manual (Volume-4, part F). A good understanding of source contribution to atmospheric emissions is important in formulation of targeted mitigation measures.

2.1 Ground Level Air Quality

The ambient air which we breathe contains mixture of gases, liquid and solid particles, some of which cause harm to human health (Manisalidis et al., 2020). The level of risk associated with these pollutants is determined by their sizes, chemical composition, toxicity and its relative abundance in the atmosphere (Humans, 2016). Airborne particles which has aerodynamic diameter equal or less than 2.5 microns is defined as fine particles and denoted as PM_{2.5} (Wu et al., 2018), and are more detrimental due to their smallness in size (Chan and Lippmann, 1980; Villar-Vidal et al., 2014). Their compositions range from sulphate ion, nitrate ion, elemental carbon EC, dust, sea salt and trace metals (Cheng et al., 2015; Chow and Watson, 2002). Fossil fuel combustion is a key source of atmospheric SO₂ and the primary sulphate particles (Gaita et al., 2014; Ngo et al., 2015). Atmospheric SO₂ is oxidized to sulphuric acid (H₂SO₄) which then condenses to form aqueous sulphate particles which in presence of ammonia gas, is neutralized to aqueous sulphate to form ammonium sulphate (NH₄)₂ SO₄ particles (Seinfeld and Pandis, 2016; Tomasi and Lupi, 2016). Secondary PM_{2.5} is also formed when nitrous oxide reacts with ammonia leading to ammonium nitrate particles (Seinfeld and Pandis, 2016).

Secondary inorganic aerosols are mainly formed by trace gases such as NO_x, SO₂, and NH₃ which emanate from anthropogenic and natural sources (Boucher, 2015). The leading anthropogenic sources air pollution in urban areas are fossil fuel combustion in industries, power generation and the transport sector (Boucher, 2015; Ngo et al., 2015). The SO₂ emissions get produced from power plants while transport sector is the major source of NO_x while wildfires and burning of biomass generate certain amount of NO₂ and SO₂ (Sudalma et al., 2015). Primary organic aerosols are emitted from vegetation (e.g. pollen grains, biomass burning) (Sudalma et al., 2015).

2.2 Air Pollution Studies in Nairobi

Air quality studies in the country started a couple of decades ago mainly focusing on the total suspended particulate matter (TSP) within Nairobi area (Karue et al., 1994). TSP measurements however could not provide adequate information on involved health implications (Dockery et al., 1994). Another study to assess elemental composition of ambient aerosols was carried out in Nairobi (Kenya) and Hanoi (Vietnam). The study reported elemental concentrations of chlorine, potassium and iron above 100 ng m⁻³ in both cities (Gatari et al., 2005). Ambient particulate matter has been reported to rise due to increased anthropogenic emissions. Road transport continue to dominate atmospheric pollution while other sources include industrial emissions, construction works, uncontrolled burning of municipal waste, biomass fuel, and wind-blown dust (Gatari et al., 2019; Kinney et al., 2011; Muindi, 2017).

Air monitoring campaign conducted in 2011 showed high concentration of black carbon (BC) in Nairobi central business district and in neighbourhoods of highways feeding into the city. These concentrations reduced at distances away from road networks thus indicating the role of motorised traffic on particulate emissions (Gatari et al., 2019). In 2015, measurements of PM₁₀, PM_{2.5}, NO_x, SO₂, CO, BC, and O₃ were taken at Nakumatt, Landhies Road, Pangani and Industrial area junctions. At Landhies roundabout, BC concentration exceeded the upper measurement limit of detector (50,000 µg m⁻³), concentrations of SO₂, O₃, PM₁₀ and PM_{2.5} in the four sites were below their WHO guidelines (Gaita et al., 2014).

Source apportionment of atmospheric aerosols has been carried out in the urban and suburban sites in Nairobi (Gaita et al., 2014). The PM_{2.5} mass concentration was found to exceed the daily WHO guidelines (25 µg m⁻³) in both sites (Gaita et al., 2014). The major sources of pollutants identified through positive factorization matrix were mineral dust, industry,

combustion, motor vehicle and a mixed factor (Gaita et al., 2014). In low income areas of Korogocho, Mathare and Viwandani, the average concentration of PM_{2.5} were 166 $\mu\text{g m}^{-3}$, $103.8 \pm 28.363 \mu\text{g m}^{-3}$, 67 $\mu\text{g m}^{-3}$ respectively (Egondi et al., 2013; Ngo et al., 2015). BC accounted approximately one-third of the measured PM_{2.5} in Mathare and emanated mainly from road transport and industries. Other sources of pollution identified in the study ranged from use of biomass fuel, trash burning, and resuspended dust (Ngo et al., 2015).

In 2016, PM_{2.5} measurements were taken on high traffic congested roads at Kamukunji, Uhuru Highway, and University Way (Mukaria, 2017). The average concentration of PM_{2.5} was highest around Kamukunji at 123.3 $\mu\text{g m}^{-3}$, while it ranged between 45.0 – 46.0 $\mu\text{g m}^{-3}$ along Uhuru Highway, and at University Way (Mukaria, 2017). Pope et al. (2018) also reported on PM₁, PM_{2.5} and PM₁₀ at urban background site (American Wing University of Nairobi), urban roadside (Fire Station-Tom Mboya Street), and rural background (Nanyuki town). It was found that peak particulate matter emissions occurred during the morning and the evening rush hours, and WHO air quality guidelines were always exceeded in roadside and urban background (Pope et al., 2018). Although limited research exists on PM₁, and while no global regulatory guidelines exists currently, its health outcome could be more severe than PM_{2.5} (Chen et al., 2017).

The models are not only effective tools which supplement air quality monitoring, but are also important in performing tasks such as scenario analysis and forecasting, which cannot be conducted by monitoring (Castell et al., 2017). They also provide opportunity to test contribution of different sources to pollution loading, and the relative contribution of primary emissions to secondary pollutants (Cretu and Deaconu, 2012).

2.3 Health Effects of Air Pollutants

Road transport is responsible for PM_{2.5}, HC, CO, CO₂, NO_x, and SO₂ emissions. Since PM_{2.5} is first deposited on the lungs, it is reported to cause airway inflammation effect (Feng et al., 2016; Habre et al., 2014; Xing et al., 2016). It leads to poor functioning of the lungs, increased incidences of asthma and chronic obstructive diseases, besides making the lungs prone to other infections (Feng et al., 2016; Habre et al., 2014). Inhaled PM_{2.5} is deposited on the surfaces of pulmonary and bronchiole and alveoli, it interacts epithelial cells and macrophages in the lungs, impairs its functioning and could even cause them to die (Deng et al., 2013; Feng et al., 2016; Gualtieri et al., 2011).

The impacts of PM_{2.5} on cardiovascular system has also been widely documented. The traffic related components of PM_{2.5} inhibits cardiac autonomic function, cause decline in heart rate variability thus leading to increasing cardiovascular morbidity and mortality (Hu et al., 2020; Thayer et al., 2010). According to Adar et al. (2013), long term exposure to PM_{2.5} is linked to cardiovascular diseases through accelerated atherosclerosis, which is a chronic disease of the arterial wall (Feng et al., 2016; Hu et al., 2020).

The HC emissions contribute to formation of smog in urban areas which reduces visibility and can result to accidents. In the presence of sunlight, NO_x, CO and HC reacts to form ground level O₃ which has potential to trigger asthma, reduce lung function as well as causing of lung diseases (WHO, 2006). The SO₂ exposure is linked to inflammatory condition to respiratory tract which cause coughing, mucus secretion and aggravation of chronic bronchitis and asthma. According to the KNES (2019), diseases of the respiratory and cardiovascular systems were the leading cause of illness among children in Nairobi.

Cumulatively, 154,636 and 489 cases of respiratory and cardiovascular conditions were reported, this constituted 12% and 11% respectively of the nationally statistics (KNBS, 2020).

2.4 WHO Air Quality Guidelines

Since vehicle exhaust emission has significant contribution to atmospheric aerosols within Nairobi, regular measurements are important in order to control their abundance in air. Vehicle exhaust emissions is composed of PM_{2.5}, SO₂, NO_x, HC, CO and CO₂. The WHO has issued safety guidelines to control atmospheric concentration of these pollutants. The guideline requires that the annual mean concentration for PM_{2.5} and NO₂ does not exceed 10 µgm⁻³ and 40 µgm⁻³ respectively, and the 24-hour mean concentration for SO₂ is 20 µgm⁻³ (WHO, 2006). Individual countries have developed their own emission limits based on which enforcement of air quality regulations is done. In Kenya, the National Environmental Management Authority (NEMA) is the body responsible for enforcement of air quality regulation. Air quality regulation is carried out in three zoned areas (table 2.1) (NEMA, 2014).

Table 2. 1 NEMA Air Quality Guidelines

Pollutant		Industrial area	Residential area	Controlled area
PM _{2.5}	Annual average	35 μgm^{-3}		
	24 hours	75 μgm^{-3}		
NO ₂	Annual average			
	24 hours	100 μgm^{-3}	0.1 ppm	
SO ₂	Annual average	80 μgm^{-3}	60 μgm^{-3}	15 μgm^{-3}
	24 hours	125 μgm^{-3}	80 μgm^{-3}	30 μgm^{-3}
O ₃	1 hour	200 μgm^{-3}	0.12 ppm	
	8 hour	120 μgm^{-3}	1.25 ppm	

2.5 Vehicle Exhaust Emissions

Combustion of fossil fuel in motor vehicles is the main cause of exhaust emissions. The major pollutant from diesel engines exhaust is PM_{2.5} (Fiebig et al., 2014). On the other hand, gasoline engines are major emitters of NO_x, CO, HC and volatile organic compounds (VOC) (Saini et al., 2013). The engine out CO emissions is generated due to incomplete combustion caused by insufficient oxygen which can adequately mix with the fuel (Bolaji and Adejuyigbe, 2006). The reaction which leads to CO formation takes place pretty fast than the one for CO₂, therefore, CO can be considered as an intermediate or final product. When internal combustion engine fails to burn fuel completely to CO₂ and water, CO forms part of the exhaust emission (Bolaji and Adejuyigbe, 2006). The concentration of CO is high in a rich air/fuel mixture owing to high amount of unburnt fuel while for a weak air/fuel mixture the amount of CO reduces considerably (Bolaji and Adejuyigbe, 2006).

CO occur as a colourless and odourless gas which is highly poisonous. This pollutant has a tendency to reacts with haemoglobin present in the blood to form carboxyhemoglobin thus suppressing the quantity of oxygen transported to the body organs (Weaver, 2009). In high concentration, CO is able to increase the risk of cardiovascular problem and impede the psychomotor functions (Heidarnazhad et al., 2004). The risks due to CO exposure are high in

children, elderly, and people with cardiovascular problems. The presence of CO in the lower troposphere increases ozone formation at the ground level (Monks et al., 2015).

The HC emissions in motor vehicles occur due to missing, worn-out or improperly tightened fuel caps (Batterman et al., 2005). Evaporation causes HC emission to occur in stationary vehicles due to diurnal temperature changes. HC emissions is also formed due to incomplete combustion of fuel due to limited O₂ supply or difference in temperatures of combustion where some fuel species burn at higher temperature than others. High quantity of HC is produced during long deceleration events (An et al., 1998). Since fuel consumption reduces considerably during deceleration, the fuel which was initially undergoing combustion process is thus released unburned (An et al., 1998).

Vehicle exhaust emissions is the principal source of nitric oxide (NO) and nitrogen dioxide (NO₂) both of which are referred in a general term as nitrogen oxides (NO_x) (Bolaji and Adejuyigbe, 2006; Lozhkina and Lozhkin, 2016). NO_x is generated due to the high temperature and pressure in the engine cylinder which cause dissociation and subsequent recombination of atmospheric N₂ and O₂ as shown by the following chemical reactions (Dimaratos et al., 2019).



NO_x and VOC react in the presence of sunlight to form ground level ozone (Chaturkova, 2015).

Carbon dioxide (CO₂) emissions is the major product of complete combustion of fuel in the vehicle engine. It occurs naturally in the atmosphere and therefore not considered as a pollutant. Since CO₂ is transparent to short wavelength radiation from the sun but opaque to the longer wavelengths radiated back to space from the earth, in high concentration, it cause heating of the earth's atmosphere and therefore global warming (Bolaji and Adejuyigbe, 2006).

2.6 Satellite Remote Sensing of Air Quality

The rise in concentrations of trace gases (NO₂, CO and SO₂) especially in urban areas have become indicator of the level of air pollution. Studies to determine spatial-temporal characteristics of these gases has therefore increased tremendously. Satellite remote sensing provides unprecedented capabilities to be able to study large-scale behaviour and evolution of

these pollutants over long periods of time. Its use for monitoring of air pollution has developed over the previous decades (Martin, 2008).

2.6.1 TROPOMI Air Quality Detector

The TROPospheric monitoring Instrument (TROPOMI) is an atmospheric detector on-board the Sentinel 5p satellite aimed at monitoring changes in global air quality and climate (Veefkind et al., 2012).

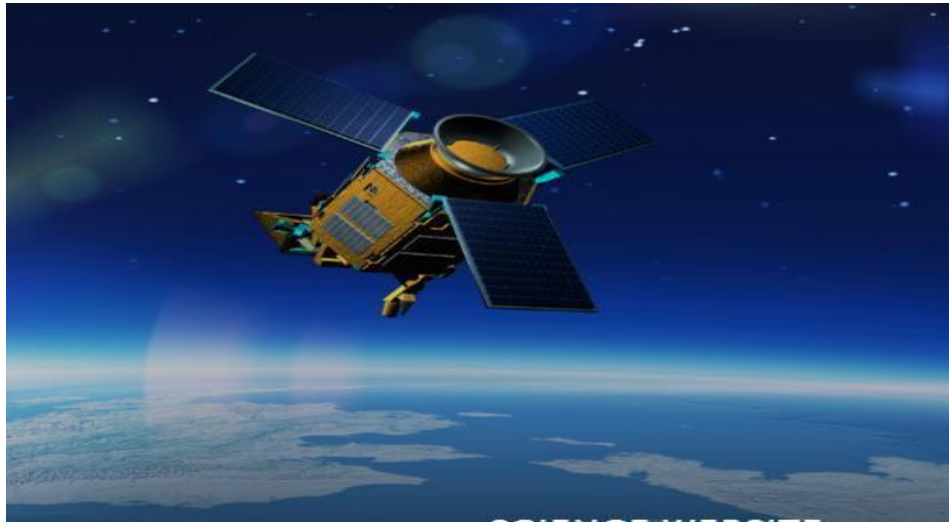


Figure 2. 1 Sentinel 5P satellite carrying TROPOMI detector on board (RBISA, 2020).

TROPOMI detector derives its properties from its predecessor instruments namely SCIAMACHY (Bovensmann et al., 1999), GOME-2 (Munro et al., 2016) and OMI (Levelt et al., 2006). TROPOMI is a multispectral imaging detector which covers spectral bands in the Ultraviolet, Visible, Near-Infrared and the Shortwave Infrared (Veefkind et al., 2012). It therefore measures a wide range of atmospheric trace gases including NO_2 , O_3 , SO_2 , CO , CH_2O , CH_4 , and clouds (Veefkind et al., 2012). The spatial resolution for all trace gases is $3.5 \times 7 \text{ km}^2$ except for CO and CH_4 which is $7 \times 7 \text{ km}^2$ (Veefkind et al., 2012). For this reason and for the first time, it is possible to detect air pollution on facility and city scale from space (Borsdorff et al., 2018). TROPOMI has two dimensional detectors, one for measuring the spatial information and the other for measuring spectral information (Veefkind et al., 2012).

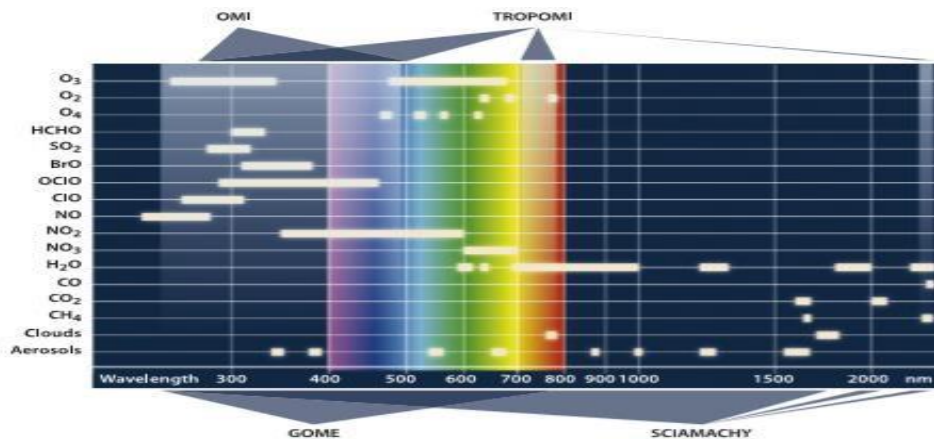


Figure 2. 2 Spectral bands for TROPOMI and its predecessors OMI, SCIAMACHY and GOME (Vries et al., 2009).

2.6.2 TROPOMI Working Principle

Atmospheric pollutants exist as molecules formed by combination of elements joined together by several type of bonds of different strength (NRC, 2003). It is possible to identify chemical compounds in the atmosphere owing to differences in mass and bonding structures which lead to unique quantized energy states associated with vibrational, rotational, stretching and bending modes of the molecules, thereby leading to identification of chemical species (NRC, 2003). The uniqueness of each chemical species is identified by observing the infrared absorption spectra or the Raman scattering intensity within the region of the spectrum, $0-4200\text{ cm}^{-1}$, which corresponds to absorption spectrum wavelengths from about 25 to $2.4\text{ }\mu\text{m}$ (Kang et al., 2009).

The Sentinel 5P has a large swath of 2600 km which provide a global coverage and the collected data sets which are available as L1B and L2 (Berger et al., 2012). The L1B is geolocated and radiometrically corrected top-of-atmosphere radiance while L2 include radiance products, solar irradiance products, aerosol products, and the total column concentration for O_3 , CO, NO_2 , SO_2 , and CH_4 trace gases (Berger et al., 2012; Virghileanu et al., 2020). The datasets are available on two different timelines, the first one is Near Real Time (NRT) which is made available three hours after sensing. The second is the Offline (OFFL) stream which is available after five days (Berger et al., 2012).

2.7 The Highway Development and Management Model (HDM-4)

The Highway Development and Management (HDM-4) model was originally developed by World Bank for pavement management (Kerali, 2000). The model is widely applied to facilitate analysis of alternatives for road maintenance and investment (Li et al., 2004). Its focus is to provide road performance prediction, project appraisal, and policy impact studies

(Kerali, 2000). It has ability to predict pavement performance based on factors relating to road design, materials, construction variability, traffic, vehicle operating costs, environmental considerations as well as maintenance and rehabilitation practices (Li et al., 2004). For HDM-4 to give reasonably accurate results, the model default parameters must be customized to reflect the local conditions (H. G. Kerali et al., 2000). The model has been customized and domesticated in numerous countries including Ethiopia, Ghana, Malawi, India, Thailand etc. Similarly, effective application of the model in Kenya adequate calibration to be conducted (Thube, 2013).

The model is broadly classified into two sub-models namely Road Deterioration and Work Effects (RDWE) and Road User Effects models (Bennett and Paterson, 2002; Kerali et al., 2000). The RDWE model simulates road deterioration for three classes of pavements namely bituminous, concrete and unsealed roads (Morosiuk et al., 2004). Since each pavement deterioration is unique, it is modelled separately in HDM-4 (Odoki and Kerali, 2000). The roadworks anticipated to be carried out during the life-cycle of the pavement must be defined during the project analysis (Morosiuk et al., 2004). The models simulate the effect of each type of roadworks on pavement condition and determine the corresponding costs (Bennett and Paterson, 1998). On the other hand, the Road User Effects (RUE) models predicts the vehicle exhaust emissions, cost of vehicle operation, road accidents and travel time cost (Prasad et al., 2013). Prediction of vehicle exhaust emissions is based on vehicle energy consumption, which on the other hand is influenced by vehicle technology, road condition, and traffic volume (Odoki and Kerali, 2000).

2.7.1 HDM-4 Data Requirement

The HDM-4 model configuration require data relating to road network, vehicle composition and their characteristics, road maintenance, improvement works, traffic flow patterns, speed flow types, accident classes and road calibration parameters (Kerali et al., 2000). The model has several data managers where this information is inputted, they are Vehicle Fleet, Road Network, Work Standards, Projects, Programmes, Strategies, and Configuration (Odoki and Kerali, 2000).

Limited studies exist on characterisation of vehicle fleet in Kenya. However, aggregated data on vehicle registration is available at National Transport and Safety Authority (NTSA) and the Kenya National Economic Surveys (Ogot et al., 2018). Recently, a study was conducted to estimate the nationwide on-road vehicle fleet, age distribution and life expectancies, emission factors, fuel consumption, mileage and the national rate of motorisation (Ogot et al.,

2018). The vehicle ages, mileage and motorization rate used in HDM-4 model was extracted from this study.

The five critical data managers within the HDM-4 model are Vehicle Fleet, Road Networks, Road Works, Maintenance Standards, and Configuration (Kerali, 2000). The Vehicle Fleet data manager stores and retrieve vehicle characteristics information which is required for calculating vehicle speeds, operating costs, travel cost time and other vehicle effects (Bennett and Greenwood, 2003). The Road Networks data manager allows one to store characteristics of one or more road sections (Kerali, 2000).

2.8 Modelling Vehicle Emissions in HDM-4

The objective is to assess the quantity of emissions, variation of these emissions with changes in road characteristics as well as vehicle technology (Hammerstrom, 1995). The formulation of emission models in HDM-4 is based on vehicle specific fuel consumption (Zhang, 2016). On the other hand, fuel consumption is dependent on vehicle characteristic, speed and road condition (Zhang, 2016). The primary data required for modelling vehicle emissions include the length of road section, section traffic volume, vehicle speeds, fuel consumption, and vehicle characteristics (Kerali et al., 2000).

2.8.1 Road Characteristics

It has been established that pavement characteristics affects traffic flow speeds and consequently the rate of fuel consumption (Svenson and Fjeld, 2016). The model road surface classification falls under paved or unpaved (Hammerstrom, 1995). Paved roads are further sub-divided into bituminous and concrete while earth roads represent the unpaved class (Hammerstrom, 1995). The data on road geometry, road surface condition, road section speed limit, and the fleet volume for motorised and non-motorised vehicles is also required (Odoki and Kerali, 2000). The road section undergoes different forms of deterioration during the analysis period caused by traffic volume and climatic conditions. These distresses can be predicted by mechanistic and empirical modelling approaches (Morosiuk et al., 2004).

Table 2. 2 Road Surface Classification (Morosiuk et al., 2004)

Bituminous	Concrete	Block *	Unsealed
Drainage	Cracking	Rutting	Gravel loss
Cracking	Joint Spalling	Roughness	Roughness
Ravelling	Joint Faulting	Surface Texture	
Potholing	Failures		
Edge Break	Roughness		
Rutting			
Roughness			
Texture Depth			
Skid Resistance			

* Not currently modelled in HDM-4

These damages can be described by road roughness on macro-scale as well as on micro-scale. On macroscale, road roughness is described by potholes, ruts, and cracks. While on microscale road roughness exist as the smoothness or roughness of the pavement surface texture (Noshadravan et al., 2013). The range of roughness values for each class of pavement has been shown below:

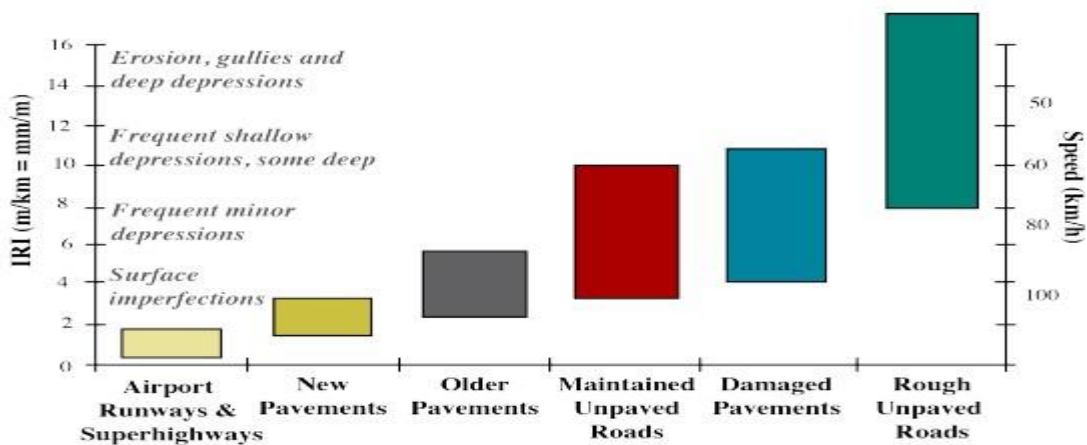


Figure 2. 3 International roughness index for various roads (Sayers, 1986)

The factors which trigger pavement deterioration include the type of construction material, construction quality, traffic volume, axle load characteristics, road geometry, environmental conditions, age of pavement, and maintenance policy pursued (Odoki and Kerali, 2000).

In Kenya, state agencies responsible for road management are main custodian of all road networks data nationally. They include Kenya Urban Roads Authority (KURA), Kenya National Highways Authority (KeNHA), and the Kenya Rural Roads Authority (KeRRA). The role of KURA is management, development, rehabilitation and maintenance of different roads in cities except the national roads (KURA, 2021). KeNHA and KeRRA are tasked with the development, rehabilitation, management and maintenance of all trunk roads and rural roads respectively (KENHA, 2021; KeRRA, 2021).

2.8.2 Traffic Characteristics

The Traffic composition play a key role in road deterioration, heavy vehicles such as trucks and buses cause more distress on road than cars (Chatti et al., 2004). The level of damage induced on a pavement is dependent on the weight of the vehicle. Detailed analysis on how each of these variable is modelled is presented in Volume-4 manual of the HDM-4 model (Morosiuk et al., 2004). This section describe the traffic data required in the model. The traffic representation in terms of categories, composition, volume and growth has been described in (Kerali et al., 1994). Both motorised and non-motorised vehicles are included in the model, the reason of non-motorised traffic is that it tends to affect traffic flow speeds which has impact on fuel consumption (Kerali et al., 1994).

Table 2. 3 Vehicle Categories Included in HDM-4 (Kerali et al., 2000)

Category	
Motorised	Motorcycle, small passenger car, medium passenger car, large passenger car, light delivery vehicle, light goods vehicle, four wheel drive, light truck, medium truck, heavy truck, articulated truck, minibus, light bus, medium bus, heavy bus, coach
Non-motorised	Pedestrian, bicycle, rickshaw, animal cart

2.8.3 Modelling Vehicle Speed

The vehicle flow speeds influence the rate of fuel consumption and subsequently affects vehicle exhaust emissions (Jaikumar et al., 2017). The modules for predicting vehicle speeds under different driving conditions are therefore included in the HDM-4. The speeds depend on vehicle specific characteristics, road geometry, road surface type and its current condition (Jaikumar et al., 2017). A travelling vehicle is associated with two types of speeds namely vehicle free speed and operating speed, unlike operating speed, free speed can be achieved on uncongested road (Eluru et al., 2013; Malaghan et al., 2020).

In the HDM-4 model, vehicle free speeds are predicted using mechanistic models. The assumption made is that the steady-state speed for each vehicle type k is a probabilistic minimum of five constraining speeds based on driving power, braking capacity, road curvature, surface roughness and the desired speed (Watanatada et al., 1987). The equations for estimating the uphill speed, downhill speed and the average round trip speed are described in Greenwood and Bennett (2003). The formulae for the uphill segment is;

$$VS_{ku} = \frac{\exp\left[\frac{\sigma^2}{2}\right]}{\left[\left(\frac{1}{VDRIVEu}\right)^{\frac{1}{\beta}} + \left(\frac{1}{VBRAKEu}\right)^{\frac{1}{\beta}} + \left(\frac{1}{VCURVE}\right)^{\frac{1}{\beta}} + \left(\frac{1}{VROUGH}\right)^{\frac{1}{\beta}} + \left(\frac{1}{VDESIR}\right)^{\frac{1}{\beta}}\right]^{\beta}} \quad (2.6)$$

Where:

VS_{ku} the predicted steady – state speed for uphill segment (ms^{-1})

$VDRIVEu$ the speed limited by gradient and used driving power for uphill section (ms^{-1})

$VBRAKEu$ the speed limited by gradient and used braking power for uphill section (ms^{-1})

$VCURVE$ the speed limited by curvature ($m s^{-1}$)

$VROUGH$ the speed limited by roughness ($m s^{-1}$)

$VDESIR$ the desired speed under ideal condition (ms^{-1})

σ SPEED_SIG Weibull model parameter

β SPEED_BETA Weibull model parameter

For the downhill segment, the speed prediction model takes the format below (Greenwood and Bennett, 1996):

$$VS_{kd} = \frac{\exp\left[\frac{\sigma^2}{2}\right]}{\left[\left(\frac{1}{VDRIVED}\right)^{\frac{1}{\beta}} + \left(\frac{1}{VBRAKED}\right)^{\frac{1}{\beta}} + \left(\frac{1}{VCURVE}\right)^{\frac{1}{\beta}} + \left(\frac{1}{VROUGH}\right)^{\frac{1}{\beta}} + \left(\frac{1}{VDESIR}\right)^{\frac{1}{\beta}}\right]^{\beta}} \quad (2.7)$$

Where:

VS_{kd} the predicted steady state speed for the uphill segment ($m s^{-1}$)

$VDRIVED$ the speed limited by gradient and used driving power for uphill section ($m s^{-1}$)

$VBRAKED$ the speed limited by gradient and used braking power for uphill section ($m s^{-1}$)

$VCURVE$ the speed limited by curvature ($m s^{-1}$)

$VROUGH$ the speed limited by roughness ($m s^{-1}$)

$VDESIR$ the desired speed under ideal condition ($m s^{-1}$)

σ SPEED_SIG Weibull model parameter

β SPEED_BETA Weibull model parameter

2.8.4 Traffic Congestion modelling

The speed-flow model in HDM-4 is shown in (figure 2.4), all variables bear the same meaning as in Hoban et al. (1994):

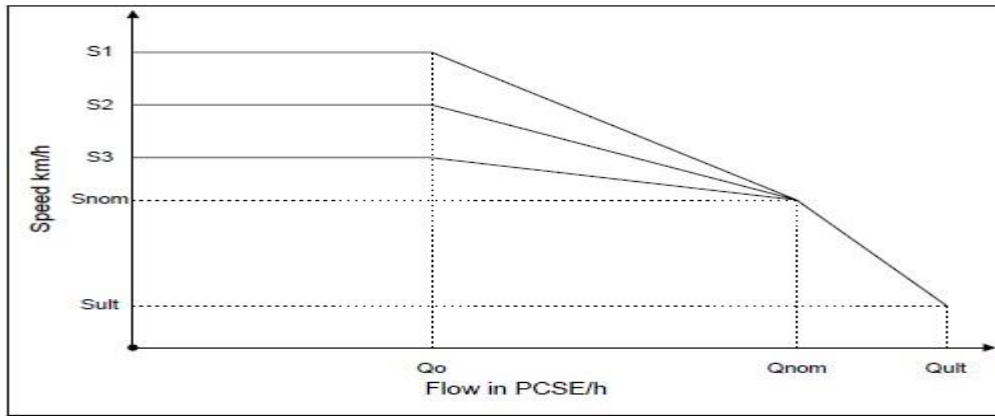


Figure 2. 4 Speed flow model in HDM-4 (Hoban et al., 1994).

Free flow speed

Traffic volume is key to the vehicle speed-flow, therefore traffic congestion model simulate vehicle speeds for different states of traffic loading. According to the model, a critical traffic volume exist below which traffic interactions are insignificant and all vehicles travel at their free speeds (Hoban et al., 1994). When traffic interactions sets in, the speeds for the individual vehicles decrease until the nominal capacity where all vehicles will be travelling at the same speed (Hoban et al., 1994). A further reduction in speeds can occur towards the ultimate capacity beyond which unstable flow will arise.

Congested speeds

Increased traffic flow lead to high vehicle interactions which then results to a reduction in speed. This reduced speed is modelled as the steady-state congested speed which is determined by the traffic flow period for both the uphill and the downhill segments(Bennett and Greenwood, 2003) . For the Uphill segment, the model equation takes the form below:

$$VU_{kp} = \text{MAX}(VU_{kp} * \text{CALIBFAC}, VSult) \quad (2.8)$$

Where:

VU_{kp} steady state congested speed of vehicle of type k during period p for uphill section (ms^{-1})

CALIBFAC speed calibration factor

$VSult$ is obtained by dividing $Sult$ by a factor of 3.6

Speed for Downhill segment

The steady-state speed for each traffic flow period is modelled using the equation presented below:

$$VD_{kp} = \text{MAX}(VD_{kp} * \text{CALIBFAC}, VS_{ult}) \quad (2.9)$$

Where:

VD_{kp} steady state congested speed of vehicle type k during period p for the uphill section (m s^{-1})

CALIBFAC speed calibration factor

VS_{ult} is obtained by dividing S_{ult} by a factor of 3.6

Round trip congested speed

The average steady-state congested speed for a round trip (km h^{-1}) at each flow period p and flow Q_p is predicted by the equation presented below (Odoki and Kerali, 2000):

$$S_{kp} = \left\{ \frac{7.2}{\left[\left(\frac{1}{VU_{kp}} \right) + \left(\frac{1}{VD_{kp}} \right) \right]} \right\} \quad (2.10)$$

Where:

S_{kp} average steady state congested speed (km h^{-1})

Vehicle operating speed

This speed is calculated by multiplying congested speeds described above by speed-bias factors. The steady-state vehicle-operating speed is therefore calculated as follows:

$$SS_{kp} = S_{kp} * \text{SPEEDBIAS} \quad (2.11)$$

Where;

SS_{kp} vehicle operating speed (km h^{-1})

S_{kp} steady state congested speed (km h^{-1}) for traffic flow period p

SPEEDBIAS speed adjustment factor to account for the bias introduced through the use of the time mean speed instead of space mean speed. where each of the variable is described in detail in Volume-4 manual of the HDM-4.

2.8.4 Fuel Consumption

Fuel consumption is a significant factor which influence vehicle exhaust emissions. Fuel consumption modelling is based on mechanistic approach, assumption being that vehicle fuel

consumption is directly proportional to the total power requirements of the engine which include tractive power, engine drag, and accessory power (Biggs, 1988; Kerali et al., 2000). Fuel consumption for a specific vehicle type is estimated by computing the vehicle uphill and downhill separately which is then averaged to obtain the fuel consumed for a round trip over the road section (Zaabar and Chatti, 2010). The instantaneous fuel consumption for the downhill for a specific vehicle type k during traffic flow period p was described by Bennet and Peterson (2003) as shown:

$$IFC_{kpu} = \text{MAX}[\text{IDLE}_{\text{FUEL}_k}, \text{ZETA}_{kpu} * \text{PTOT}_{kpu} * (1 + \text{dFUEL}_{kpu})] \quad (2.12)$$

The fuel consumption for the downhill segment is estimated using the equation below:

$$IFC_{kpd} = \text{MAX}[\text{IDLE}_{\text{FUEL}_k}, \text{ZETA}_{kpd} * \text{PTOT}_{kpd} * (1 + \text{dFUEL}_{kpd})] \quad (2.13)$$

Where:

IFC_{kpd} instanteneous fuel consumption m/s

$\text{IDLE}_{\text{FUEL}_k}$ idle rate of fuel consumption (ml s^{-1})

ZETA_{kpd} uphill fuel to power efficiency factor of vehicle type k ($\text{ml kW}^{-1} \text{s}^{-1}$)

PTOT_{kpd} uphill total requirement for steady state motion (kW)

dFUEL_{kpd} additional fuel consumption factor due to vehicle speed change cycles

The specific fuel consumption (ml) per vehicle-kilometre on a particular road section was developed by Biggs (1988)

$$\text{SFC}_{kp} = 500 \left[\frac{\text{IFC}_{kpu}}{\text{VU}_{kp}} + \frac{\text{IFC}_{kpd}}{\text{VD}_{kp}} \right] \quad (2.14)$$

Where:

SFC_{kp} specific fuel consumption (ml km^{-1})

IFC_{kpu} instanteneous fuel consumption for uphill travel (ml s^{-1})

IFC_{kpd} instanteneous fuel consumption for downhill travrl (ml s^{-1})

VU_{kp} uphill speed (m s^{-1}) of vehicle type k in traffic flow period p

VD_{kp} downhill speed (m s^{-1})

The annual fuel consumption for a specific vehicle type is reported in litres per 1000 vehicle kilometre as shown (*symbols explained in HDM-4 Calibration manual Vol. 4*) (Biggs, 1988; Kerali et al., 2000):

$$FC_{kav} = \frac{\sum_{p=1}^n HRYR_p \times HV_p \times FC_{kp}}{\sum_{p=1}^n HRYR_p \times HV_p} \quad (2.15)$$

2.9 Calibration of Vehicle Emission Models

The model must be properly calibrated before any modelling activity is undertaken (Bennett and Paterson, 2002). The ability to calibrate the HDM-4 model relies on the type of application, resources and time available to the user (Bennett and Paterson, 2002). **Level 1** calibration was undertaken in this study. This was a desk study based on data collected from secondary sources such as government agencies (KURA, NTSA), industrial publications, operator organizations or various RUE reports from previous studies (Bennett and Paterson, 2002). The default variables that were adjusted in this study are shown in Appendix A. **Level 2** and **Level 3** were beyond the scope of the study since they involve major field surveys and research to improve data collection, therefore they were not possible at this stage. The HDM4 calibration was carried out by adjusting the default coefficients contained in the exhaust emissions model. The model was run with the adjusted coefficients and the exhaust emissions output compared against the Edgar-DICE emission inventory. The DICE Africa emissions inventory was developed for the year 2013 (Marais and Wiedinmyer, 2016) while the Edgar-v4.3.2 global emission inventory was developed for the year 2012 (Crippa et al., 2018). They were merged in similar procedure as that of Marais and Wiedinmyer (2016), to generate a new inventory (Edgar-DICE) emissions.

2.10 Format of Vehicle Emission Models in HDM-4

The HDM-4 emission models compute quantity of each emission component (CO, CO₂, NO_x, SO₂, PM_{2.5}) separately (Bennett and Paterson, 2000). The exhaust emissions are predicted based on vehicle fuel consumption (Tong et al., 2000). The total annual emission of each component is obtained by summing over the contribution of each vehicle type (Bennett and Greenwood, 2003). In general, vehicle emissions can be directly related to changes in pavement conditions, traffic characteristics as well as vehicle technology (Wang et al., 2014). The CO₂ emissions was calculated from carbon balance assumptions (Bennett and Greenwood, 2003). The engine out emissions are acted by catalytic converter (if present) to

yield tailpipe emissions which is then released into the environment. Below is the format of the model catalytic converter as described by An et al. (1997)

$$TPE_i = EOE_i * CPF_i \quad (2.16)$$

and

$$CPF_i = [1 - \varepsilon_i \exp(-b_i IFC \text{ MassFuel})] \min \left[\left(1 + \frac{r_i}{100} AGE \right), MDF_i \right] \quad (2.17)$$

The quantities of CO, SO₂, NO_x, HC, PM_{2.5}, and CO₂ are predicted as follows (Bennett and Greenwood, 2003)

Carbon Monoxide model

It is based on the rate of fuel consumption and engine out emissions which are directly related (An et al., 1997):

$$EOE_{CO} = a_{CO} \times FC \quad (2.18)$$

EOE_{CO} engine out carbon monoxide emission in grams per vehicle kilometre
ratio of engine out emission per gram of fuel consumed for emission CO

FC is the fuel consumption (including congestion effects) in g km⁻¹

Sulphur Dioxide model

Its formulation is based on the assumption that the amount of SO₂ emitted is related directly to the quantity of sulphur present in the fuel (Bennett and Greenwood, 2003). The engine out emissions for SO₂ is therefore presented as (Bennett and Greenwood, 2003)

$$EOE_{SO_2} = 2a_{SO_2} FC \quad (2.19)$$

EOE_{SO₂} engine out sulphur dioxide emission in grams per vehicle kilometre

a_{SO₂} ratio of engine out emission per gram of fuel consumed for emission SO₂

Nitrous oxide model

The relationship used to model NO_x component of exhaust emission is described below (An et al., 1997):

$$EOE_{NO_x} = \max \left[a_{NO_x} \left(FC - \frac{FR_{NO_x}}{V} \right), 0 \right] \quad (2.20)$$

Where:

EOE_{NO_x} engine out nitrous oxide emissions in grams per vehicle kilometer

a_{NO_x} ratio of engine out emissions per gram of fuel consumed for emission NOx

FR_{NO_x} the fuel threshold below which NOx emission are very low

Hydrocarbons model

The model for predicting engine out emission takes the format below (Bennett and Greenwood, 2003):

$$EOE_{HC} = a_{HC}FC + \frac{r_{HC}}{V} 1000 \quad (2.21)$$

and

$$FC = \frac{IFC \text{ MassFuel } 1000}{V} \quad (2.22)$$

EOE_{HC} is the engine out hydrocarbon emission in grams per vehicle kilometer

a_{HC} is the ratio of engine out emission per gram of fuel consumed for emission HC

r_{HC} is a constant to account for incomplete combustion in gs^{-1}

IFC instantaneous fuel consumption $ml s^{-1}$

FC is the fuel consumption in $g km^{-1}$

v is the vehicle speed in ms^{-1}

MassFuel is the mass of fuel in $g mL^{-1}$

Each coefficient hold the same meaning as described by (Bennett and Greenwood, 2003)

Particulates model

The model for particulate emissions (PM2.5) takes the format below (Bennett and Greenwood, 2003):

$$EOE_{PM2.5} = a_{PM2.5}FC + \frac{r_{PM2.5}}{V} 1000 \quad (2.23)$$

Where:

EOE_{PM} engine out particulate emissions in grams per vehicle kilometres

$a_{PM2.5}$ ratio of engine out emissions per gram of fuel consumed for emission PM2.5

FC is the fuel consumption (including congestion effects) in $g\ km^{-1}$

r_{HC} is a constant to account for incomplete combustion in $g\ s^{-1}$

v is the vehicle speed in ms^{-1}

Carbon Dioxide

This model is described in HDM-4 *Manual Volume-4* (Bennett and Greenwood, 2003):

$$TPE_{CO_2} = 44.011 \left[\frac{FC}{12.011 + 1.008 a_{CO_2}} - \frac{TPE_{CO}}{28.011} - \frac{TPE_{HC}}{13.018} - \frac{TPE_{PM2.5}}{12.011} \right] \quad (2.24)$$

TPE_{CO_2} tail pipe carbon dioxide emissions in grams per vehicle kilometer

a_{CO_2} fuel dependent model parameter representing the ratio of hydrogen to carbon atom in the fuel

2.11 Summary

The sparse air quality datasets collected from short monitoring campaigns have shown levels of air quality which exceed the WHO guidelines. The situation is only likely to worsen due to high cost of acquiring and maintaining air quality monitors which has proved unaffordable to most developing cities like Nairobi. There is need for air quality data of good spatial and temporal resolution upon which policies and regulation of air quality can be based on. The vehicle emission models in HDM-4 and Sentinel 5P tropospheric measurements provide information regarding atmospheric emissions which can be exploited to studies air quality. Properly calibrated HDM-4 emission models have been shown to model vehicle emissions with reasonable degree of accuracy. Sentinel 5P provide long term measurements of atmospheric pollutants at high resolution, thus making it possible to study air quality at city scale.

CHAPTER THREE

METHODOLOGY

3.0 Customization and Calibration of HDM-4 Model v2.0

The HDM-4 model is a commercial software distributed by HDMGLOBAL, the software was downloaded and installed in Windows 10 laptop computer. The licence was acquired through ASAP (*A Systems Approach to Air Pollution*) project of East Africa. The disk space required to run the program files was about 50MB.

The data for pavements, vehicle fleet, maintenance standards, and model configuration parameters within Nairobi county was collected from secondary sources. The data was manually obtained from KURA (Kenya Urban Roads Authority KURA) Nairobi road networks data and Nairobi AADT data.

The key variables extracted from the data were classified into two broad categories namely pavement physical characteristics and pavement geometry. The road physical characteristics included road section name, identification code, carriage width, shoulder width, length, speed flow type, directions of flow, surface class, last surfacing, traffic flow pattern, climate zone, traffic and last construction year. The inputs for pavement geometry included road curvature, pavement gradient, number of rise and falls (Appendix A).

Another information also obtained from KURA was the Nairobi Annual Average Daily Traffic (AADT) data. The vehicle classes in the data included motorcycles, passenger cars, 14-seater vans (Matatus), small bus, medium bus, small trucks, medium trucks, Heavy trucks, articulated trucks, and others. The AADT for each road section was also contained in this data. Thirteen road networks were generated from this data and defined in the **Road Network** data manager of the HDM-4 model. Each network was built from multiple sections of road and the model input parameters for the sections summarised in Appendix A. The rate of traffic growth for each class of vehicles and along different road categories were manually obtained from a draft report by the Kenya Roads Board (Appendix B).

The vehicle fleet data was also obtained upon request from KURA. It contained information in terms of Annual Average Daily Traffic (AADT). The classes of vehicles in this data included motorcycles, passenger cars, small buses, large buses, light trucks, medium trucks, heavy trucks, and articulated trucks. The model default values were used for the PCSE, number of wheels and operating weight. The vehicle mileage, average life and operating

weight (Appendix C). The fleet was defined in the **Vehicle Fleet** data manager of the HDM-4 and for modelling.

Then calibration of Engine Output models involved adjustment of default emission coefficients for HC, CO, NO_x, SO₂, and PM_{2.5}. The model was run repeatedly with the adjusted factors, each time comparing the agreement of output emissions with the Edgar-DICE emissions. **Level 1** calibration of Engine output models was achieved this way.

3.1 Sensitivity Test

The vehicle exhaust emissions have been shown to depend on vehicle physical parameters, road characteristics as well as traffic characteristics (Prasad et al., 2013a). Thirty-five Input variables that influence exhaust emissions were identified, sixteen were engine related, four vehicle physical inputs, while the rest constituted road geometric and traffic characteristics. The engine related variables were beyond the scope, therefore they were dropped from this analysis.

The variables considered in this analysis included vehicle average life, vehicle operating weight, vehicle number of wheels, PCSE, pavement roughness, pavement carriage width, number of rise and falls, average rise and fall, speed reduction of motorised traffic due to non-motorised traffic (XNMT), speed reduction of motorised traffic due to roadside activities (XFRI), pavement curvature, the altitude and speed limit. Fourteen simulations were run to generate random Latin Hypercube Samples (LHS), this technique is documented in the work of Prasad et al. (2013a). A rectangular grid of 14 x13 sample points was thus generated, each sample acting as a single data point (Sheikholeslami and Razavi, 2017). The Spearman's rank correlation coefficient was computed for these inputs. The degree to which these variables impact on the components of vehicle emissions i.e. HC, CO, SO₂, NO_x, was hence visualized as Tornado plots.

3.2 Modelling Annual Exhaust Emissions

This simulation was done through *project analysis* which is incorporated in the HDM-4. A project was created for each road network used in the model. The duration of simulation was taken to be one year. Then model was run and the output was in form of a report which had information on traffic, Deterioration and Work Effects, Road User Effects, and Environment Effects. This was repeated for the thirteen road networks, and the output analysed for vehicle exhaust emissions.

3.3 Effects Traffic Growth on Vehicle Exhaust Emissions

Integrated in the HDM-4 are powerful tools for investigating the role of future economic development on exhaust emissions. Due to the ever increasing population, construction of new roads and expansion of existing networks, the on-road traffic is bound to increase. It is therefore necessary to investigate the impacts on Nairobi air quality. Three test scenarios were set to carry out this analysis. They included High, Base, and Low traffic growth scenarios.

This analysis was conducted for a period of twenty years starting from 2020. The annual traffic growth for that year was 14% which was adopted from (Notter et al., 2019). Three test scenarios (Base, High and Low traffic growth scenarios) were set in order to investigate variations in vehicle emissions, fuel consumption, and the road surface condition. By taking the Base traffic growth scenario as 100%, the High and Low traffic growth scenarios were generated by adding and subtracting 14% to the Base scenario respectively. The multiplication factors for the High, Low and Base scenarios were 1.14, 0.86, and 1 respectively. The pavement maintenance activities defined for the analysis included potholing, crack sealing and overlay. The output of this simulation was in form of a report containing information on traffic growth, average fuel consumption, average traffic operating speeds, and the pavement deterioration in form of the roughness index (IRI). The relationship of these parameters with the vehicle tailpipe emission analysed and presented in results.

3.4 Mapping NO₂ Concentration Over Nairobi

The TROPOMI is air quality detector on-board the Sentinel 5P satellite. The air quality data acquired by TROPOMI detector is stored in the Copernicus website (Guzonato et al., 2020). Two data streams are available from this detector namely the Near Real Time (NRTI) and the Offline (OFFL) data products. The NRTI product is available a few hours after it has been sensed by the satellite. It is considered raw data and therefore data processing is required for research. The OFFL product is processed and quality assured. It is made available after a few days and is therefore recommended for research. In this study, Level 2 data product was used. The NO₂ tropospheric column data was retrieved for the spatial grid with longitude/latitude points shown below.

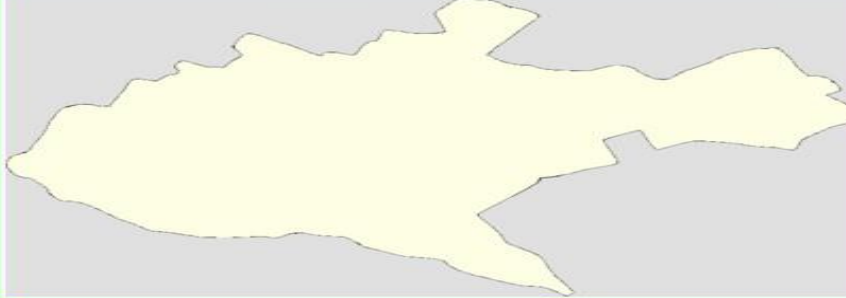
name	Nairobi		
border coordinates	-1.17		
	36.67	←↕→	37.21
	-1.46		
map center	🌐 1.315°S 36.94°E		
image	Nairobi_location_map.png		
			

Figure 3. 1. Illustrates the horizontal grid over which NO₂ tropospheric column data was retrieved (source:(Wikipedia, 2018).

Random days were chosen depending on availability of the satellite image. A single TROPOMI orbit contains datasets stored in fourteen granules. The granule cutting through the grid shown in figure 3.1 was selected and downloaded. Data processing and visualization was done using python programming language which has highly advanced software tools for analysis for geospatial analysis. The data was filtered for contaminants such as clouds and snow cover, all pixels with quality assurance values less than 75% were therefore removed.

CHAPTER FOUR

RESULTS AND DISCUSSION

4.0 Sensitivity Test Results

The Spearman's Rank Correlation coefficient of the model input variables were determined and visualized as Tornado plots (Figure 4.1). The variables whose value of the Spearman's rank correlation coefficient was equal to one or negative one had the highest impact on that particular pollutant, while that having a value closer to zero is least significant. The variable with a positive value of Spearman's Rank Correlation coefficient indicates a direct relationship with that particular pollutant, the opposite is true to variables with a negative sign.

The two variables which showed significant influenced on CO emissions were vehicle life and road surface roughness. The carriage width of the road section, number of rise and falls, and the number of wheels of the vehicle showed a strong negative influence. For HC emissions, road section rise and fall, and vehicle operating weight showed strong positive effect. On the other hand, road carriage width and the vehicle number of wheels had strong negative impact. The vehicle life and operating weight was reported to impact directly on NOx emissions while section carriage width and the number of rise and falls had negative effects on these emissions. The vehicle life had major impact on PM2.5 emissions which on the other hand was affected negatively by road section curvature.

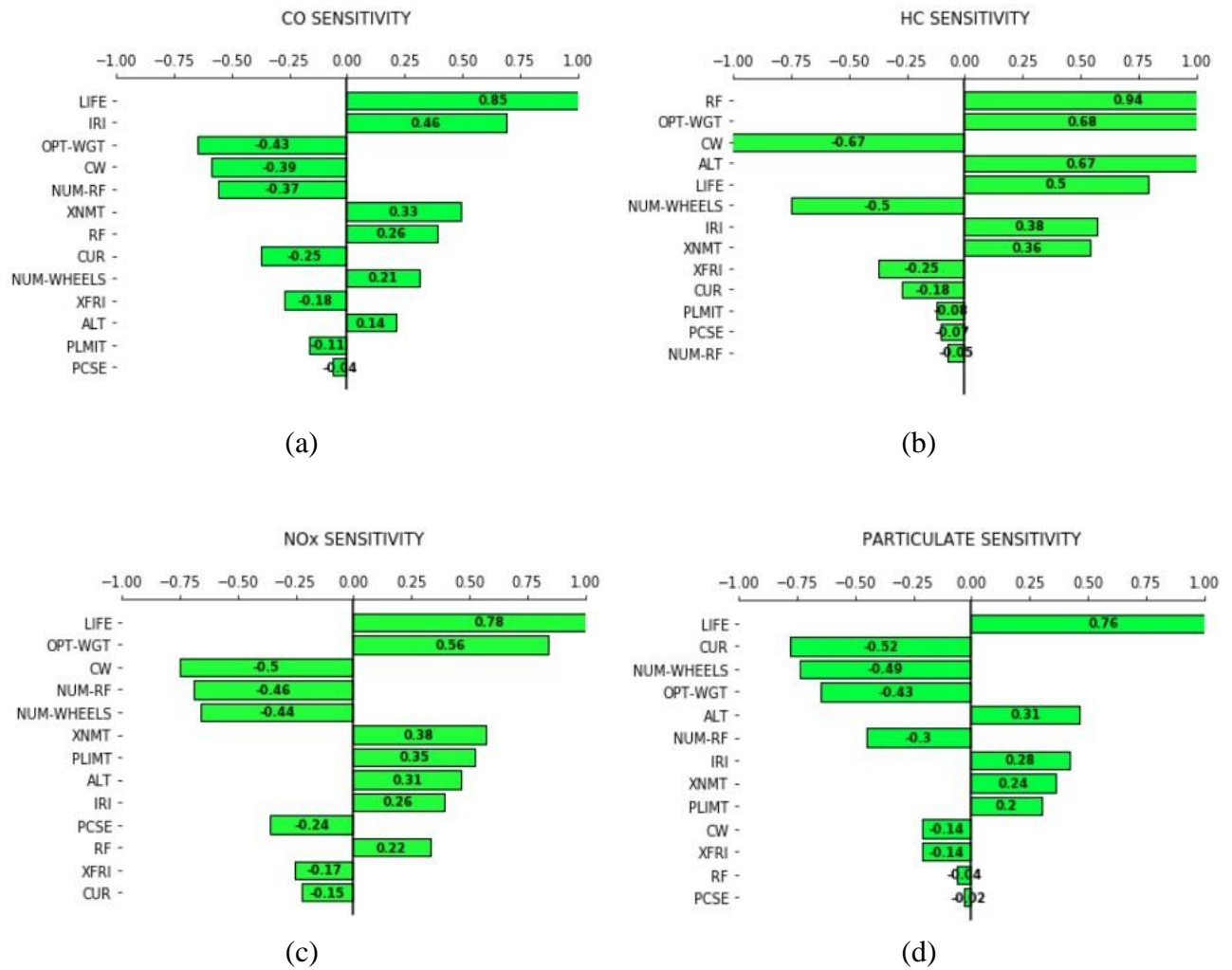


Figure 4. 1 Tornado plots showing sensitivity of the model input variables to (a) CO, (b) HC, (c) NO_x, and (d) PM_{2.5} emissions.

4.1 Modelled Exhaust Emissions

The vehicle exhaust emissions were modelled using un-calibrated and calibrated forms of the model (Figure 4.2). The un-calibrated model had weak emissions prediction power which resulted to the huge margins between HDM-4 and Edgar-DICE exhaust emissions.

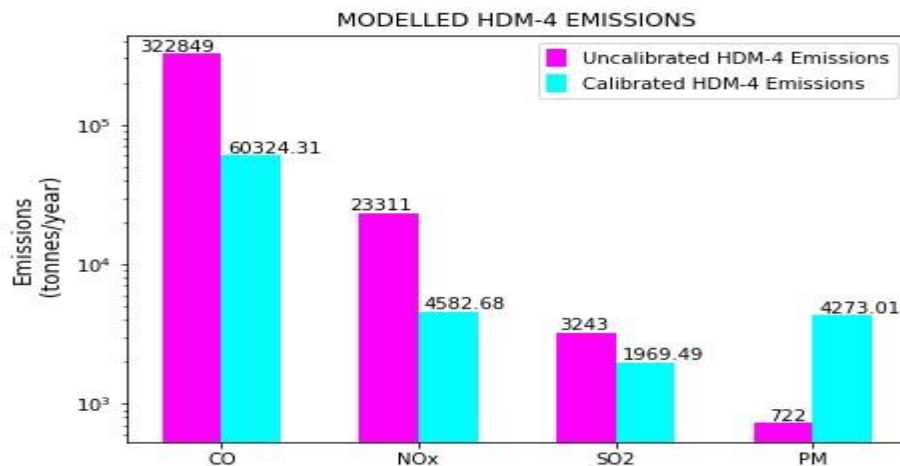


Figure 4. 2 Comparison of un-calibrated HDM-4 exhaust emissions Edgar-DICE emissions.

Figure 4.3 illustrates the exhaust emissions from calibrated HDM-4 model and the Edgar-DICE. A huge difference was observed between modelled SO₂ and the Edgar-DICE SO₂ emissions which was attributed to a bug in the model. The Edgar-DICE emissions has been validated for PM_{2.5} relative to the impact of primary emissions. However, it has not been done for gaseous pollutants which might explain the huge difference between the two sets of emissions. It was found that road transport contributed approximately 4273 tonnes of PM_{2.5} emissions annually. Its significance to air quality in Nairobi has been underscored in previous studies. Pope et al. (2018) showed that motorised traffic was the dominant source of emissions in the city contributing approximately 48.1%, 47.5% and 57.2% of PM₁₀, PM_{2.5} and PM₁ respectively. Mukaria et al. (2017) recorded concentrations ranging from 124.3 μg m⁻³ to 45.0 μg m⁻³, 45.0 μg m⁻³ at Railways Roundabout and University Way Roundabout respectively. Shilenje et al. (2016) recorded extremely high levels of BC along Landhies Road. It was further noted that exhaust emission was bound to increase owing to huge fleet of old and poorly maintained vehicles.

Until now, limited studies exist which concern monitoring of pollutant gases in Nairobi. Shilenje et al. (2016) reported SO₂, CO, and O₃ concentration along Ladhies road, Nakumatt junction, and Pangani Roundabout. For the four sampling locations, SO₂ and O₃ concentrations were below their respective WHO recommendations. The mean CO in all sites was above the background concentration 0.05-0.12 ppm. It was however pointed out that lack of instrument calibration could limit the accuracy of recorded results. Although the results were not directly comparable to air quality reporting standards, it provided useful insights on the role of traffic emissions to air pollution in the study area. Emission fluxes derived from

the study form important component of urban emissions that can be used in chemistry transport models to predict air quality.

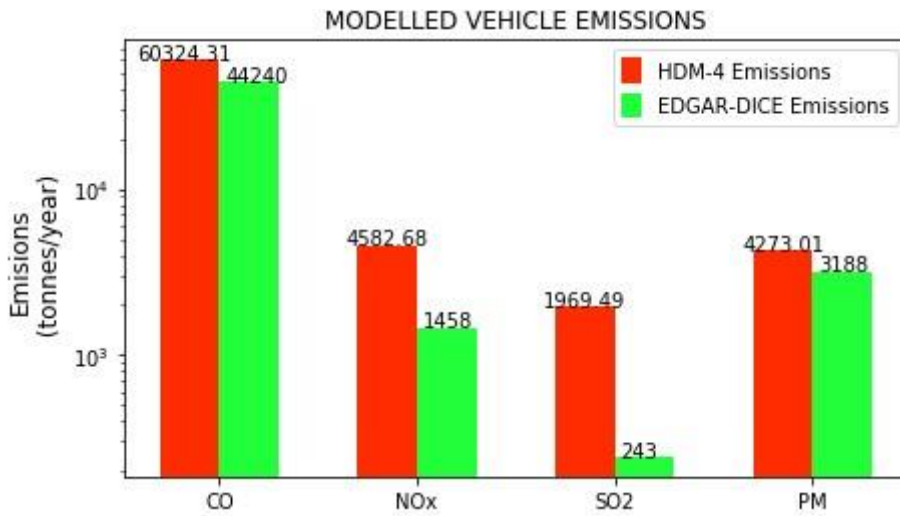


Figure 4. 3 Illustrates comparison between HDM-4 and Edgar-DICE emissions

4.2 Results of Change in Exhaust Emissions Due to Traffic Growth

The High, Base and Low traffic growth scenarios were analysed for nine major road networks. For each network, the road surface condition (IRI), average vehicle operating speeds were analysed to understand their influence on vehicle exhaust emissions

4.2.1 Jogoo Road Results

Figure 4.4 (a) illustrates changes in road surface roughness, and (b) is the respective change in vehicle average speed for the three analysis scenarios. This increase in IRI signified poor road surface condition which was likely to impact on vehicle operating speeds 4.4 (b). Low vehicle operating speed is associated with high fuel consumption, therefore causing more exhaust emissions.

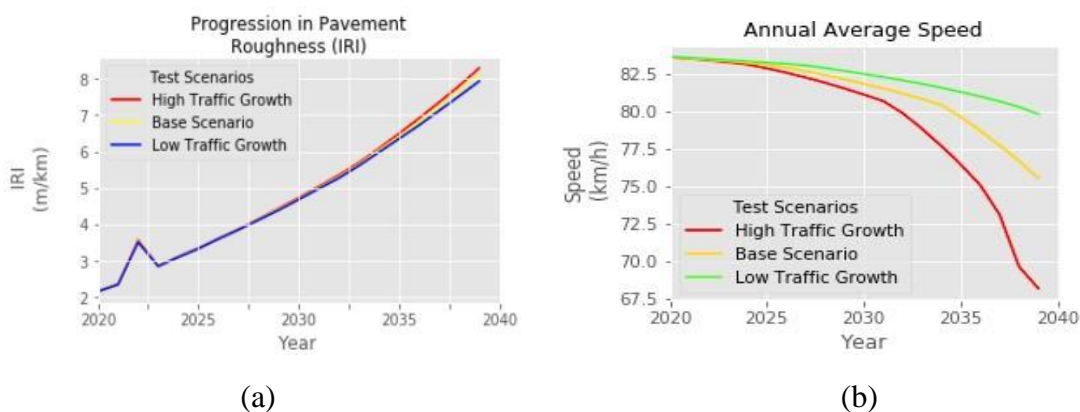


Figure 4. 4 (a). Shows variation in IRI and (b) is the vehicle operating speed.

Fuel Consumption

Figure 4.5 illustrates the annual average vehicle fuel consumption for trucks, buses, passenger cars, and motorcycles. It was observed that vehicle fuel consumption followed fleet operating speed. Therefore, at speed of 82.5 km/hr, fuel consumption was lowest except for the motorcycles which is not affected by traffic congestion. Generally, fuel consumption increased for all test scenarios. It was however significant for High traffic growth scenario thus causing more exhaust emissions.

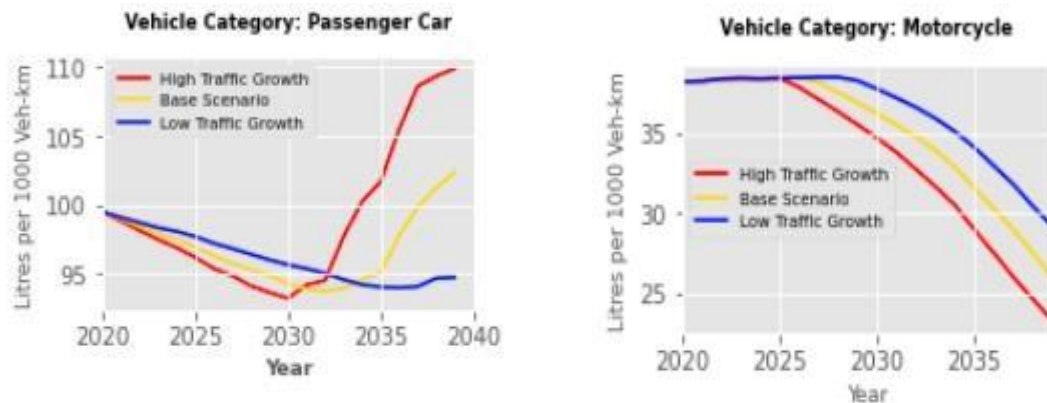
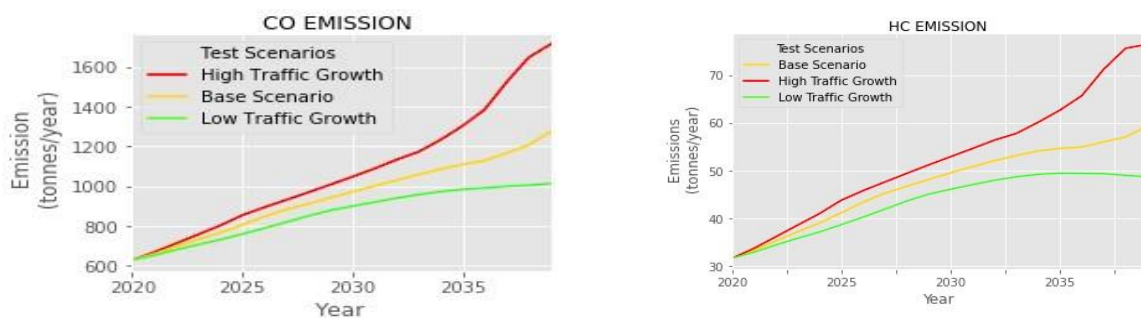


Figure 4. 5 The modelled annual average fuel consumption for Jogoo road

Modelled Vehicle Exhaust Emissions for Jogoo Road

The exhaust emissions in form of CO, HC, PM, SO₂, and NO_x was modelled and presented in figure 4.6. For all components of exhaust emissions, the quantities were highest in the High Traffic Growth scenario followed by the Base scenario and the Low Traffic Growth. The High and the Low Traffic Growth scenarios were evaluated against the Base scenario. The modelled CO, HC, SO₂, NO_x and PM_{2.5} increased by 14%, 12%, 17%, 14% and 10% respectively for the High Traffic Growth scenario. Similarly, these emission components decreased by 9%, 8%, 12%, 9% and 9.4% respectively for the Low Traffic Growth scenario.



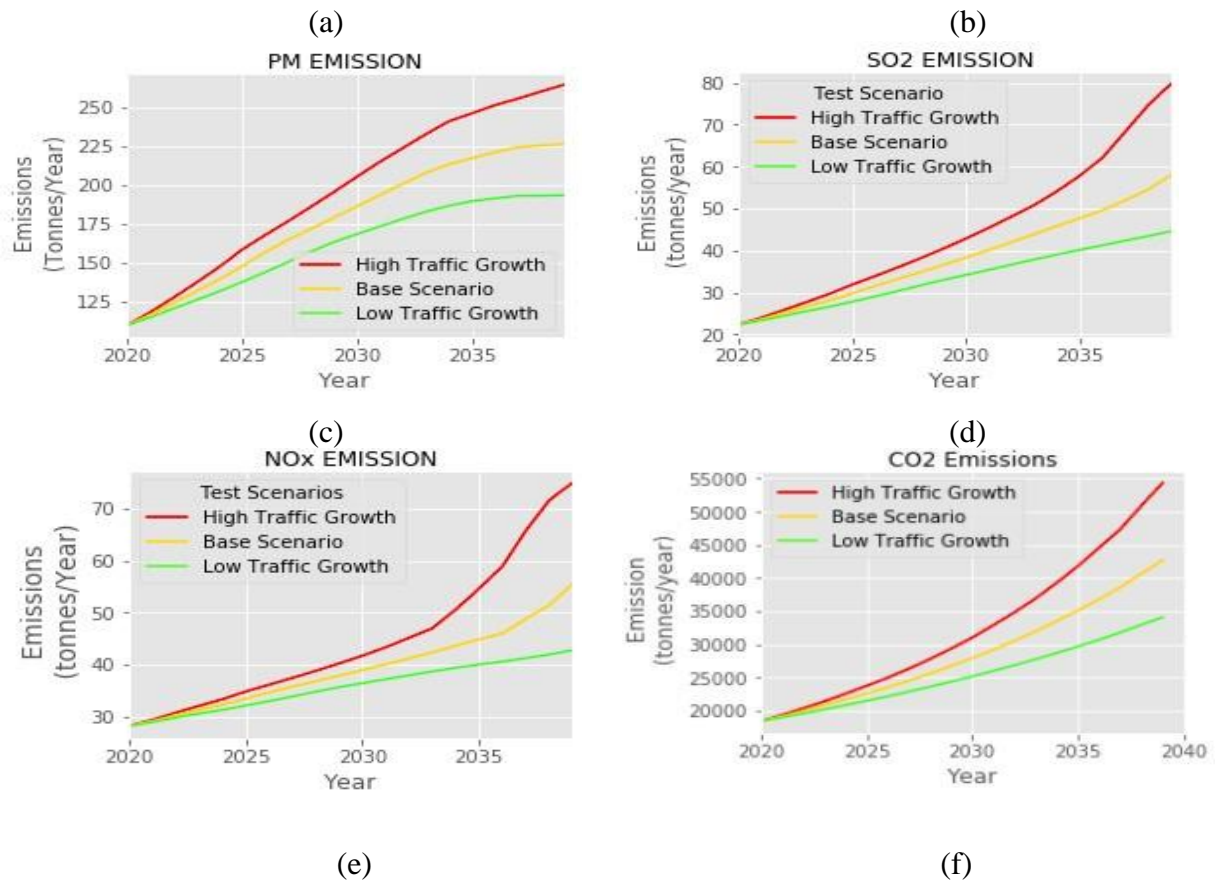


Figure 4. 6 Illustrates the modelled exhaust emissions for Jogoo road

4.2.2 Mombasa Road Results

The road surface condition, vehicle operating speeds, and emissions for Mombasa road was modelled, analysed and reported in Figure 4. 7. A sharp rise in road surface roughness was observed for the high traffic growth which signified faster rate of deterioration, the opposite was true for the low traffic growth. The high level of traffic experienced during the high traffic growth resulted in congestion which gradually slowed vehicle operating speed. The reduction in traffic speeds from 87 km/hr to 77 km/hr and from 87km/hr to 80km/hr was noted for the high and the low traffic growth scenarios respectively.

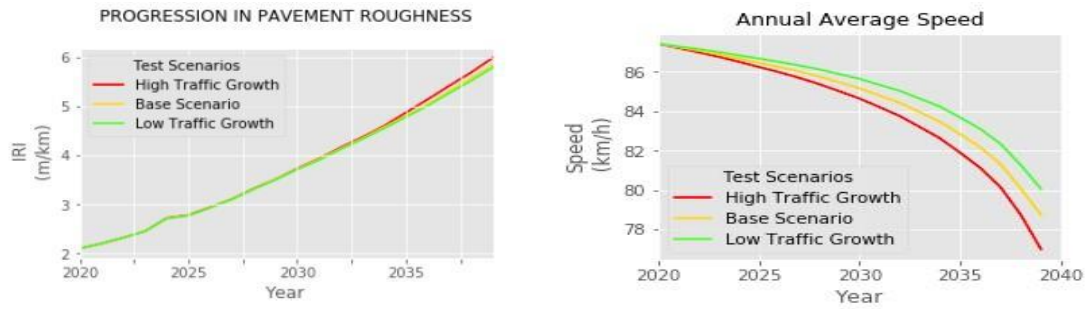


Figure 4. 7 (a) Variation in pavement IRI and (b) are the changes in annual average operating speed.

Fuel consumption

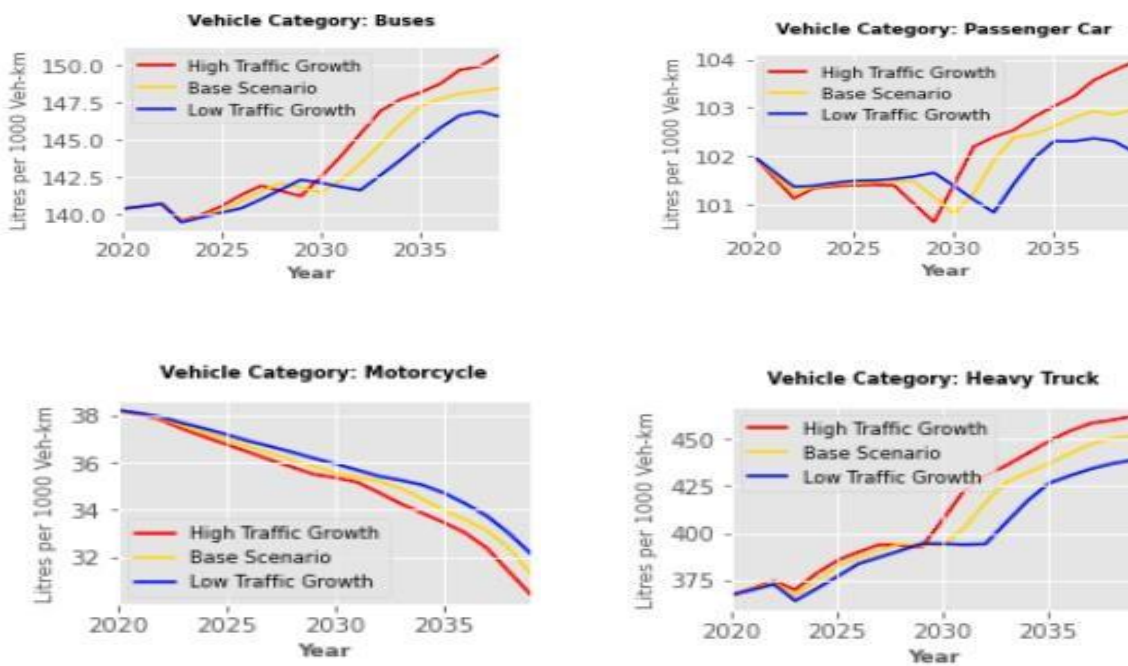


Figure 4. 8 Shows the modelled annual average fuel consumption for Mombasa road

Modelled Vehicle Exhaust Emissions for Mombasa Road

The results of vehicle exhaust emissions for Mombasa road was presented in figure 4.9. The five components of emissions showed a general increasing trend throughout the simulation period. For CO emissions, an increment of approximately 9% was reported for the high traffic growth scenario while a reduction of approximately 8% was observed during the low traffic growth scenario. For HC, an increment of approximately 9% was noted during the high traffic growth scenario which then reduced by almost 8% for the low traffic growth scenario. PM emissions increased by approximately 12% during the high traffic growth

scenario while it reduced by approximately 11% during the low traffic growth scenario. The quantity of NO_x increased by 6% for the high traffic growth scenario, however this reduced by 5% for the low traffic growth scenario.

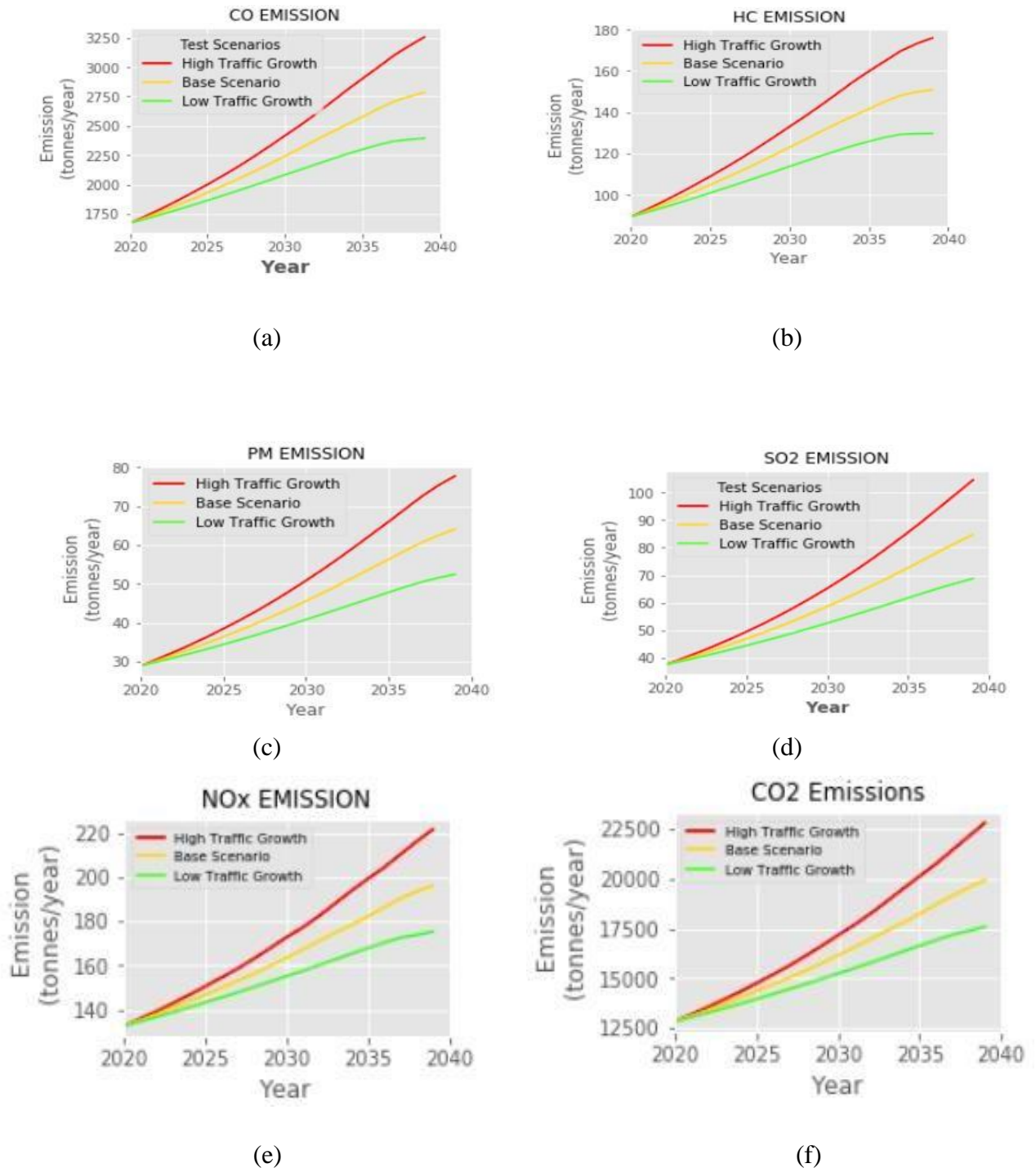


Figure 4. 9 Predicted exhaust emissions for Mombasa road

4.2.3 Ngong Road Results

Analysis of road surface roughness, vehicle operating speed and emissions for Ngong road was reported in this section. The results showed a sharp rise in pavement roughness at the

start of analysis which was altered by pavement maintenance. The variations in the road condition and the growth in traffic volume along this road section has subsequent effect of reducing the average vehicle operating speeds (figure 4.10 (b)). Consequently, the traffic operating speeds affect the rate of fuel consumption and consequently the vehicle emissions.

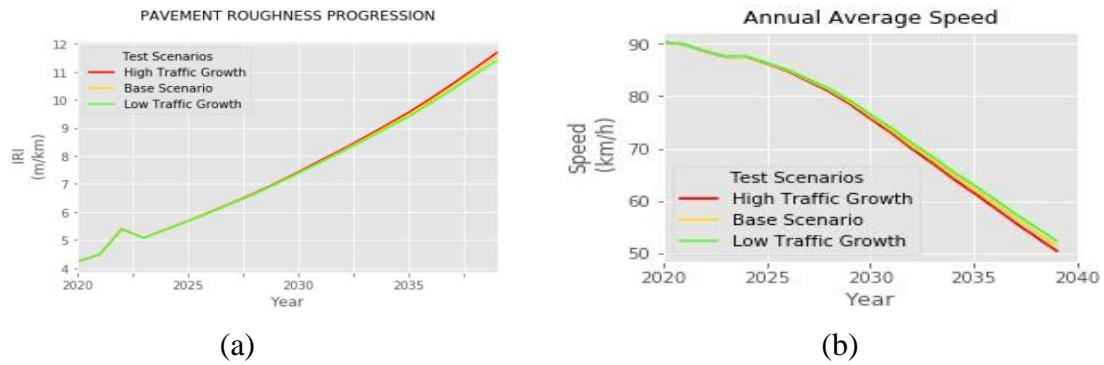
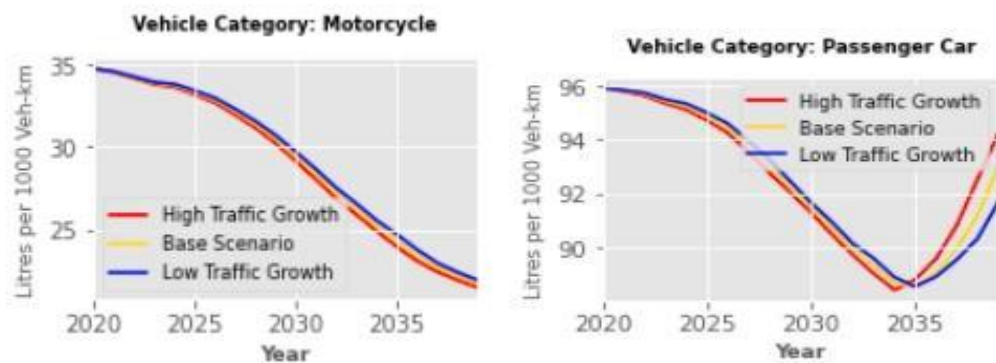


Figure 4. 10 (a) Illustrates predicted pavement surface condition (IRI) and (b) is the annual average vehicle operating speed.

Fuel consumption



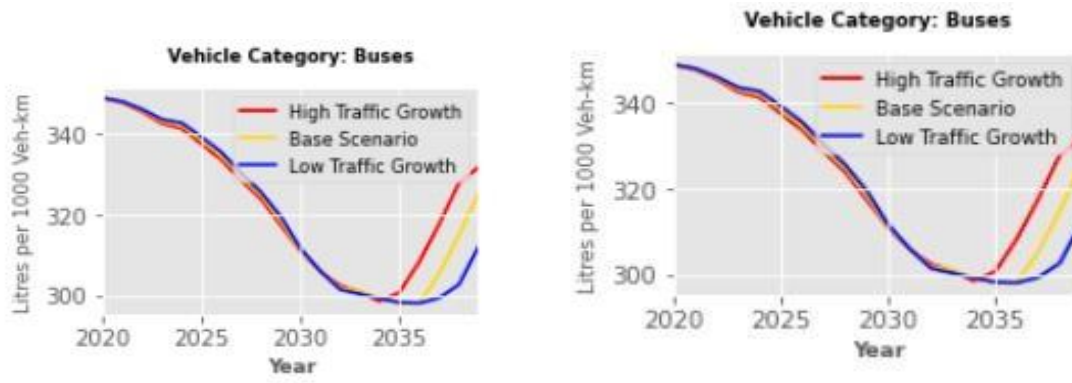
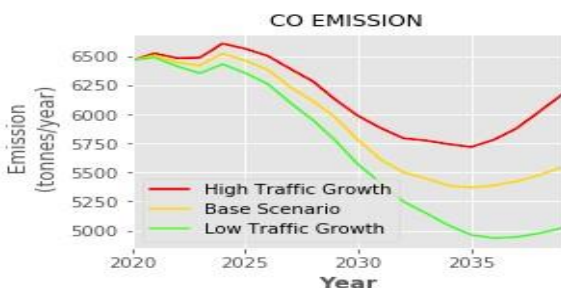


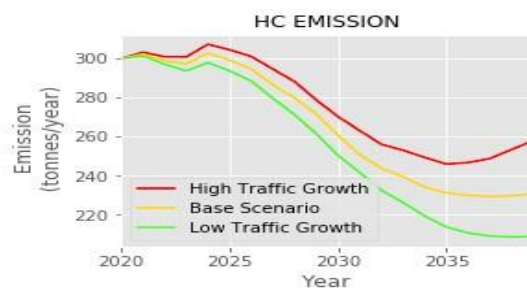
Figure 4. 11 illustrates the modelled annual average fuel consumption for Ngong road

Vehicle Exhaust Emissions for Ngong Road

Analysis of the modelled CO, HC, NO_x, SO₂, and PM was done for the high and low traffic growth scenarios as reported in figure 4.12. The cumulative emissions for these scenarios were evaluated with the base scenario. The highest quantities of CO and HC emissions was reported at 90km/hr and reduced as vehicle operating speed slowed. However, a dramatic increase in these emissions was observed below 60km/hr. In comparison to the base scenario, cumulative emissions for CO and HC increased by approximately 4% for the high traffic growth scenario, while it reduced by approximately 4% for the low traffic growth scenario. For PM, emissions increment of approximately 10% was reported for high traffic growth scenario while a reduction of approximately 9% reduction was recorded for the low traffic growth scenario. The quantity of SO₂ emissions increased by approximately 12% during the high traffic growth while it reduced by approximately 11% for the low traffic growth scenario. Approximately 6% increase in NO_x emissions occurred for the high traffic growth scenario while a 5% reduction was reported for the low traffic growth scenario.



(b)



(a)

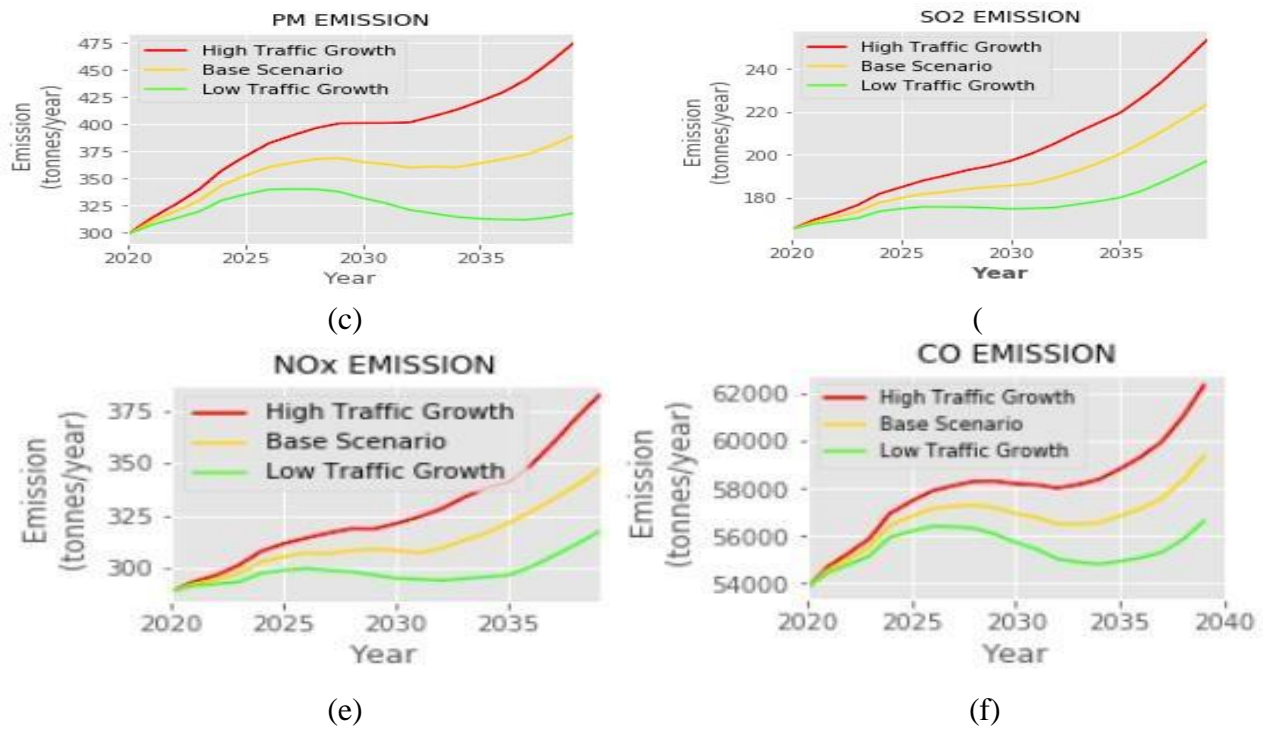


Figure 4. 12 Illustrate predicted vehicle exhaust emissions for Ngong road.

4.2.4 Outer-Ring Road Results

The results of pavement roughness, annual average vehicle speed and vehicle emissions for Outer-Ring road has been analysed and presented in this section. According to figure 4.13(a), the road surface underwent deterioration throughout during the period of analysis. This had the effect of lowering the average vehicle operating speed along the road section.

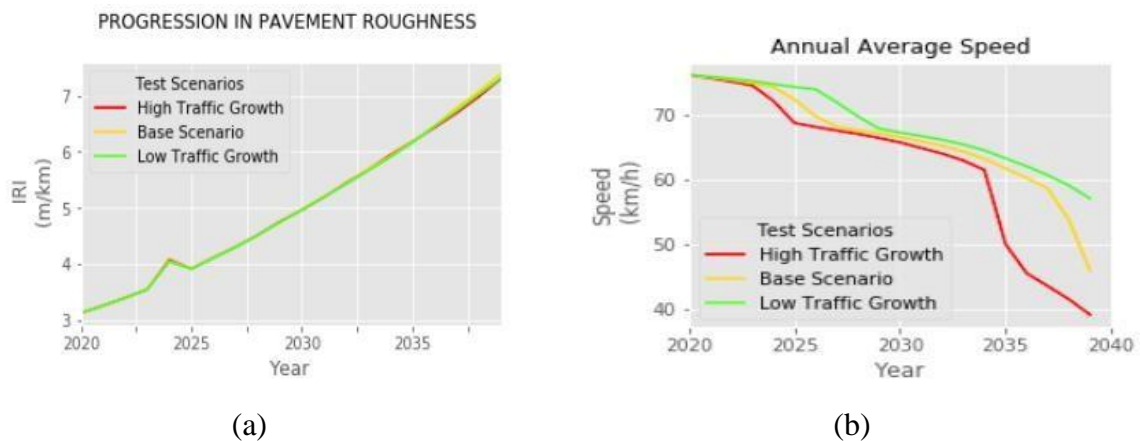


Figure 4. 13 Illustrates change in modelled pavement surface condition (a), and variations in modelled vehicle average operating speeds (b)

Fuel consumption

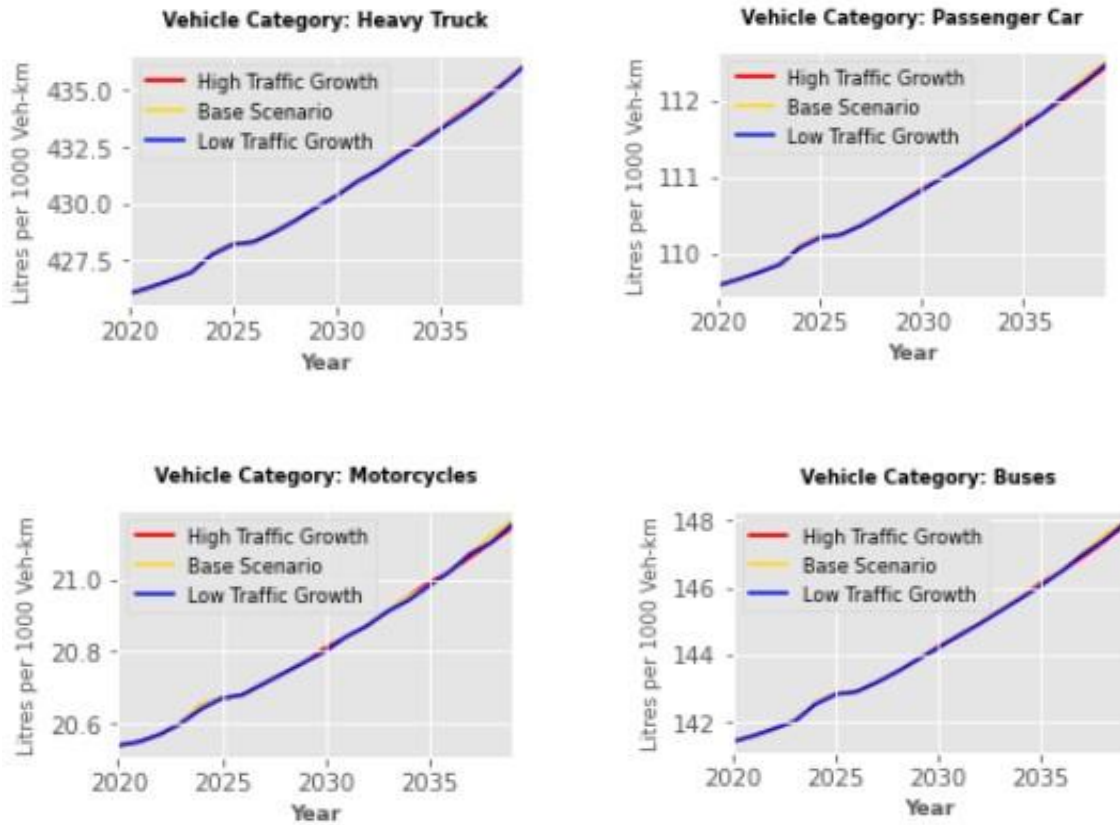


Figure 4. 14 The modelled annual average fuel consumption for Outer-Ring road.

Vehicle Exhaust Emissions for Outer-Ring Road

The cumulative emissions for the high and the low traffic growth scenarios were evaluated against the base traffic growth scenario as follows:

High traffic growth scenario

The exhaust emission for the high traffic growth case was estimated and compared to the base scenario. The cumulative CO, HC, PM, SO₂, increased by approximately 4%, 5%, 18%, and 9% respectively. However, NO_x emissions reduced by approximately 0.6% during this period. It is therefore evident that particulate emission is high at low vehicle operating speeds and the opposite is true for NO_x.

Low traffic growth scenario

The cumulative emissions of CO, HC, PM, and SO₂ reduced by 3%, 4%, 15%, and 8% respectively, however an increment by 0.4% was recorded for NO_x emissions.

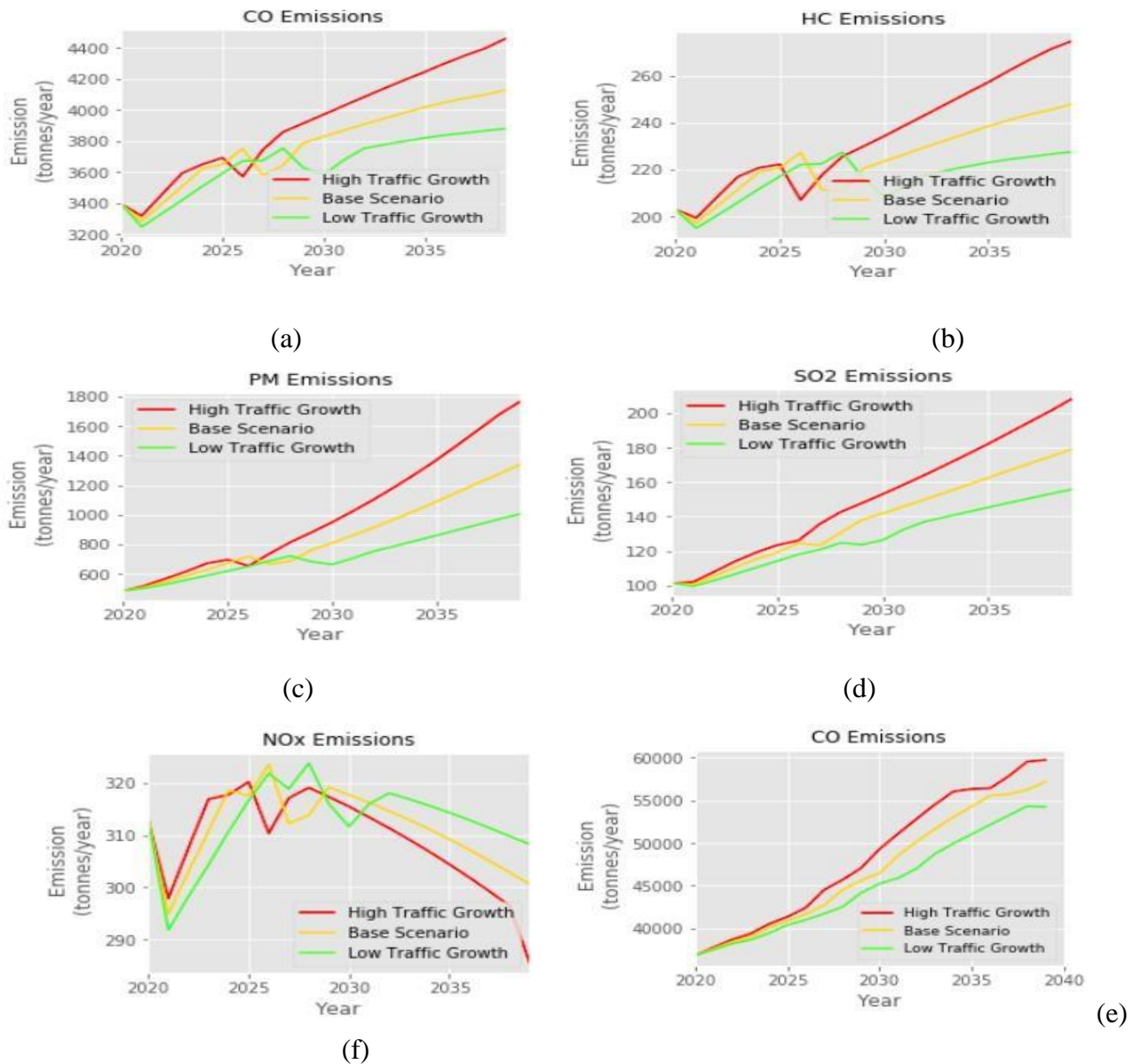


Figure 4. 15 Predicted exhaust emissions for Outer-ring road for CO, HC, PM_{2.5}, SO₂, NO_x, CO₂

4.2.5 Waiyaki Way Results

The modelled road surface roughness, vehicle operating speed and the traffic emissions was analysed for Waiyaki Way. The pavement surface condition changed almost linearly except during which road maintenance was carried out. The pavement surface condition changed almost linearly except during which road maintenance was carried out. At the start of analysis, the average vehicle operating of 65 km/hr was recorded, it however reduced gradually owing to increasing vehicle fleet and road deterioration reaching a minimum of 40 km/hr.

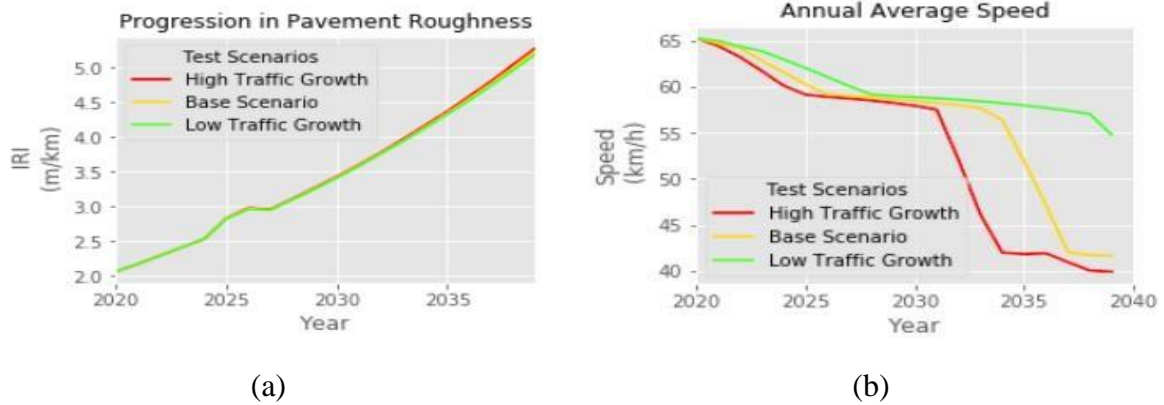


Figure 4. 16 Predicted annual pavement surface roughness (IRI) (a), and the modelled vehicle operating speed.

Predicted Emissions for Waiyaki Way

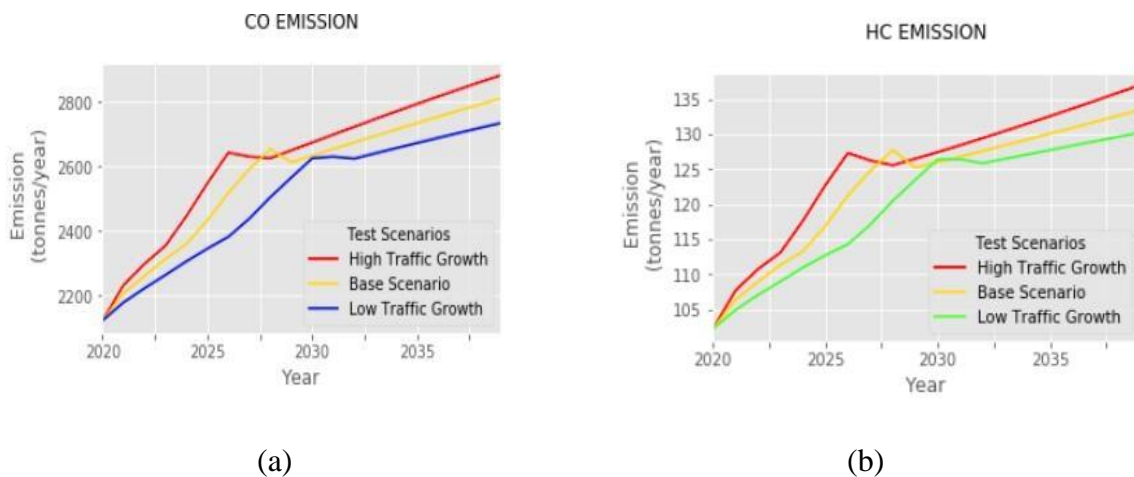
Emissions for Waiyaki Way has been analysed for the high and the low traffic growth scenarios. The cumulative emissions for each scenario was then compared with the base scenario to evaluate which the effect of traffic growth regimes on vehicle emissions:

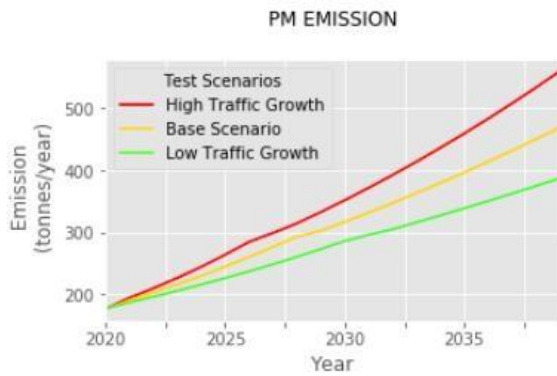
High Traffic Growth Scenario

In this case, cumulative emissions of CO, HC, PM, and SO₂ increased by 2%, 2%, 12%, 6% respectively, while NO_x recorded a reduction of 2%. The vehicle operating speed reduced considerably for this scenario therefore the negative growth in NO_x emissions.

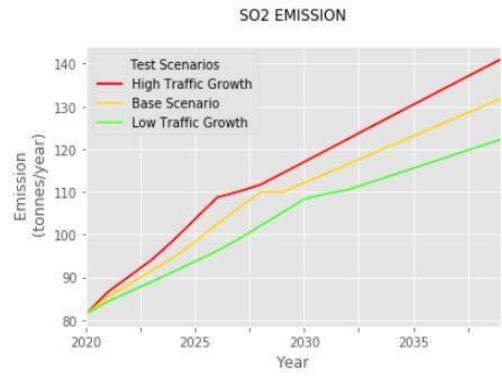
Low Traffic Growth Scenario

The CO, HC, PM, and SO₂ emissions recorded an increment of 2%, 2%, 11%, and 5% respectively, contrary to NO_x which increased by 1%. The reason for high quantity of NO_x reported is due to the fact that the vehicle speeds remains relatively high unlike in high traffic growth scenario, which is the favourable condition for NO_x emissions

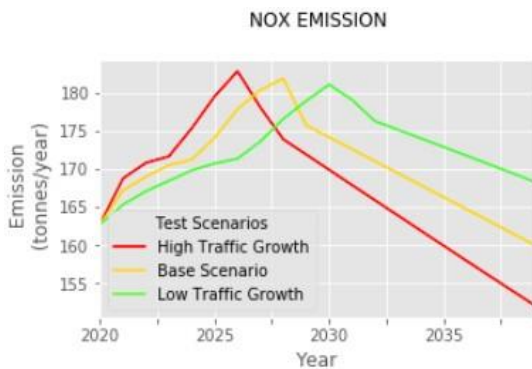




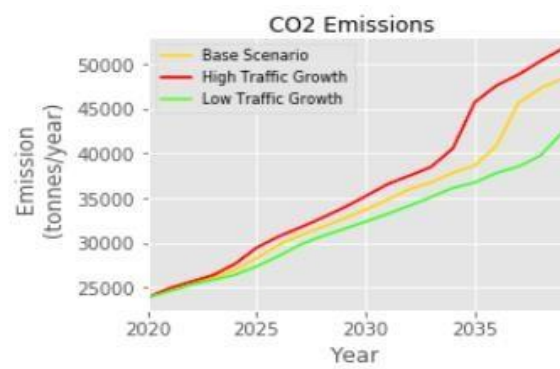
(c)



(d)



(e)



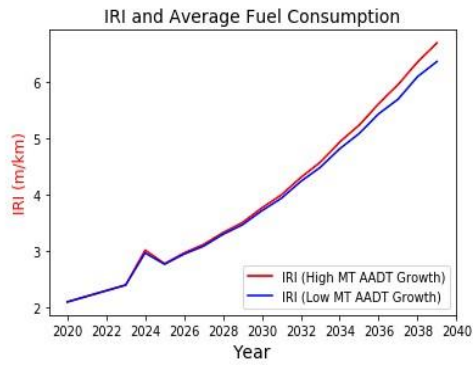
(f)

Figure 4. 17 Illustrate changes in modelled vehicle exhaust emissions

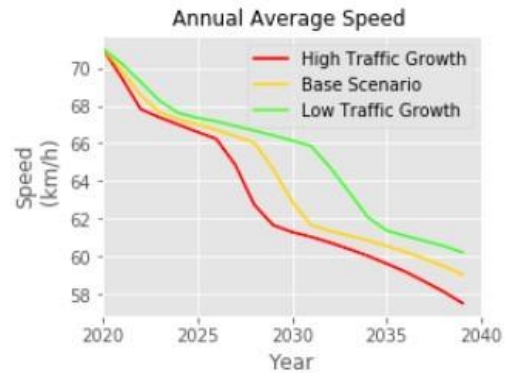
4.2.6 Thika Road Results

The trend in IRI for the Thika road network was modelled and analysed for the low and high traffic growth scenarios. The road condition was observed to increase rapidly for the high traffic growth compared to the low traffic growth. It signified serious damage on road surface condition for the high traffic growth.

On the other hand, the vehicle average operating speeds for the high, base, and the low traffic growth scenarios was also analysed. The traffic flow speed impacts on the rate of fuel consumption which consequently affect vehicle exhaust emissions. The general increment in the vehicle fleet and the IRI impacts on the average operating vehicle speed, which then influence vehicle fuel consumption which is then related to vehicle emissions.



(a)



(b)

Figure 4. 18 illustrates predicted IRI and the average vehicle speed

Modelled Vehicle Exhaust Emissions for Thika Road

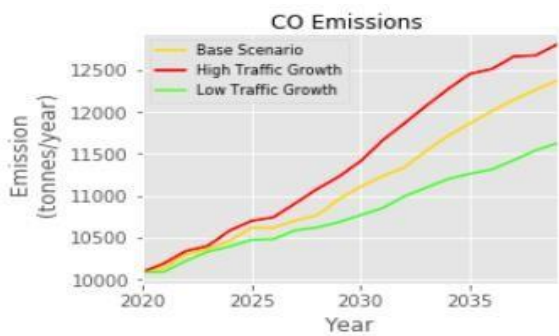
Exhaust emissions was analysed and the changes in cumulative emissions for low and high traffic growth scenarios compared with the base scenario:

High Traffic Growth

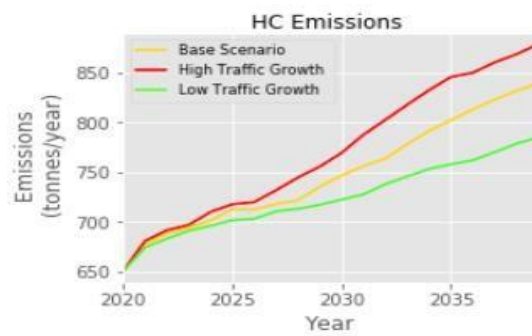
The trend for all emission components increased throughout the analysis period. The quantities of CO, PM, NO_x, HC, SO₂, and CO₂ varied from the base scenario by approximately 3%, 8%, 2%, 3%, 4%, and 3% respectively.

Low Traffic Growth Scenario

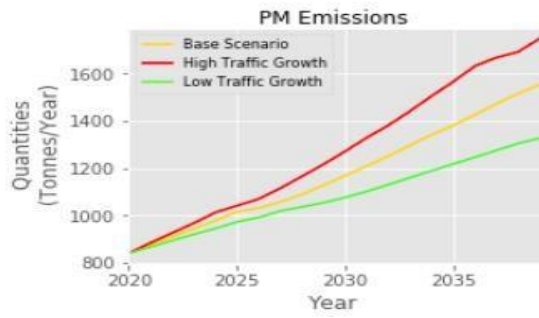
The trend in exhaust emissions also observed to gradually increase throughout the modelling period. Compared to the base scenario, the quantities of CO, PM, NO_x, HC and SO₂ emissions reduced by about 3%, 8%, 3%, 3%, 4%, and 3% respectively.



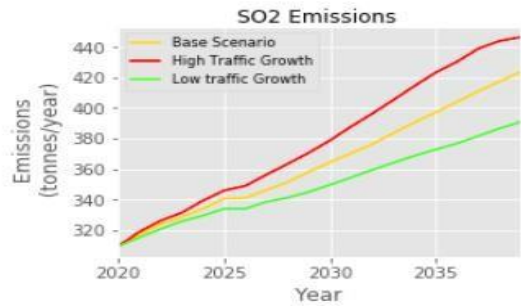
(a)



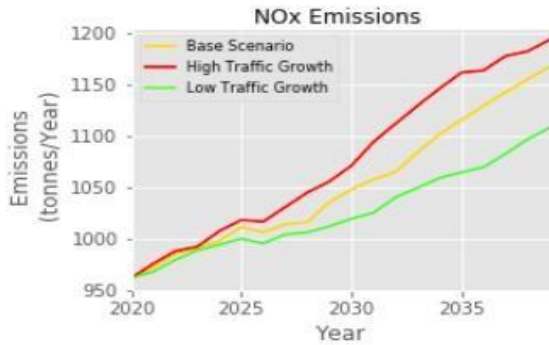
(b)



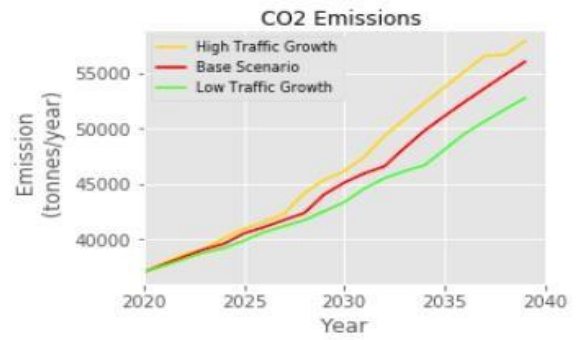
(c)



(d)



(e)

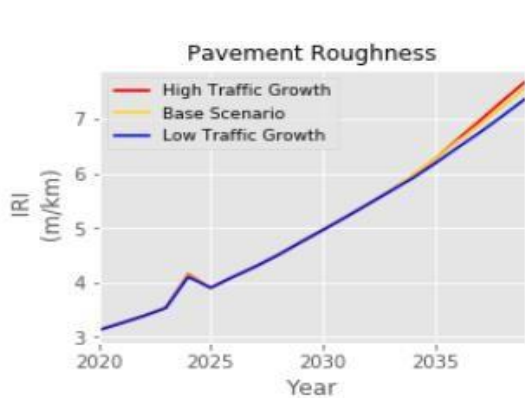


(f)

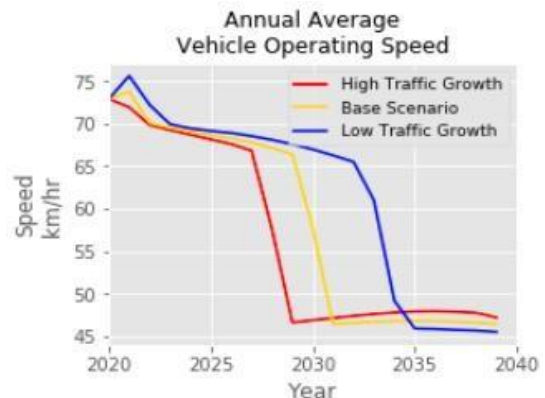
Figure 4. 19 Illustrates modelled exhaust emissions for Thika road

4.2.7 Langata Road Results

As illustrated in figure 4.20 (a), distinct pavement deterioration was observed for the three test scenarios. Consequently, the average vehicle operating speed slowed gradually reaching the lowest values towards the end of analysis.



(a)



(b)

Figure 4. 20 (a) illustrates variation in pavement roughness and (b) is the annual average traffic operating speed.

Fuel consumption

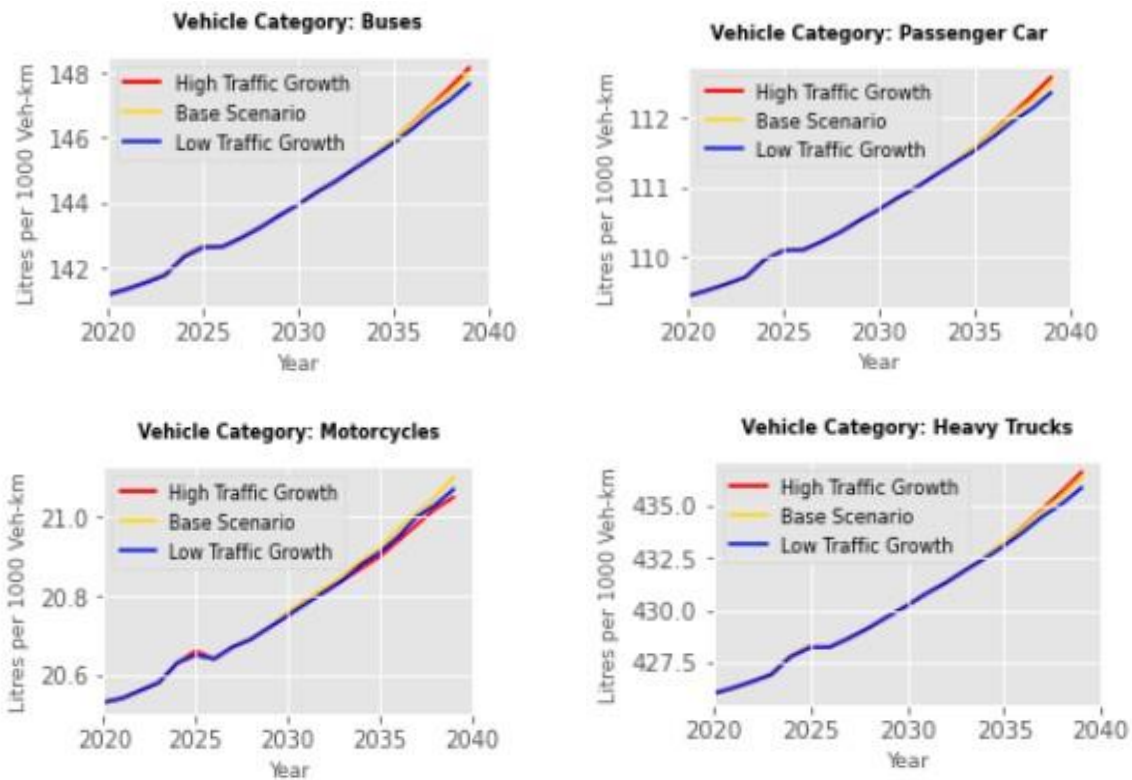


Figure 4. 21 The annual average vehicle fuel consumption along Langata road

Modelled Vehicle Exhaust Emissions for Langata Road

Figure 4.22 shows the modelled exhaust emissions for Langata road network. Each emission component was analysed for the high and low traffic growth scenarios was compared to the base scenario.

High traffic growth scenario

Generally, the trend in quantity of vehicle emissions increased with reducing vehicle speeds except for NO_x. Cumulative emissions were then evaluated against the base scenario. The relative change in CO, HC, PM, SO₂, and CO₂ emissions was 1%, 0.6%, 5%, 3%, and 2% respectively. Traffic congestion was attributed to this significant increment in exhaust emissions. A relative reduction in the quantity of NO_x emissions by 1.7% was reported which was likely due to high decrease in vehicle operating speed observed in for scenario.

Low traffic growth scenario

The trend in vehicle emission during the period of analysis was similar with the high traffic growth scenario. The relative change in CO, HC, PM, SO₂, and CO₂ emissions was approximately 2%, 1%, 5%, 4%, and 3% respectively. On the other hand, the relative

increment in quantity of NOx was about 1.6%. This increase in NOx emissions occurred since vehicle operating speed for this scenario remained slightly higher, therefore contributing to more NOx emissions.

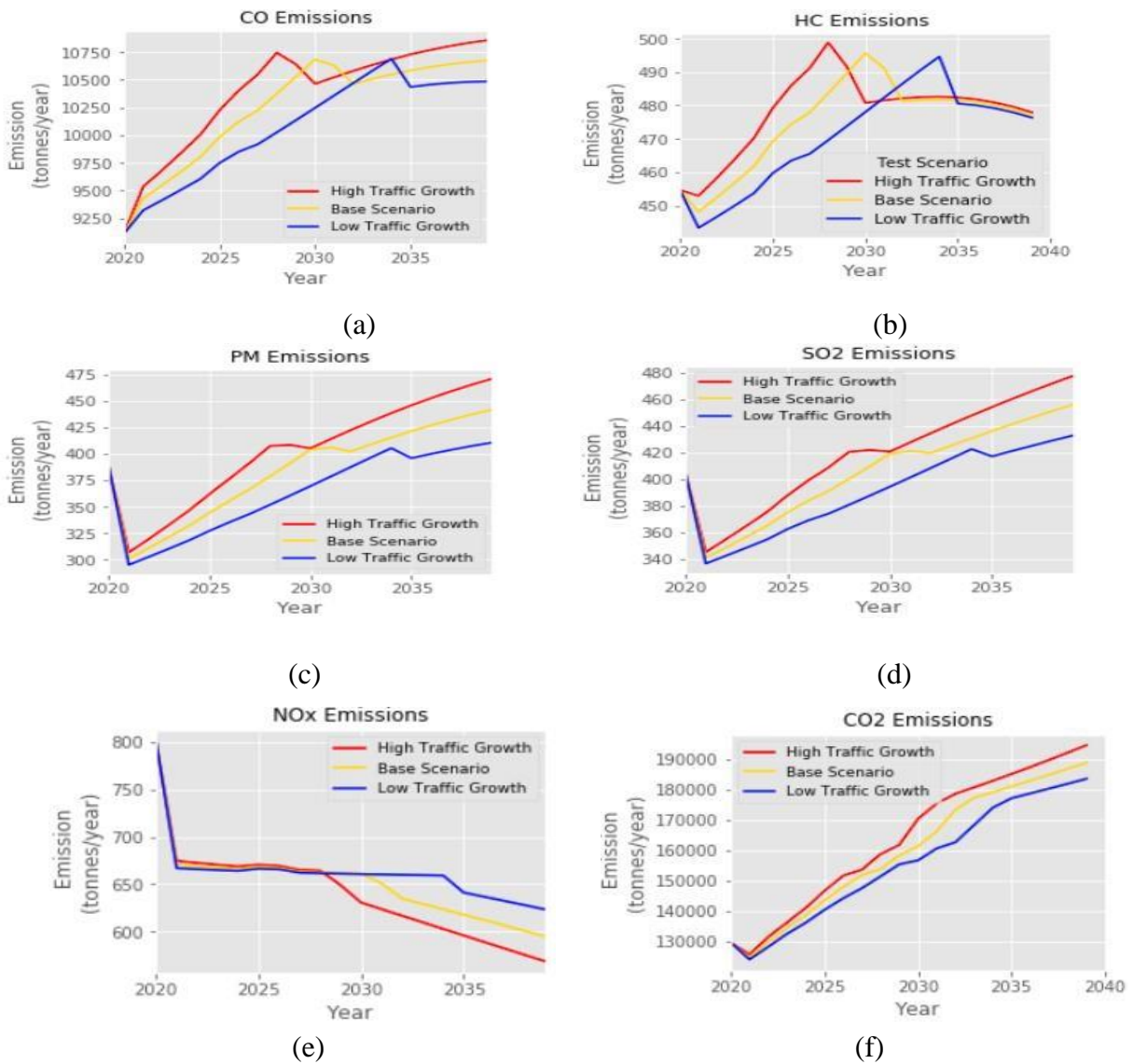
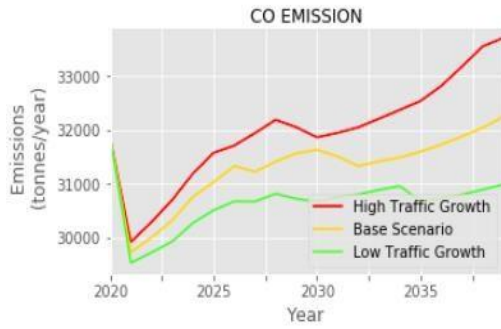


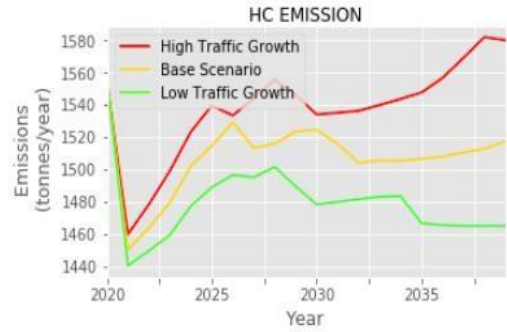
Figure 4. 22 Reports changes in vehicle emissions for Langata road

4.3 Predicted Cumulative Exhaust Emissions for Nairobi Road Networks

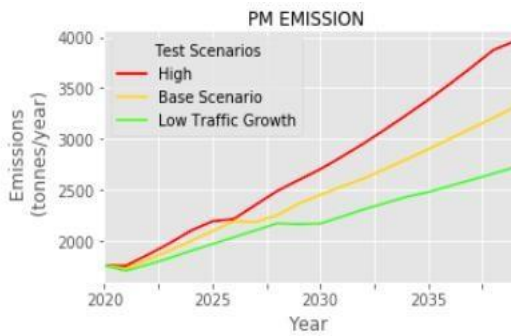
Figure 4.23 illustrates predicted cumulative emissions for all Nairobi road networks. For the High traffic growth, PM_{2.5}, SO₂, and CO emissions increased by about 11.5%, 5.8%, and 2.2% respectively. For the Low traffic growth, they reduced by 10.1%, 3.7%, and 2.1% respectively.



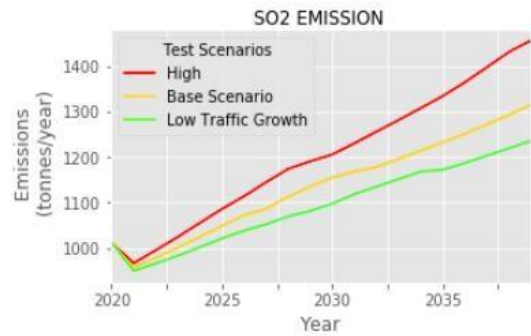
(a)



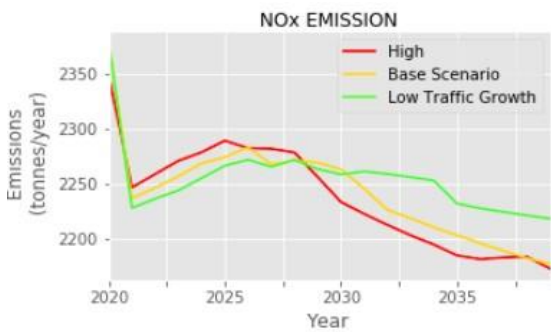
(b)



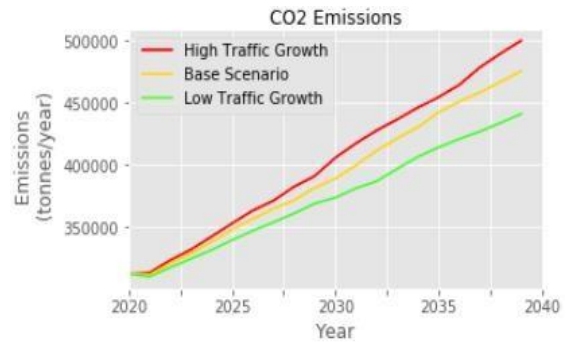
(c)



(d)



(e)



(f)

Figure 4. 23 Cumulative vehicle emissions for Nairobi road networks and their annual variations for the three test scenarios.

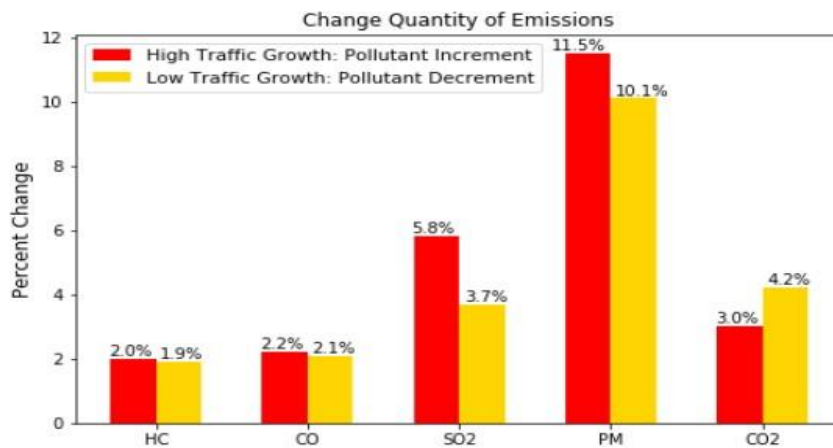


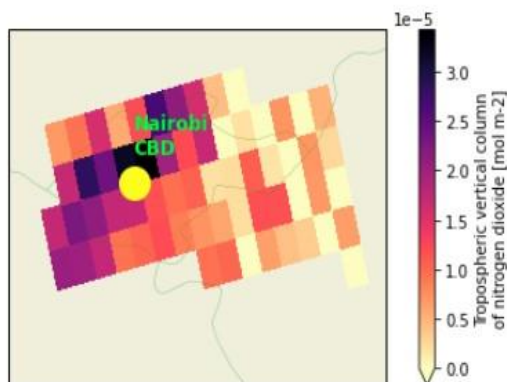
Figure 4. 24 Relative change in emissions for the high and low traffic growth in comparison to the base scenario

4.4 Spatial Distribution of NO₂ Emissions over Nairobi

The atmospheric emission was mapped for six days during which satellite images were available. The quantity of emissions was high within Nairobi central business district and diminished towards the city periphery. Emission concentration was also high in the neighbourhoods of busy traffic routes connecting the links t city. High level of NO₂ concentration was observed along Thika road, Mombasa road, and Ngong road.

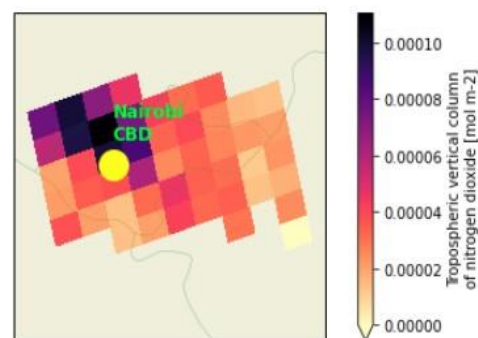
Although there was no data in north eastern part of the city which could have occurred due to cloud masking. The level was however high at the city centre and trailed the route of Waiyaki Way. It is therefore possible that high atmospheric concentration along major transport routes was due to traffic congestion. Road transport is thus import source of air pollution which requires to be monitored regularly. These results point out the important role of traffic emissions with regard to air quality in Nairobi. Despite NO₂ being a precursor of ground level ozone as well as secondary particulate matter, much remain to be explored on its important role on air quality within the city. The long-term data from Sentinel 5P provides a unique opportunity for investigating the temporal behaviour of this pollutant. However, the big size of TROPOMI data involved renders computational challenges at for this analysis.

NO₂ Concentration over Nairobi (2019-01-12)
Quality Flag Layer > 0.75



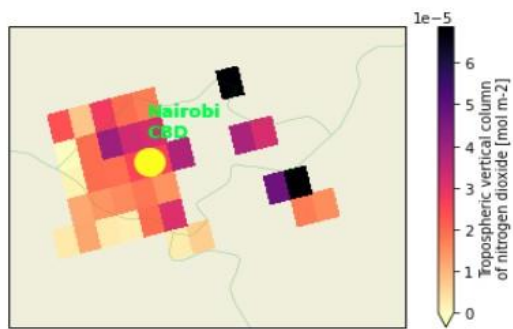
(a)

NO₂ Concentration over Nairobi (2020-09-17)
Quality Flag Layer > 0.75



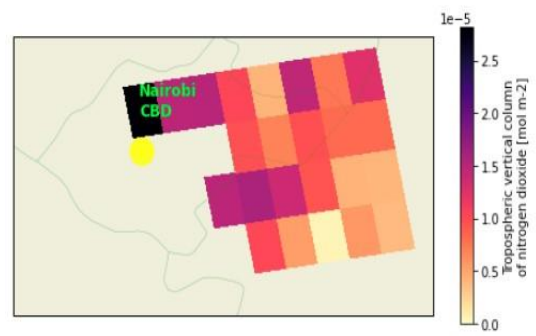
(b)

NO₂ Concentration over Nairobi (2020-08-10)
Quality Flag Layer > 0.75



(c)

NO₂ Concentration over Nairobi (2019-01-16)
Quality Flag Layer > 0.75



(d)

Figure 4. 25 Total NO₂ tropospheric column over Nairobi observed in different days of the year.

CHAPTER FIVE

CONCLUSION

The recent development in population growth and motorisation has compromised the quality of air in Nairobi, thus posing serious health risks to over four million residents of the city. These effects can be greatly minimised through continuous monitoring and source apportionment of air quality. The study employed HDM-4 vehicle emission models and Sentinel 5P data to study the impact of air pollution on air pollution in the study area.

The default factors in HDM-4 were customized with local pavements and vehicle fleet data. The model was configured to reflect the traffic flow patterns, speed flow types, and accident classes for study road networks. The existing climatic conditions was also defined in the model since it is known to affect the rate of pavement deterioration.

Adjustment of the model default emission factors was done for the study vehicles fleet till the output emissions compared to the Edgar-DICE. The annual exhaust emissions in Nairobi was then predicted using calibrated HDM-4 model. The annual predicted quantities of CO, NO_x, SO₂, and PM_{2.5} emissions were approximately 60324, 4582, 1969, and 4273 tonnes respectively. HDM-4 overestimated PM_{2.5} emissions by 24% in comparison to Edgar-DICE emissions. The HDM-4 improvement in prediction of particulate emissions was attributed to its bottom-up approach. Since the HDM-4 emission models have been calibrated, they can be used to predict vehicle exhaust emissions in places which have similar pavement and vehicle fleet characteristics as Nairobi. Ground monitoring of vehicle emissions is however necessary for validation of model predicted emissions.

The effect of traffic growth on exhaust emissions was analysed for a period of twenty years. Cumulative PM_{2.5} emissions from the thirteen study road networks recorded increment of approximately 11.5% during the twenty-year analysis period. The SO₂, CO, and HC emissions were predicted to rise by 5.8, 2.2, and 2.0 respectively. For the low traffic growth, PM_{2.5}, SO₂, and CO emissions was likely to reduce by approximately 10.1, 3.7, 2.1, and 1.9% respectively. Since future introduction of Bus Rapid Transport, electric vehicles and commuter trains is likely to reduce the public service vehicles, its overall impact on exhaust emissions needs to be investigated.

The spatial distribution of NO₂ over the study area was mapped using Sentinel 5P total NO₂ tropospheric column measurements. The data was retrieved, processed and mapped using

python packages developed by RUS. High emission hotspots were identified within Nairobi central business district and in neighbourhoods of busy traffic routes. Since significant number of industries are located in Nairobi and Thika, it is important to estimate the contribution of this sector to atmospheric emissions.

RECOMMENDATIONS

It has been demonstrated that the model for road management (HDM-4) and satellite remote sensing provide opportunity for improved estimation of atmospheric emissions in areas with limited coverage of ground air monitoring networks like Nairobi. If regularly conducted, studies of this nature can provide comprehensive data through which policy formulation and air quality regulation can be done.

However, proper characterisation of vehicle fleet and the pavements are necessary to improve the accuracy of the modelled results. Assessment of contribution of industries, municipal waste, and biomass burning to atmospheric emissions need to be done to give insights to the key drivers of air quality in Nairobi. Furthermore, it can provide high spatial and temporal resolved data which improves the prediction of air quality. Routine monitoring of air quality is also needed in the study area since it can capture long term trends in air quality.

References

- Adar, S. D., Sheppard, L., Vedal, S., Polak, J. F., Sampson, P. D., Roux, A. V. D., Budoff, M., Jacobs Jr, D. R., Barr, R. G., & Watson, K. (2013). Fine particulate air pollution and the progression of carotid intima-medial thickness: A prospective cohort study from the multi-ethnic study of atherosclerosis and air pollution. *PLoS Med*, *10*(4), e1001430.
- An, F., Barth, M., Norbeck, J., & Ross, M. (1997). Development of comprehensive modal emissions model: Operating under hot-stabilized conditions. *Transportation Research Record*, *1587*(1), 52–62.
- An, F., Barth, M., Scora, G., & Ross, M. (1998). Modeling enleanment emissions for light-duty vehicles. *Transportation Research Record*, *1641*(1), 48–57.
- Baskin, A., de Jong, R., Dumitrescu, E., Akumu, J., Stannah, V. R., Mwangi, A., Diabate, F., Quirama, L. F., & Maina, G. (2020). *Used Vehicles and the Environment: A Global Overview of Used Light Duty Vehicles-Flow, Scale and Regulation*.
- Batterman, S. A., Yu, Y., Jia, C., & Godwin, C. (2005). Non-methane hydrocarbon emissions from vehicle fuel caps. *Atmospheric Environment*, *39*(10), 1855–1867.
- Bennett, C. R., & Greenwood, I. D. (2003). Volume 7: Modeling road user and environmental effects in HDM-4, Version 3.0, international study of highway development and management tools (ISOHDM), World Road Association (PIARC). *World Road Association (PIARC), Paris*.
- Bennett, C. R., & Paterson, W. D. O. (2002). Volume V: A guide to calibration and adaptation. *HDM-4 Manual (Version 1.3)*, 524–529.
- Bennett, Christopher R., & Paterson, W. D. (2000). A guide to calibration and adaptation. *HDM-4. Volume 5. The Highway Development and Management Series*.
- Berger, M., Moreno, J., Johannessen, J. A., Levelt, P. F., & Hanssen, R. F. (2012). ESA’s sentinel missions in support of Earth system science. *Remote Sensing of Environment*, *120*, 84–90.
- Biggs, D. C. (1988a). *ARFCOM: Models for Estimating Light to Heavy Vehicle Fuel Consumption*.
- Biggs, D. C. (1988b). *ARFCOM: Models for Estimating Light to Heavy Vehicle Fuel Consumption*.
- Bolaji, B. O., & Adejuyigbe, S. B. (2006). *Vehicle emissions and their effects on the natural environment*.
- Borsdorff, T., Aan de Brugh, J., Hu, H., Aben, I., Hasekamp, O., & Landgraf, J. (2018). Measuring carbon monoxide with TROPOMI: First results and a comparison with ECMWF-IFS analysis data. *Geophysical Research Letters*, *45*(6), 2826–2832.
- Boucher, O. (2015). Atmospheric aerosols. In *Atmospheric Aerosols* (pp. 9–24). Springer.
- Bovensmann, H., Burrows, J. P., Buchwitz, M., Frerick, J., Noël, S., Rozanov, V. V., Chance, K. V., & Goede, A. P. H. (1999). SCIAMACHY: Mission objectives and measurement modes. *Journal of the Atmospheric Sciences*, *56*(2), 127–150.
- Castell, N., Dauge, F. R., Schneider, P., Vogt, M., Lerner, U., Fishbain, B., Broday, D., & Bartonova, A. (2017). Can commercial low-cost sensor platforms contribute to air quality monitoring and

- exposure estimates? *Environment International*, 99, 293–302.
<https://doi.org/10.1016/j.envint.2016.12.007>
- Chama, N. C. C. (2013). Investigating for Contributory Factors to Traffic Congestion in Nairobi City, Kenya. *International Journal of Science and Research (IJSR)*, 4(5), 3253–3256.
- Chan, T. L., & Lippmann, M. (1980). Experimental measurements and empirical modelling of the regional deposition of inhaled particles in humans. *American Industrial Hygiene Association Journal*, 41(6), 399–409. <https://doi.org/10.1080/15298668091424942>
- Chatti, K., Salama, H., & El Mohtar, C. (2004). Effect of heavy trucks with large axle groups on asphalt pavement damage. *Proceedings of the 8th International Symposium on Heavy Vehicle Weights and Dimensions, Muldersdrift, South Africa*.
- Chen, G., Li, S., Zhang, Y., Wenyi, Z., Li, D., Wei, X., He, Y., Bell, M., Williams, G., Marks, G., Jalaludin, B., Abramson, M., & Guo, Y. (2017). Effects of ambient PM 1 air pollution on daily emergency hospital visits in China: An epidemiological study. *The LANCET*, 1, e221–e229.
[https://doi.org/10.1016/S2542-5196\(17\)30100-6](https://doi.org/10.1016/S2542-5196(17)30100-6)
- Cheng, Y., Lee, S., Gu, Z., Ho, K., Zhang, Y., Huang, Y., Chow, J. C., Watson, J. G., Cao, J., & Zhang, R. (2015). PM_{2.5} and PM_{10-2.5} chemical composition and source apportionment near a Hong Kong roadway. *Particuology*, 18, 96–104. <https://doi.org/10.1016/j.partic.2013.10.003>
- Chow, J. C., & Watson, J. G. (2002). Review of PM_{2.5} and PM₁₀ Apportionment for Fossil Fuel Combustion and Other Sources by the Chemical Mass Balance Receptor Model. *Energy & Fuels*, 16(2), 222–260. <https://doi.org/10.1021/ef0101715>
- Chuturkova, R. (2015). *OZONE AND OZONE PRECURSORS IN URBAN ATMOSPHERE*. 8.
- Council, N. R. (2003). *Beyond the molecular frontier: Challenges for chemistry and chemical engineering*.
- Cretu, M., & Deaconu, M. (2012). Air Quality—monitoring and modelling. *INCAS Bulletin*, 4(4), 127.
- Crippa, M., Guizzardi, D., Muntean, M., Schaaf, E., Dentener, F., van Aardenne, J. A., Monni, S., Doering, U., Olivier, J. G. J., Pagliari, V., & Janssens-Maenhout, G. (2018). Gridded emissions of air pollutants for the period 1970–2012 within EDGAR v4.3.2. *Earth System Science Data*, 10(4), 1987–2013. <https://doi.org/10.5194/essd-10-1987-2018>
- Deng, X., Zhang, F., Rui, W., Long, F., Wang, L., Feng, Z., Chen, D., & Ding, W. (2013). PM_{2.5}-induced oxidative stress triggers autophagy in human lung epithelial A549 cells. *Toxicology in Vitro*, 27(6), 1762–1770.
- Díaz, G., Macia, H., Valero, V., Boubeta-Puig, J., & Cuartero, F. (2020). An Intelligent Transportation System to control air pollution and road traffic in cities integrating CEP and Colored Petri Nets. *Neural Computing and Applications*, 32(2), 405–426.
- Dimaratos, A., Toumasatos, Z., Doulgeris, S., Triantafyllopoulos, G., Kontses, A., & Samaras, Z. (2019). Assessment of CO₂ and NO_x emissions of one diesel and one bi-fuel gasoline/CNG euro 6 vehicles during real-world driving and laboratory testing. *Frontiers in Mechanical Engineering*, 5, 62.
- Dockery, D., Pope, C., Xu, X., Spengler, J., Ware, J., Fay, M., Ferris, B., & Speizer, F. (1994). An Association Between Air Pollution and Mortality in Six U.S. Cities. *The New England Journal of Medicine*, 329, 1753–1759. <https://doi.org/10.1056/NEJM199312093292401>

- Ebinger, J., & Vergara, W. (2011). *Climate impacts on energy systems: Key issues for energy sector adaptation*. The World Bank.
- Egondi, T., Kyobutungi, C., Ng, N., Muindi, K., Oti, S., Vijver, S., Ettarh, R., & Rocklöv, J. (2013). Community Perceptions of Air Pollution and Related Health Risks in Nairobi Slums. *International Journal of Environmental Research and Public Health*, *10*, 4851–4868. <https://doi.org/10.3390/ijerph10104851>
- Eluru, N., Chakour, V., Chamberlain, M., & Miranda-Moreno, L. F. (2013). Modeling vehicle operating speed on urban roads in Montreal: A panel mixed ordered probit fractional split model. *Accident Analysis & Prevention*, *59*, 125–134.
- Feng, S., Gao, D., Liao, F., Zhou, F., & Wang, X. (2016a). The health effects of ambient PM_{2.5} and potential mechanisms. *Ecotoxicology and Environmental Safety*, *128*, 67–74.
- Feng, S., Gao, D., Liao, F., Zhou, F., & Wang, X. (2016b). The health effects of ambient PM_{2.5} and potential mechanisms. *Ecotoxicology and Environmental Safety*, *128*, 67–74.
- Fiebig, M., Wiartalla, A., Holderbaum, B., & Kiesow, S. (2014). Particulate emissions from diesel engines: Correlation between engine technology and emissions. *Journal of Occupational Medicine and Toxicology*, *9*(1), 1–18.
- Gachanja, J. (2015). Mitigating Road Traffic Congestion in the Nairobi Metropolitan Region. *The Kenya Institute for Public Policy Research and Analysis (KIPPRA) Policy Brief*, *2*.
- Gaita, S., Boman, J., Gichuru, M., Pettersson, J., & Janhäll, S. (2014). Source apportionment and seasonal variation in PM_{2.5} in Sub-Saharan African city: Nairobi, Kenya. *ATMOSPHERIC CHEMISTRY AND PHYSICS*, *14*. <https://doi.org/10.5194/acpd-14-9565-2014>
- Gaita, S. M., Boman, J., Gatari, M. J., Pettersson, J. B., & Janhäll, S. (2014). Source apportionment and seasonal variation of PM_{2.5} in a Sub-Saharan African city: Nairobi, Kenya. *Atmospheric Chemistry and Physics*, *14*(18), 9977–9991.
- Gatari, M. J., Kinney, P. L., Yan, B., Sclar, E., Volavka-Close, N., Ngo, N. S., Gaita, S. M., Law, A., Ndiba, P. K., & Gachanja, A. (2019). High airborne black carbon concentrations measured near roadways in Nairobi, Kenya. *Transportation Research Part D: Transport and Environment*, *68*, 99–109.
- Gatari, M., Wagner, A., & Boman, J. (2005). Elemental composition of tropospheric aerosols in Hanoi, Vietnam and Nairobi, Kenya. *Science of the Total Environment*, *341*(1–3), 241–249.
- Gichuru, M., Wagner, A., & Boman, J. (2005). Elemental Composition of Tropospheric Aerosols in Hanoi, Vietnam and Nairobi, Kenya. *The Science of the Total Environment*, *341*, 241–249. <https://doi.org/10.1016/j.scitotenv.2004.09.031>
- Gonzales, E. J., Chavis, C., Li, Y., & Daganzo, C. F. (2009). *Multimodal transport modeling for Nairobi, Kenya: Insights and recommendations with an evidence-based model*.
- Greenwood, I. D., & Bennett, C. R. (1996). The effects of traffic congestion on fuel consumption. *Road and Transport Research*, *5*(2). <https://trid.trb.org/view/1167306>
- Gualtieri, M., Øvrevik, J., Møllerup, S., Asare, N., Longhin, E., Dahlman, H.-J., Camatini, M., & Holme, J. A. (2011). Airborne urban particles (Milan winter-PM_{2.5}) cause mitotic arrest and cell

- death: Effects on DNA, mitochondria, AhR binding and spindle organization. *Mutation Research/Fundamental and Molecular Mechanisms of Mutagenesis*, 713(1–2), 18–31.
- Guzzonato, E., Mora, B., Remondière, S., & Palazzo, F. (2020). RUS Copernicus: An Expert Service for New Sentinel Data Users. *IOP Conference Series: Earth and Environmental Science*, 509(1), 012022.
- Habre, R., Moshier, E., Castro, W., Nath, A., Grunin, A., Rohr, A., Godbold, J., Schachter, N., Kattan, M., & Coull, B. (2014). The effects of PM 2.5 and its components from indoor and outdoor sources on cough and wheeze symptoms in asthmatic children. *Journal of Exposure Science & Environmental Epidemiology*, 24(4), 380–387.
- Hammerstrom, U. (1995). Proposal for a Vehicle Exhaust Model in HDM-4 ISOHDM Supplementary Technical Relationships Study Draft Report. *Swedish National Road Administration, Road and Traffic Management Division, Borlange Sweden*, 120–145.
- Hoban, C. J., Reilly, W., & Archondo-Callo, R. (1994). Economic Analysis of Road Projects with Congested Traffic, World Bank Publication. *Washington DC*.
- Hu, J., Fan, H., Li, Y., Li, H., Tang, M., Wen, J., Huang, C., Wang, C., Gao, Y., & Kan, H. (2020). Fine particulate matter constituents and heart rate variability: A panel study in Shanghai, China. *Science of The Total Environment*, 747, 141199.
- Humans, I. W. G. on the E. of C. R. to. (2016). *Outdoor air pollution*. International Agency for Research on Cancer.
- Jaikumar, R., Nagendra, S. S., & Sivanandan, R. (2017a). Modeling of real time exhaust emissions of passenger cars under heterogeneous traffic conditions. *Atmospheric Pollution Research*, 8(1), 80–88.
- Jaikumar, R., Nagendra, S. S., & Sivanandan, R. (2017b). Modeling of real time exhaust emissions of passenger cars under heterogeneous traffic conditions. *Atmospheric Pollution Research*, 8(1), 80–88.
- Kang, M. S., Nazarkin, A., Brenn, A., & Russell, P. S. J. (2009). Tightly trapped acoustic phonons in photonic crystal fibres as highly nonlinear artificial Raman oscillators. *Nature Physics*, 5(4), 276–280.
- Karue, J., Kinyua, A. M., & Njau, L. (1994). *Air pollution in Kenya*.
- KENHA. (2021). *Kenya National Highway Authority*. <https://www.kenha.co.ke>
- Kerali, H. G., Odoki, J. B., & Stannard, E. E. (2000). Overview of HDM-4. *The Highway Development and Management Series, Volume One, World Road Association, PIARC. World Bank, Washington DC, USA*.
- Kerali, H. R., Odoki, J. B., & Wightman, D. C. (1994). *Vehicle Fleet Representation*. Working Paper. International Study of Highway Development and Management
- KeRRA. (2021). *Kenya Rural Roads Authority (KeRRA)*. <https://www.kerra.go.ke/index.php/about-us/our-role>
- Kinney, P. L., Gichuru, M. G., Volavka-Close, N., Ngo, N., Ndiba, P. K., Law, A., Gachanja, A., Gaita, S. M., Chillrud, S. N., & Sclar, E. (2011a). Traffic impacts on PM2.5 air quality in Nairobi, Kenya. *Environmental Science & Policy*, 14(4), 369–378.
- Kinney, P. L., Gichuru, M. G., Volavka-Close, N., Ngo, N., Ndiba, P. K., Law, A., Gachanja, A., Gaita, S. M., Chillrud, S. N., & Sclar, E. (2011b). Traffic impacts on PM2.5 air quality in Nairobi, Kenya. *Environmental Science & Policy*, 14(4), 369–378. <https://doi.org/10.1016/j.envsci.2011.02.005>

- KNBS. (2016). *Kenya National Bureau of Statistics. County Statistical abstract- Nairobi County, 2016*. www.knbs.or.ke
- KNBS. (2019). *2019 Kenya Population and Housing Census Volume I: Population by County and Sub-County*.
- KNBS. (2020). *Kenya National Bureau of Statistics. Nairobi County Statistics*. www.knbs.or.ke
- Koistinen, K. J., Kousa, A., Tenhola, V., Hänninen, O., Jantunen, M. J., Oglesby, L., Kuenzli, N., & Georgoulis, L. (1999). Fine Particle (PM₂₅) Measurement Methodology, Quality Assurance Procedures, and Pilot Results of the *EXPOLIS* Study. *Journal of the Air & Waste Management Association*, *49*(10), 1212–1220. <https://doi.org/10.1080/10473289.1999.10463916>
- Kumar, P., Morawska, L., Martani, C., Biskos, G., Neophytou, M., Di Sabatino, S., Bell, M., Norford, L., & Britter, R. (2015). The rise of low-cost sensing for managing air pollution in cities. *Environment International*, *75*, 199–205.
- KURA. (2021). *Road Network Conditions. The Kenya Urban Roads Authority (KURA)*. <https://maps.krb.go.ke/kenya-roads-board12769/maps/110400/2-road-network-conditions#>
- Levelt, P., Oord, G. H. J., Dobber, M., Mälkki, A., Visser, H., Vries, J., Stammes, P., Lundell, J., & Saari, H. (2006). The Ozone Monitoring Instrument. *IEEE T. Geoscience and Remote Sensing*, *44*, 1093–1101. <https://doi.org/10.1109/TGRS.2006.872333>
- Li, J., Muench, S. T., Mahoney, J., White, G., Peirce, L., & Sivaneswaran, N. (2004). Application of HDM-4 in the WSDOT Highway System. *Washington State Transportation Commission*, 1–106.
- Lozhkina, O. V., & Lozhkin, V. N. (2016). Estimation of nitrogen oxides emissions from petrol and diesel passenger cars by means of on-board monitoring: Effect of vehicle speed, vehicle technology, engine type on emission rates. *Transportation Research Part D: Transport and Environment*, *47*, 251–264.
- Malaghan, V., Pawar, D. S., & Dia, H. (2020). Speed prediction models for heavy passenger vehicles on rural highways based on an instrumented vehicle study. *Transportation Letters*, 1–10.
- Manisalidis, I., Stavropoulou, E., Stavropoulos, A., & Bezirtzoglou, E. (2020). Environmental and Health Impacts of Air Pollution: A Review. *Frontiers in Public Health*, *8*. <https://doi.org/10.3389/fpubh.2020.00014>
- Marais, E. A., & Wiedinmyer, C. (2016). Air quality impact of diffuse and inefficient combustion emissions in Africa (DICE-Africa). *Environmental Science & Technology*, *50*(19), 10739–10745.
- Martin, R. V. (2008). Satellite remote sensing of surface air quality. *Atmospheric Environment*, *42*(34), 7823–7843.
- Mazzeo, A., Quinn, A., Burrow, M., Marais, E., Singh, A., & Pope, F. (2019). *Air pollution modelling in East Africa Impact of anthropogenic emissions on urban air quality of Nairobi, Kenya*. <https://doi.org/10.13140/RG.2.2.19678.18240>
- Mbandi, A. M., Böhnke, J. R., Schwela, D., Vallack, H., Ashmore, M. R., & Emberson, L. (2019). Estimating on-road vehicle fuel economy in Africa: A case study based on an urban transport survey in Nairobi, Kenya. *Energies*, *12*(6), 1177.
- Monks, P. S., Archibald, A. T., Colette, A., Cooper, O., Coyle, M., Derwent, R., Fowler, D., Granier, C., Law, K. S., Mills, G. E., Stevenson, D. S., Tarasova, O., Thouret, V., von Schneidmesser, E.,

- Sommariva, R., Wild, O., & Williams, M. L. (2015). Tropospheric ozone and its precursors from the urban to the global scale from air quality to short-lived climate forcer. *Atmospheric Chemistry and Physics*, 15(15), 8889–8973. <https://doi.org/10.5194/acp-15-8889-2015>
- Morosiuk, G., Riley, M. J., & Odoki, J. B. (2004). Modelling road deterioration and works effects-version 2-Highway Development and Management-HDM-4. *Highway Development and Management Series*.
- Muguro, J. K., Sasaki, M., Matsushita, K., & Njeri, W. (2020). Trend analysis and fatality causes in Kenyan roads: A review of road traffic accident data between 2015 and 2020. *Cogent Engineering*, 7(1), 1797981.
- Muindi, K. (2017). *Air pollution in Nairobi slums: Sources, levels and lay perceptions* [PhD Thesis]. Ume\aa University.
- Mukaria, S. M. (2017). *Traffic Police Knowledge, Attitude and Practices Concerning Motor Vehicle Air Pollution at Key Nairobi Road Junctions* [PhD Thesis]. University of Nairobi.
- Munir, S., Mayfield, M., Coca, D., Jubb, S. A., & Osammor, O. (2019). Analysing the performance of low-cost air quality sensors, their drivers, relative benefits and calibration in cities—A case study in Sheffield. *Environmental Monitoring and Assessment*, 191(2), 94.
- Munro, R., Lang, R., Klaes, D., Poli, G., Retscher, C., Lindstrot, R., Huckle, R., Lacan, A., Grzegorski, M., & Holdak, A. (2016). The GOME-2 instrument on the Metop series of satellites: Instrument design, calibration, and level 1 data processing—an overview. *Atmospheric Measurement Techniques*, 9(3), 1279–1301.
- Nakagawa, Y., Nishida, J., Asao, H., Mukoko, B., & Tamura, K. (2018). Application of AMP Collectors in Nairobi CBD for Transport Planning. *Transportation Research Procedia*, 34, 107–114.
- NCAQAP. (2018). *Air Quality Action Plan (2019-2023)*. Nairobi City County. https://www.eci-africa.org/wp-content/uploads/2019/05/Nairobi-Air-Quality-Action-Plan_Final_ECI_31.12.2018.pdf
- NCIDP, N. C. (2018). County integrated development plan (CIDP) 2018–2022. *Nairobi: NCC*.
- Ndegwa, P. (2017). *Factors influencing supply of petroleum products in Kenya: A case of Kenya pipeline company Eldoret depot, Uasin Gishu County, Kenya* [PhD Thesis]. University of Nairobi.
- Ngo, N. S., Gatari, M., Yan, B., Chillrud, S. N., Bouhamam, K., & Kinneym, P. L. (2015). Occupational exposure to roadway emissions and inside informal settlements in sub-Saharan Africa: A pilot study in Nairobi, Kenya. *Atmospheric Environment (Oxford, England : 1994)*, 111, 179–184. <https://doi.org/10.1016/j.atmosenv.2015.04.008>
- Noshadravan, A., Wildnauer, M., Gregory, J., & Kirchain, R. (2013). Comparative pavement life cycle assessment with parameter uncertainty. *Transportation Research Part D: Transport and Environment*, 25, 131–138.
- Notter, B., Weber Felix, & , Jürg, F. (2019). *Updated Transport Data in Kenya* (INFRAS Urda Eichhorst, GIZ). https://www.changing-transport.org/wp-content/uploads/2019_Updated-transport-data-in-Kenya.pdf
- Odoki, J. B., & Kerali, H. G. (2000). Highway Development and Management (HDM-4) Volume 4: Analytical Framework and Model Descriptions. *The World Road Association (PIARC), Paris and the World Bank, Washington, DC*.

- Ogot, M., Nyang'aya, J., & Muriuki, R. (2018). Characteristics of the in-service vehicle fleet in Kenya. *Draft Report*.
- Omwenga, M. (2011). Integrated transport system for liveable city environment: A case study of Nairobi Kenya. *47th ISOCARP Congress*. Retrieved Jun, 15, 2015.
- Organization, W. H. (2006a). *Air quality guidelines: Global update 2005: particulate matter, ozone, nitrogen dioxide, and sulfur dioxide*. World Health Organization.
- Organization, W. H. (2006b). *WHO Air quality guidelines for particulate matter, ozone, nitrogen dioxide and sulfur dioxide: Global update 2005: summary of risk assessment*. World Health Organization.
- Pj, L., R, F., Njr, A., O, A., R, A., Nn, B., Ab, B., R, B., S, B.-O., Ji, B., Pn, B., T, C., C, M., Am, C.-S., Ml, C., J, F., V, F., M, G., A, H., ... M, Z. (2018). The Lancet Commission on pollution and health. *Lancet (London, England)*, *391*(10119). [https://doi.org/10.1016/S0140-6736\(17\)32345-0](https://doi.org/10.1016/S0140-6736(17)32345-0)
- Pope, F. D., Gatari, M., Ng'ang'a, D., Poynter, A., & Blake, R. (2018). Airborne particulate matter monitoring in Kenya using calibrated low-cost sensors. *Atmospheric Chemistry and Physics*, *18*(20), 15403–15418.
- Pope, F., Gichuru, M., Ng'ang'a, D., Poynter, A., & Blake, R. (2018). Airborne particulate matter monitoring in Kenya using calibrated low-cost sensors. *Atmospheric Chemistry and Physics*, *18*, 15403–15418. <https://doi.org/10.5194/acp-18-15403-2018>
- Prasad, C., Swamy, A. K., & Tiwari, G. (2013a). Calibration of HDM-4 emission models for Indian conditions. *Procedia-Social and Behavioral Sciences*, *104*, 274–281.
- Prasad, C., Swamy, A. K., & Tiwari, G. (2013b). Calibration of HDM-4 emission models for Indian conditions. *Procedia-Social and Behavioral Sciences*, *104*, 274–281.
- Rajé, F., Tight, M., & Pope, F. D. (2018). Traffic pollution: A search for solutions for a city like Nairobi. *Cities*, *82*, 100–107.
- Sadd, J., Morello-Frosch, R., Pastor, M., Matsuoka, M., Prichard, M., & Carter, V. (2014). The Truth, the Whole Truth, and Nothing but the Ground-Truth: Methods to Advance Environmental Justice and Researcher–Community Partnerships. *Health Education & Behavior*, *41*(3), 281–290. <https://doi.org/10.1177/1090198113511816>
- Saini, B., Verma, R., Himanshu, S. K., & Gupta, S. (2013). Analysis of exhaust emissions from gasoline powered vehicles in a sub-urban Indian town. *International Research Journal of Environmental Science*, *2*, 37–42.
- Sassykova, L. R., Aubakirov, Y. A., Sendilvelan, S., Tashmukhambetova, Z. K., Faizullaeva, M. F., & Bhaskar, K. (2019). The Main Components of Vehicle Exhaust Gases and Their Effective Catalytic Neutralization. *Oriental Journal of Chemistry*, *35*(1), 110–127.
- Sawyer, R. F. (2010). Vehicle emissions: Progress and challenges. *Journal of Exposure Science & Environmental Epidemiology*, *20*(6), 487–488.
- Saxena, P., & Sonwani, S. (2019). Primary criteria air pollutants: Environmental health effects. In *Criteria Air Pollutants and their Impact on Environmental Health* (pp. 49–82). Springer.
- Sayers, M. W. (1986). *Guidelines for conducting and calibrating road roughness measurements*. University of Michigan, Ann Arbor, Transportation Research Institute.

- Seinfeld, J. H., & Pandis, S. N. (2016). *Atmospheric chemistry and physics: From air pollution to climate change*. John Wiley & Sons.
- Sheikholeslami, R., & Razavi, S. (2017). Progressive Latin Hypercube Sampling: An efficient approach for robust sampling-based analysis of environmental models. *Environmental Modelling & Software*, *93*, 109–126.
- Shilenje, Z. W., Thiong'o, K., Ongoma, V., Phillip, S. O., Nguru, P., & Ondimu, K. (2016). Roadside air pollutants along elected roads in Nairobi City, Kenya. *Journal of Geology & Geophysics*, *5*(5), 1–10.
- Singh, A., Avis, W. R., & Pope, F. D. (2020). Visibility as a proxy for air quality in East Africa. *Environmental Research Letters*, *15*(8), 084002.
- Sudalma, S., Purwanto, P., & Santoso, L. W. (2015). The effect of SO₂ and NO₂ from transportation and stationary emissions sources to SO₄²⁻ and NO₃⁻ in rain water in Semarang. *Procedia Environmental Sciences*, *23*, 247–252.
- Svenson, G., & Fjeld, D. (2016). The impact of road geometry and surface roughness on fuel consumption of logging trucks. *Scandinavian Journal of Forest Research*, *31*(5), 526–536.
- Thayer, J. F., Yamamoto, S. S., & Brosschot, J. F. (2010). The relationship of autonomic imbalance, heart rate variability and cardiovascular disease risk factors. *International Journal of Cardiology*, *141*(2), 122–131.
- Thube, D. T. (2013). Highway Development and Management Model (HDM-4): Calibration and adoption for low-volume roads in local conditions. *International Journal of Pavement Engineering*, *14*(1), 50–59.
- Tomasi, C., & Lupi, A. (2016). *Primary and Secondary Sources of Atmospheric Aerosol* (pp. 1–86). <https://doi.org/10.1002/9783527336449.ch1>
- Tong, H. Y., Hung, W. T., & Cheung, C. S. (2000). On-road motor vehicle emissions and fuel consumption in urban driving conditions. *Journal of the Air & Waste Management Association*, *50*(4), 543–554.
- Veefkind, J. P., Aben, I., McMullan, K., Förster, H., de Vries, J., Otter, G., Claas, J., Eskes, H. J., de Haan, J. F., Kleipool, Q., van Weele, M., Hasekamp, O., Hoogeveen, R., Landgraf, J., Snel, R., Tol, P., Ingmann, P., Voors, R., Kruizinga, B., ... Levelt, P. F. (2012). TROPOMI on the ESA Sentinel-5 Precursor: A GMES mission for global observations of the atmospheric composition for climate, air quality and ozone layer applications. *Remote Sensing of Environment*, *120*, 70–83. <https://doi.org/10.1016/j.rse.2011.09.027>
- Villar-Vidal, M., Lertxundi, A., Martínez López de Dicastillo, M. D., Alvarez, J. I., Santa Marina, L., Ayerdi, M., Basterrechea, M., & Ibarluzea, J. (2014). Air Polycyclic Aromatic Hydrocarbons (PAHs) associated with PM_{2.5} in a North Cantabric coast urban environment. *Chemosphere*, *99*, 233–238. <https://doi.org/10.1016/j.chemosphere.2013.11.006>
- Vîrghileanu, M., Săvulescu, I., Mihai, B.-A., Nistor, C., & Dobre, R. (2020). Nitrogen Dioxide (NO₂) Pollution Monitoring with Sentinel-5P Satellite Imagery over Europe during the Coronavirus Pandemic Outbreak. *Remote Sensing*, *12*(21), 3575.
- Vries, J., Voors, R., Mika, A., Otter, G., Valk, N., Aben, I., Hoogeveen, R. W. M., Gloudemans, A., Dobber, M., Veefkind, P., & Levelt, P. (2009). TROPOMI, the solar backscatter satellite instrument

for air quality and climate, heads towards detailed design. *Proc SPIE*.
<https://doi.org/10.1117/12.830087>

Wang, T., Harvey, J., & Kendall, A. (2014). Reducing greenhouse gas emissions through strategic management of highway pavement roughness. *Environmental Research Letters*, 9(3), 034007.

Watanatada, T., Harral, C. G., Paterson, W. D. O., Dhareshwar, A. M., Bhandari, A., & Tsunokawa, K. (1987). THE HIGHWAY DESIGN AND MAINTENANCE STANDARDS MODEL. VOLUME 1, DESCRIPTION OF THE HDM-III MODEL. VOLUME 2, USER'S MANUAL FOR THE HDM-III MODEL. *WORLD BANK HIGHWAY DESIGN AND MAINTENANCE STANDARDS SERIES*.
<https://trid.trb.org/view/451315>

Weaver, L. K. (2009). Carbon monoxide poisoning. *New England Journal of Medicine*, 360(12), 1217–1225.

Winkler, S. L., Anderson, J. E., Garza, L., Ruona, W. C., Vogt, R., & Wallington, T. J. (2018). Vehicle criteria pollutant (pm, no x, co, hcs) emissions: How low should we go? *Npj Climate and Atmospheric Science*, 1(1), 1–5.

Wu, J., Zheng, H., Zhe, F., Xie, W., & Song, J. (2018). Study on the relationship between urbanization and fine particulate matter (PM_{2.5}) concentration and its implication in China. *Journal of Cleaner Production*, 182, 872–882.

Xing, Y.-F., Xu, Y.-H., Shi, M.-H., & Lian, Y.-X. (2016). The impact of PM_{2.5} on the human respiratory system. *Journal of Thoracic Disease*, 8(1), E69.

Xiong, X., Wenny, B. N., & Barnes, W. D. (2009). Overview of NASA Earth Observing Systems Terra and Aqua moderate resolution imaging spectroradiometer instrument calibration algorithms and on-orbit performance. *Journal of Applied Remote Sensing*, 3(1), 032501.

Zaabar, I., & Chatti, K. (2010). Calibration of HDM-4 models for estimating the effect of pavement roughness on fuel consumption for US conditions. *Transportation Research Record*, 2155(1), 105–116.

Zhang, M. (2016). Effects of Road Maintenance on Vehicle Emissions Evaluating by the Model of Highway Development and Management. *2015 4th International Conference on Sustainable Energy and Environmental Engineering*.

APPENDICES

Appendix A: Vehicle Growth Rates for Different Road Categories (source: KENHA)

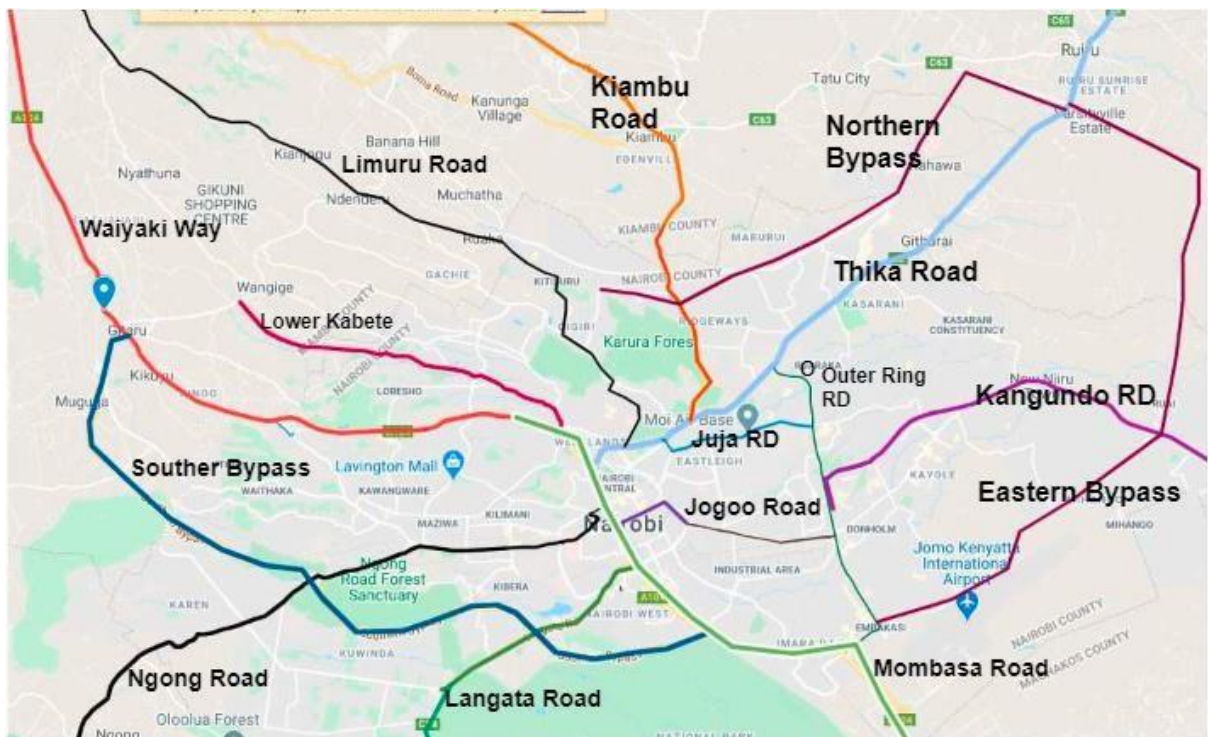
Vehicle category	Inter-urban Roads (A, B & C)			Minor Urban Roads			Rural Roads (D, E, SP)			Major Urban Roads/Multilane Highways		
	Low	Medium	High	Low	Medium	High	Low	Medium	High	Low	Medium	High
Motorcycles	3.9	6.0	10.4	3.9	10.4	19.6	2.6	3.9	10.0	9	11.0	19.6
Cars	3.9	6.4	10.0	4.4	7.5	11.5	2.5	4.4	8.4	10.0	11.0	11.5
Pickup/Vans	2.5	5.8	10.4	2.5	6.8	10.4	1.3	2.5	7.5	6.8	10.4	14
Matatu/Minibus	3.5	5.3	8.2	3.5	7.2	10.0	2.2	3.5	7.8	7	12.0	14.5
Buses	3.5	5.4	8.2	3.5	7.5	8.4	1.9	3.5	7.5	3.5	7.5	12.0
Trucks	2.9	5.6	7.8	3.5	5.7	8.4	1.9	3.5	7.5	3.5	5.7	12.0
Non-motorised Transport (NMT)	-	-	-	2.9	4.3	6.0	-	-	-	2.9	4.3	6.0

Appendix B: Vehicle Parameters Required for Modelling; source (Notter et al., 2019)

Vehicle Class	Heavy Truck	Passenger Car	Buses	Light Trucks	Motorcycles	Matatus
Fleet type	Motorised	Motorised	motorised	motorised	Motorised	motorised

Service life	8 years	14 years	5 years	10 years	4 years	17 years
Mass (tonnes)	7.5-12	1.8	3.5	3.5	0.25	2.5
Vehicle Utilization (km/year)	63,205	22,223	43,815	29,862	17,807	19,536
No. Wheels	10	4	6	4	2	4
Fuel type	Diesel	Petrol	diesel	Diesel	Petrol	Petrol
Tyre type	rubber	Rubber	rubber	Rubber	Rubber	Rubber
Fuel consumption (l/100km)	27.8	9.2	31.5	8	4.4	12.1

Appendix C: The Study Road Networks (Google.(n.d))



Appendix D: Model Input parameters for the Road Networks

Mombasa road Section ID:	A4/20	Road Name:	Nairobi Nyayo stadium-Syokimau	
Definition and Geometry:	Length (km):	27	Lanes (n):	2
	Carriage-width (m):	6	Altitude (m):	1660
	Shoulder-width (m):	2	flow-directions:	2
	Speed Limit (km/h):		Climate Zone:	Sub-humid dry
	Rise and Fall(m/km):	10	Hor. Curvature (°/km):	15
Pavement:	Pavement Type:	Bituminous	Last regravelling (year):	-
Conditions:	Gravel Thickness (mm):		AADT (annual):	32843
	Roughness (IRI):	3	Conditions for Year:	2016

Haile SelassieSection ID:	K10/1	Road Name:	Haile Selassie Avenue	
Definition and Geometry:	Length (km):	1.4	Lanes (n):	4
	Carriage-width (m):	6	Altitude (m):	1660
	Shoulder-width (m):	2	flow-directions:	2
	Speed Limit (km/h):	50	Climate Zone:	Sub-humid dry
	Rise and Fall(m/km):	10	Hor. Curvature (°/km):	15

Pavement:	Pavement Type:	Bituminous	Last regravelling (year):	-
Conditions:	Gravel Thickness (mm):	-	AADT (annual):	17977
	Roughness (IRI):	4	Conditions for Year:	2016

Moi Avenue

Section ID:		Road Name:	Moi avenue	
Definition and Geometry:	Length (km):	2	Lanes (n):	4
	Carriage-width (m):	6	Altitude (m):	1660
	Shoulder-width (m):	2	flow-directions:	2
	Speed Limit (km/h):	50	Climate Zone:	Sub-humid dry
	Rise and Fall(m/km):	10	Hor. Curvature (°/km):	15
Pavement:	Pavement Type:	Bituminous	Last regravelling (year):	-
Conditions:	Gravel Thickness (mm):	-	AADT (annual):	32798
	Roughness (IRI):	5	Conditions for Year:	2016

Tom Mboya Street

Section ID:	K4-Nairobi-1	Road Name:	Tom mboya Street	
-------------	--------------	------------	------------------	--

Definition and Geometry:	Length (km):	2.6	Lanes (n):	4
	Carriage-width (m):	6	Altitude (m):	1660
	Shoulder-width (m):	2	flow-directions:	2
	Speed Limit (km/h):	50	Climate Zone:	Sub-humid dry
	Rise and Fall(m/km):	10	Hor. Curvature (°/km):	15
Pavement:	Pavement Type:	Bituminous	Last regravelling (year):	-
Conditions:	Gravel Thickness (mm):		AADT (annual):	16779
	Roughness (IRI):	5	Conditions for Year:	2016

Jogoo Road

Section ID:	H2-NAIROBI-2	Road Name:	Jogoo road	
Definition and Geometry:	Length (km):	16.2	Lanes (n):	2
	Carriage-width (m):	6	Altitude (m):	1660
	Shoulder-width (m):	2	flow-directions:	2
	Speed Limit (km/h):	50	Climate Zone:	Sub-humid dry
	Rise and Fall(m/km):	10	Hor. Curvature (°/km):	15
Pavement:	Pavement Type:	Bituminous	Last regravelling (year):	-

Conditions:	Gravel Thickness (mm):	Two lane road	AADT (annual):	21917
	Roughness (IRI):	3	Conditions for Year:	2016
Section ID:	J7-NAIROBI-1	Road Name:	Lusaka road	
Definition and Geometry:	Length (km):	10.4	Lanes (n):	2
	Carriage-width (m):	6	Altitude (m):	1660
	Shoulder-width (m):	-	flow-directions:	2
	Speed Limit (km/h):	50	Climate Zone:	IV-Subhumid dry
	Rise and Fall(m/km):	10	Hor. Curvature (°/km):	15
Pavement:	Pavement Type:	Bituminous	Last regravelling (year):	-
Conditions:	Gravel Thickness (mm):	-	AADT (annual):	17932
	Roughness (IRI):	4	Conditions for Year:	2016

Limuru Road

Section ID:	J15-NAIROBI-1	Road Name:	Limuru road	
Definition and Geometry:	Length (km):	11.1	Lanes (n):	4
	Carriage-width (m):	6	Altitude (m):	1660
	Shoulder-width (m):	-	flow-directions:	2

	Speed Limit (km/h):	50	Climate Zone:	IV-Sub humid dry
	Rise and Fall(m/km):	10	Hor. Curvature (°/km):	15
Pavement:	Pavement Type:	Bituminous	Last regravelling (year):	-
Conditions:	Gravel Thickness (mm):	-	AADT (annual):	23487
	Roughness (IRI):	2	Conditions for Year:	2016

Section ID:	K40-NAIROBI-1	Road Name:	First parkland avenue	
Definition and Geometry:	Length (km):	3.7	Lanes (n):	2
	Carriage-width (m):	6	Altitude (m):	1660
	Shoulder-width (m):	2	Row-directions:	2
	Speed Limit (km/h):	50	Climate Zone:	IV-Sub humid dry
	Rise and Fall(m/km):	10	Hor. Curvature (°/km):	15
Pavement:	Pavement Type:	Bituminous	Last regravelling (year):	-
Conditions:	Gravel Thickness (mm):	-	AADT (annual):	7429
	Roughness (IRI):	3	Conditions for Year:	2016

Thika road

Section ID:	K6-NAIROBI-1	Road Name:	Muranga road-Ngara fig tree	
-------------	--------------	------------	-----------------------------	--

Definition and Geometry:	Length (km):	1	Lanes (n):	4
	Carriage-width (m):	7	Altitude (m):	1660
	Shoulder-width (m):	0	Row-directions:	2
	Speed Limit (km/h):	50	Climate Zone:	IV-Sub humid dry
	Rise and Fall(m/km):	10	Hor. Curvature (°/km):	15
Pavement:	Pavement Type:	Bituminous	Last regravelling (year):	-
Conditions:	Gravel Thickness (mm):	-	AADT (annual):	21,767

	Roughness (IRI):	3	Conditions for Year:	2016
Section ID:	K10-Nairobi-1	Road Name:	Ngara fig tree – Desai	
Definition and Geometry:	Length (km):	1.3	Lanes (n):	12
	Carriage-width (m):	7	Altitude (m):	1660
	Shoulder-width (m):	2	flow-directions:	2
	Speed Limit (km/h):	50	Climate Zone:	IV-Sub humid dry
	Rise and Fall(m/km):	10	Hor. Curvature (°/km):	15
Pavement:	Pavement Type:	Bituminous	Last regravelling (year):	-
Conditions:	Gravel Thickness (mm):	-	AADT (annual):	17,177

	Roughness (IRI):	2.5	Conditions for Year:	
Section ID:	J24-Nairobi-1	Road Name:	Nguru Nanak – pangani Police station	
Definition and Geometry:	Length (km):	0.5	Lanes (n):	8
	Carriage-width (m):	7	Altitude (m):	1660
	Shoulder-width (m):	2	Row-directions:	2
	Speed Limit (km/h):	50	Climate Zone:	IV-Sub humid
	Rise and Fall(m/km):	10	Hor. Curvature (°/km):	15
Pavement:	Pavement Type:	Bituminous	Last regravelling (year):	-
Conditions:	Gravel Thickness (mm):	-	AADT (annual):	18,856
	Roughness (IRI):	2.5	Conditions for Year:	2016
Section ID:	A2/5	Road Name:	Ruaraka - Kamakis junction	
Definition and Geometry:	Length (km):	11.1	Lanes (n):	8
	Carriage-width (m):	7	Altitude (m):	1660
	Shoulder-width (m):	2	Row-directions:	2
	Speed Limit (km/h):	80	Climate Zone:	IV-Sub humid dry
	Rise and Fall(m/km):	10	Hor. Curvature (°/km):	15

Pavement:	Pavement Type:	Bituminous	Last regravelling (year):	-
Conditions:	Gravel Thickness (mm):	-	AADT (annual):	55896
	Roughness (IRI):	2.5	Conditions for Year:	2016

Ngong Road

Section ID:	H4-NAIROBI-1	Road Name:	Ngong road – Karen hospital	
Definition and Geometry:	Length (km):	39	Lanes (n):	
	Carriage-width (m):	6	Altitude (m):	1660
	Shoulder-width (m):	2	Row-directions:	2
	Speed Limit (km/h):	50	Climate Zone:	IV-Sub humid dry
	Rise and Fall(m/km):	10	Hor. Curvature (°/km):	15
Pavement:	Pavement Type:	Bituminous	Last regravelling (year):	-
Conditions:	Gravel Thickness (mm):	--	AADT (annual):	13,312
	Roughness (IRI):	4	Conditions for Year:	2016
Section ID:	K21-Nairobi-1	Road Name:	Argwings Kodhek-Suna road	

Definition and Geometry:	Length (km):	1.22	Lanes (n):	4
	Carriage-width (m):	7	Altitude (m):	1660
	Shoulder-width (m):	2	Row-directions:	2
	Speed Limit (km/h):	50	Climate Zone:	IV-Sub humid dry
	Rise and Fall(m/km):	10	Hor. Curvature (°/km):	15
Pavement:	Pavement Type:	Bituminous	Last regravelling (year):	-
Conditions:	Gravel Thickness (mm):	-	AADT (annual):	8,770
	Roughness (IRI):	5	Conditions for Year:	2016

Outer-Ring Road

Section ID:	H2-NAIROBI-1	Road Name:	Allsoaps – Meerkat Kenya LTD.	
Definition and Geometry:	Length (km):	16.2	Lanes (n):	4
	Carriage-width (m):	6	Altitude (m):	1660
	Shoulder-width (m):	2	Row-directions:	2
	Speed Limit (km/h):	50	Climate Zone:	IV-Sub humid dry
	Rise and Fall(m/km):	10	Hor. Curvature (°/km):	15
Pavement:	Pavement Type:	Bituminous	Last regravelling (year):	-

Conditions:	Gravel Thickness (mm):	-	AADT (annual):	19,098
	Roughness (IRI):	3	Conditions for Year:	2016

Eastern bypass road sections

Section ID:	H6-Nairobi-3	Road Name:	Basco paints Mombasa road - Utawala	
Definition and Geometry:	Length (km):	16.2	Lanes (n):	2
	Carriage-width (m):	6	Altitude (m):	1660
	Shoulder-width (m):	0	Row-directions:	2
	Speed Limit (km/h):	50	Climate Zone:	IV-Sub humid dry
	Rise and Fall(m/km):	10	Hor. Curvature (°/km):	15
Pavement:	Pavement Type:	Concrete	Last regravelling (year):	-
Conditions:	Gravel Thickness (mm):	-	AADT (annual):	31,348
	Roughness (IRI):	3	Conditions for Year:	2016
Section ID:	H6-Nairobi-1	Road Name:	Nairobi Utawala- Nairobi Ruai	
Definition and Geometry:	Length (km):	15	Lanes (n):	
	Carriage-width (m):	6	Altitude (m):	1660
	Shoulder-width (m):	0	Row-directions:	2

	Speed Limit (km/h):	50	Climate Zone:	IV-Sub humid dry
	Rise and Fall(m/km):	10	Hor. Curvature (°/km):	15
Pavement:	Pavement Type:	Concrete	Last regravelling (year):	-
Conditions:	Gravel Thickness (mm):	-	AADT (annual):	21,369
	Roughness (IRI):	2	Conditions for Year:	2016
Section ID:	H3-Nairobi-1	Road Name:	Nairobi Ruai- Nairobi Ruiru	
Definition and Geometry:	Length (km):	15	Lanes (n):	2
	Carriage-width (m):	6	Altitude (m):	1660
	Shoulder-width (m):	2	Row-directions:	2
	Speed Limit (km/h):	50	Climate Zone:	IV-Sub humid dry
	Rise and Fall(m/km):	10	Hor. Curvature (°/km):	15
Pavement:	Pavement Type:	Concrete	Last regravelling (year):	-
Conditions:	Gravel Thickness (mm):	-	AADT (annual):	22,994
	Roughness (IRI):	2.5	Conditions for Year:	2016

Langata Road

Section ID:	H4-Nairobi-3	Road Name:	Nairobi Langata cemetery	
Definition and Geometry:	Length (km):	39	Lanes (n):	
	Carriage-width (m):	6	Altitude (m):	1660
	Shoulder-width (m):	2	Row-directions:	2
	Speed Limit (km/h):	50	Climate Zone:	IV-Sub humid dry
	Rise and Fall(m/km):	10	Hor. Curvature (°/km):	15
Pavement:	Pavement Type:	Concrete	Last regravelling (year):	-
Conditions:	Gravel Thickness (mm):	-	AADT (annual):	31,372
	Roughness (IRI):	2.5	Conditions for Year:	2016
Section ID:	J22-Nairobi-1	Road Name:	Mbagathi Road	
Definition and Geometry:	Length (km):	15	Lanes (n):	2
	Carriage-width (m):	6	Altitude (m):	1660
	Shoulder-width (m):	2	Row-directions:	2
	Speed Limit (km/h):	50	Climate Zone:	IV-Sub humid dry
	Rise and Fall(m/km):	10	Hor. Curvature (°/km):	15
Pavement:	Pavement Type:	concrete	Last regravelling (year):	-
Conditions:	Gravel Thickness (mm):	-	AADT (annual):	18,095

	Roughness (IRI):	3.0	Conditions for Year:	2016
--	------------------	-----	----------------------	------

Southern Bypass

Section ID:	H6-Nairobi-3	Road Name:	Nairobi Northern Bypass	
Definition and Geometry:	Length (km):	39	Lanes (n):	
	Carriage-width (m):	6	Altitude (m):	1660
	Shoulder-width (m):	2	Row-directions:	2
	Speed Limit (km/h):	50	Climate Zone:	IV-Sub humid dry
	Rise and Fall(m/km):	10	Hor. Curvature (°/km):	15
Pavement:	Pavement Type:	Concrete	Last regravelling (year):	-
Conditions:	Gravel Thickness (mm):	-	AADT (annual):	21,000
	Roughness (IRI):	2.5	Conditions for Year:	2016

Northern Bypass

Section ID:	J22-Nairobi-1	Road Name:	Northern Bypass	
Definition and Geometry:	Length (km):	15	Lanes (n):	2
	Carriage-width (m):	6	Altitude (m):	1660
	Shoulder-width (m):	2	Row-directions:	2
	Speed Limit (km/h):	50	Climate Zone:	IV-Sub humid dry
	Rise and Fall(m/km):	10	Hor. Curvature (°/km):	15
Pavement:	Pavement Type:	concrete	Last regravelling (year):	-

Conditions:	Gravel Thickness (mm):	-	AADT (annual):	18.792
	Roughness (IRI):	3.0	Conditions for Year:	2016